Seamless Coverage for the Next Generation Wireless Communication Networks

Aysenur TURKMEN

Submitted in fulfilment of the requirements for the

Degree of Doctor of Philosophy

School of Engineering

College of Science and Engineering

University of Glasgow

October 2022

Abstract

Data demand has exponentially increased due to the rapid growth of wireless and mobile devices traffic in recent years. With the advent of the fifth generation, 5G, and beyond networks, users will be able to take advantage of additional services beyond the capability of current wireless networks while maintaining a high-quality experience. The exploitation of millimeter-wave (mm-wave) frequency in 5G promises to meet the demands of future networks with the motto of providing high data rate coverage with low latency to its users, which will allow future networks to function more efficiently. However, while planning a network using mm-wave frequencies, it is important to consider their small coverage footprints and weak penetration resistance. Heterogeneous network planning with the dense deployment of the small cells is one way of overcoming these issues, yet, without proper planning of the integrated network within the same or different frequencies could lead to other problems such as coverage gaps and frequent handovers; due to the natural physics of mm-wave frequencies.

Therefore this thesis focuses on bringing ultra-reliable low-latency communication for mm-wave indoor users by increasing the indoor coverage and reducing the frequency of handovers. Towards achieving this thesis's aim, a detailed literature review of mm-wave coverage is provided in Chapter 2. Moreover, a table that highlights the penetration loss of materials at various frequencies is provided as a result of thorough research in this field, which will be helpful to the researchers investigating this subject. According to our knowledge, this is the first table presenting the most studies that have been conducted in this field.

Chapter 3 examines the interference effect of the outdoor base station (BS) inside the building in the context of a heterogeneous network environment. A single building model scenario is created, and the interference analysis is performed to observe the effects of different building materials used as walls. The results reveal the importance of choosing the material type when outdoor BS is close to the building. Moreover, the interference effect of outdoor BS should be minimized when the frequency re-use technique is deployed over very short distances.

Chapter 4 presents two-fold contributions, in addition to providing a comprehensive handover study of mm-wave technology. The first study starts with addressing the problem of modelling users' movement in the indoor environment. Therefore, a user-based indoor mobility prediction via Markov chain with an initial transition matrix is proposed, acquired from Q-learning algorithms. Based on the acquired knowledge of the user's mobility in the indoor environment, the second contribution of this chapter provides a pre-emptive handover algorithm to provide seamless connection while the user moves within the heterogeneous network. The implementation and evaluation of the proposed algorithm show a reduction in the handover signalling costs by more than 50%, outperforming conventional handover algorithms.

Lastly, Chapter 5 contributes to providing robust signal coverage for coverage blind areas and implementing and evaluating the proposed handover algorithm with the intelligent reflective surface. The results show a reduction in the handover signalling costs by more than 33%, outperforming conventional handover algorithms with the pre-emptive handover initiation.

University of Glasgow

College of Science & Engineering

Statement of Originality

Name: Aysenur Turkmen

Registration Number: xxxxxxx

I certify that the thesis presented here for examination for a PhD degree of the University of Glasgow is solely my own work other than where I have clearly indicated that it is the work of others (in which case the extent of any work carried out jointly by me and any other person is clearly identified in it) and that the thesis has not been edited by a third party beyond what is permitted by the University's PGR Code of Practice.

I declare that the thesis does not include work forming part of a thesis presented successfully for another degree.

I declare that this thesis has been produced in accordance with the University of Glasgow's Code of Good Practice in Research.

I acknowledge that if any issues are raised regarding good research practice based on the review of the thesis, the examination may be postponed pending the outcome of any investigation of the issues.

Signature: Aysenur TURKMEN

Date: .....

Contents

List of Tables

List of Figures

Acknowledgements

"My success is not but through Allah. Upon Him I have relied and to Him I return." (Hud, 11:88)

First, I would like to express my deepest gratitude to my supervisor, Prof. Muhammad Ali Imran, for his support, motivation, and valuable guidance. I always felt granted about having him as my supervisor, whose mentorship, patience and motivation meant a lot to me. What I had to endure throughout my PhD was my starstruck syndrome since I idolize him greatly. Thank you, Prof. Imran, for being a great example to your students. Thank you so much for believing in me even when I doubted myself.

Second, I would like to express my deepest gratitude to my co-supervisor, Prof. Lei Zhang, for the exceptional support, encouragement, and patience. My discussions with him have taught me a lot, and his feedback has greatly improved my skills. Thank you Prof. Lei, for thoroughly reading all my drafts, and giving all the feedback to polish this thesis. You helped me keep going when I lost motivation during my PhD journey, and I sincerely appreciate it.

I also thank my scholarship provider, the Republic of Turkey Ministry of National Education, for providing this great opportunity.

Special thanks to the Communications Sensing and Imaging (CSI) research group members, especially to Dr Paulo V. Klaine and Dr Shuja Ansari for sharing their experience whenever I needed their help and to Dr Yusuf Sambo for his continued encouragement.

I would also like to acknowledge the support and help of all my friends during

the PhD; without them, this journey would have been much harder and arduous. A very special thanks to my dear friend, Dr Sofiat Olaosebikan, who became my mentor, my couch to 5k run, my therapist, and most importantly, for being my family in Glasgow. I am so grateful that our paths crossed, and to have you as a lifelong friend/sister.

I would like to thank M.Fettah eH. for opening the doors of this great journey of my life, and my sincere love and gratitude to A.Baki eH, for being the foundation/resource of my life.

Last but not least, I would like to thank my family for all the support throughout this journey, in special my parents, Mebruke & Ibrahim Turkmen, my siblings Mehmet, Fatmanur and my always baby sister Esmanur. I appreciate all your patience during all the years we had to live apart. Lastly, I send my gratitude to my dear cat Aslan, who came into my life at a very needed time and brought great enjoyment.

Chapter 1

Introduction

5G has already been deployed in major cities worldwide [1]. In 5G, mm-wave frequencies are exploited to handle increased wireless data traffic associated with smart connected devices. The mm-wave band's high-frequency range promises to achieve high data rate communications with minimal latency. However, they are highly prone to penetration losses due to the physical nature of high-frequency radio communications, which may cause some coverage problems. In order to ensure robust coverage of mm-wave frequencies, small cells can be deployed where mm-wave frequency-driven BSs are placed closer to each other [2]. The density of small cell deployment is likely to result in frequent handovers without proper management and regulation. Otherwise, these increased handovers may degrade users' quality of Service (QoS) and Quality of Experience (QoE) [3]. Unless these handovers are reduced, the QoS and the QoE of a user may suffer.

Therefore this thesis contributes to provide low latency communication and robust coverage to mm-wave users, especially for indoor residents, as there needs to be more concentration in that area. Firstly, the effect of frequency-dependent materials on the interference examined that users could experience in the indoor environment under multiple frequency multi-tier networks. Next, based on previous investigations of the impact of interference on indoor users, a smart handover algorithm is implemented to reduce the number of handovers with machine learn-

ing techniques. As a final step, a solution is proposed to address coverage hole areas within the frequency-dependent building and proposed another handover algorithm to reduce handover delays.

The following provides an overview of handover and mobility management in the cellular network.

1.1 Handover Management Overview

Handover or handoff is a procedure for maintaining a steady connection of a UE to the network when it moves out from the serving cell's coverage to another cell's coverage. The procedure is done by changing the current cell's channel into a new channel whenever the UE moves into a new cell [4].

Fig. 1.1 demonstrates a simple handover scenario where the UE attached to BS_1 has an ongoing call while moving toward the coverage area of BS_2. The UE continuously monitors the signal strength of the two base stations (BS_1 and BS_2). If the measured signal strength of the BS_2 goes higher than BS_1 in the overlapping area, and the BS_2 can provide the required resources that the UE needs; a handover process will be performed to connect the UE to the BS_2, avoiding disconnection of the ongoing call.

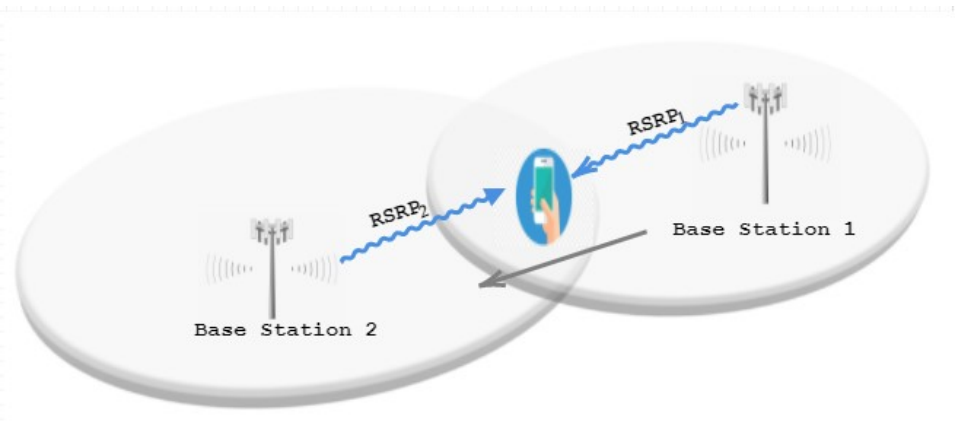

Figure 1.1: Handover illustration.

The call dropping probability (CDP) and the call blocking probability (CBP)

are two essential parameters that give a clear indicator for the QoS of a network in the context of mobility [5]. CD happens when the handover process is rejected, and the connection is dropped due to the required resources of the connection not being supported by the new BS. Alternatively, the probability of new connection access being denied by the target BS due to current traffic congestion is called CBP. The use of bandwidth (channel) or the efficient utilisation of frequency bands within a network is another fundamental parameter of QoS. For more information about CDP and CBP, readers should go to [5].

Generally, there are three phases in a handover procedure: measurement, handover decision and handover execution. The outcome of the first stage, the measurement report, is used as input along with the handover algorithms of the second stage. In the last stage, handover is executed by assigning the UE to the new BS; hence, the old connection is terminated. In the handover decision phase, if measurements are done by the UE and the network conducts the handover decision, it is called Mobile Assisted Handover (MAHO). Whereas if the network makes the decision using the measurements collected from the UEs at several BSs, it is called Network Controlled Handover (NCHO). Lastly, Mobile Controlled Handover (MCHO) is where each UE thoroughly assists in the handover process [4].

In addition, a HO can also be categorised as a soft or hard handover. In the hard handover, mostly employed in Time Division Multiple Access (TDMA) and Frequency Division Multiple Access (FDMA), the connection with the existing BS is ended before a new connection is made with the target BS. The soft handover, mostly utilised in Code Division Multiple Access (CDMA), preserved the existing connection while making a new connection with a target BS.

Handover Requirements

Handovers in the wireless network might negatively affect both the QoS and the network's capacity if the aspects mentioned below are not taken into account [6].

- Handover latency should be kept as low as possible.
- The total number of handovers should be kept minimum in case of knowing the particular trajectory of a UE.
- Additional signals should be lowered during the handover process.
- Handover impact on QoS should be minimized, such as lowering CDPs and CBPs and traffic between the neighbouring cells.

Some factors also need to be considered from the designers' aspect to achieve the desired features of handovers. Some of them are:

- *Cellular structure* has an important effect on handover occurrence, depending on the cell size. For instance, if the cell size decreases, handover becomes more frequent for a given mobile user scenario. Macro-cell, micro-cell, pico-cell, and femtocell are wireless network types, ordered by their cell size [7].
- *Mobility*, referring to the user's direction and speed, also impacts handovers. For example, the handover requirements might differ for a user who moves fast, in a car, train etc., and a user with a normal speed. Therefore, the handover algorithms should address the different requirements based on the user's needs.
- The decrease in QoS, such as bandwidth, BER or packet loss, might trigger the handover in order to find another BS that can provide a better QoS.

Handover Schemes and Resource Management

Good management of wireless network tools such as; code channels, time slots, transmission capacity, frequency channels, transceiver numbers, and battery power grants the service providers enhancement in the service quality, saving costs and increasing wireless network productivity and effectiveness. Good resource management also decreases the probability of handover drops and preserves the QoS

during and after the handover. As shown in Fig.1.2, handover-related resource management consists of admission control, bandwidth reservation and power control. In admission control, ongoing and new calls can be handled differently to ensure the system is not overloaded. For instance, new calls may be queued while handovers may be prioritized. The bandwidth in a wireless system is one of the most important resources. A handover request can proceed when a channel is available or bandwidth reservation is done. A basic solution for bandwidth needs in a handover process is reserving fractional bandwidths in a cell and using these preserved bandwidths for a handover request instead of a new call request. Power control is also very important in mobile systems due to its significant role in battery life, resource and spectrum allocation. Detailed information on resource management in a wireless network can be found in [8].

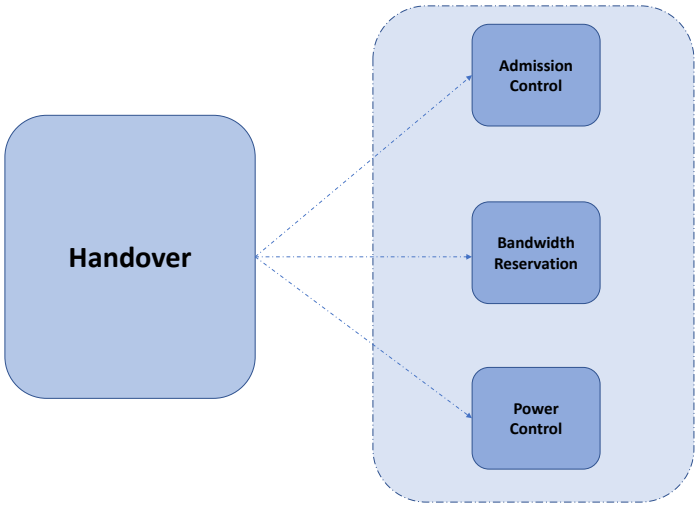

Figure 1.2: Handover resource management.

Handover Algorithms

Handover algorithms can be divided into two groups as [9], [10]:

1. Conventional handover algorithms are based on the received signal strength (RSS), signal-to-interference ratio (SIR), power, distance, velocity and budget.

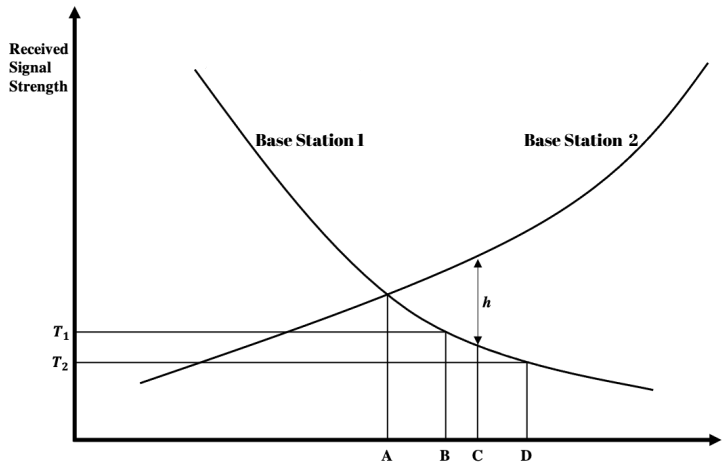

Figure 1.3: Received Signal Strength as UE moving towards the handover area.

2. Intelligent Handover algorithms based on AI technologies, such as neural networks, fuzzy logic, pattern recognition and prediction.

Relative Signal Strength: The BSs' RSSs are measured over time in this process, and the BS with the highest signal strength is chosen to initiate the handover. Fig.1.3 shows the RSS alteration of two BSs, while UE moves towards the handover area. When UE enters the handover area, point A, the RSS of BS_1 decreases while measured RSS by UE from BS_2 increases. Therefore, UE needs to handover from BS_1 to BS_2. Multiple fading can cause back-and-forth handovers, called ping-pong handovers. For instance, if the UE senses an increase in the RSS of BS_1, then it might handover back to BS_1. Occurrences of ping-pong handovers reduce the QoS considerably. Therefore, the below methods are mostly applied with the RSS to mitigate the ping-pong effect.

- *RSS with threshold:* In this method, handover proceeds when the serving BS' RSS value goes under the threshold value. As shown in Fig.1.3, handover will proceed at point B, where RSS of BS_1 is lower than threshold T_1. Having a threshold value helps to reduce the handover occurrences in the system. However, there is an important point that needs to be taken into account when determining this threshold value. An optimum value for the threshold should be chosen carefully; otherwise, handover problems may

arise. For example, a user might face call drops if the threshold is chosen low; or the ping-pong effect might be seen if it gets closer to point A, in the case shown in Fig.1.3.

- *RSS with Hysteresis:* Handover is only allowed in this method if the RSS of BS_2 is higher than BS_1 with a hysteresis value of h. Hence in Fig.1.3, handover will be executed at point C. The ping-pong effect will be reduced with this method. However, similar problems in the abovementioned method are also present if the appropriate value for h is not chosen. Such as, if h is chosen too high, call drop may happen since RSS of BS_1 will not be strong enough to support the UE, or unnecessary handovers may occur if h value is chosen very low.

- *RSS with Threshold and Hysteresis:* Both threshold and hysteresis values are used together in this technique to minimize unnecessary handovers. The handover occurs if the RSS of BS_1 is lower than the threshold value and the RSS of BS_2 is higher than the BS_1 with a hysteresis value of h. As shown in Fig.1.3, handover will occur at point C if this method is used.

T_2 value in Fig.1.3 is a threshold value for the receiver, ensuring the minimum value for RSS that maintains the ongoing call. In case the RSS of the receiver goes under the T_2 value, an ongoing call will be dropped. The network will try to accommodate the UE to the target BS, the time slot from point A to point D.

SIR Based Algorithms: Signal to Interference Ratio is one of the most important measures to evaluate the communication system's QoS. Once the serving BS' SIR value is lower than the threshold and if the neighbouring BS provides better SIR, handover will be executed to the neighbouring BS.

Velocity Based Algorithms: The time delay throughout the handover may cause call drops for fast-moving users. In [11], a fast handover algorithm with velocity adaptation is presented for a typical NLOS scenario of urban communication. Their velocity-adapted handover algorithm shows a decrease in handover

delay. Using the first moment of the instantaneous frequency, IF, of the received signal, a mobile station velocity estimator is presented in [12]. Their IF-based velocity estimator algorithm showed more robustness to the shadowing effects than other velocity estimators.

Direction Biased Algorithms: The study in [13] used direction biased algorithm by grouping the BSs in two; users are approaching group 1, and users are moving away from group 2. In order to encourage the handovers to the group 1 BSs, the adjustment is done by assigning the hysteresis values to each group; lower hysteresis to group 1 and higher hysteresis to group 2. This algorithm helps increase the handover efficiency by reducing the mean number of handovers and simultaneously decreasing the delay in handover.

Minimum Power Algorithms: This algorithm is proposed in [14], where the transmission power is used as a handover criteria, and a timer is utilized alongside the algorithm to avoid the ping-pong effect.

Conventional handover algorithm methods, in which inputs can be SIR, power, the signal strength, are mostly easy to deploy. The intelligent algorithms presented below can be utilized alongside conventional algorithms to increase the performance of the handover algorithm.

Fuzzy Logic Based Algorithms: A fuzzy logic algorithm integrated with an existing cross-layer handover protocol is proposed in [15] for providing a seamless handover for next-generation wireless systems. In comparing their proposed method with the existing protocol, and based on their simulation results, the proposed fuzzy logic-based handover algorithm performs better than the conventional protocol. The fuzzy logic algorithm is utilized in [16] for saving the energy of mobile devices while keeping QoE at satisfactory levels for energy-efficient seamless vertical handover in the heterogeneous network environment.

Neural Based Algorithms: Handover algorithms based on neural networks are presented in [17]- [18]. The study in [17] uses data rate, while the algorithm used in [17] employs the data rate, monetary cost and RSSI information as input

to create vertical handover decision systems. Significant decreases are observed in the handover latency and the number of handovers using their algorithm. A hybrid method; using artificial neural network-based prediction with fuzzy logic is proposed in [18]. Their results show that the algorithm used in the study is able to reduce the ping-pong effect associated with other handover techniques.

Pattern Recognition Based Algorithms: A pattern recognition handover algorithm is proposed in [19], which uses the signal strength measurements at the location where handovers may be needed. The signal strengths from BSs are used as patterns; hence, handover will be executed when signal strength measurements match these patterns. The algorithm outperforms the traditional handovers at the same hysteresis and threshold by reducing handover decisions and unnecessary handovers. Authors extended their pattern recognition algorithm for reducing the corner effect by introducing two-stage decision; machine-regular and alert [20]. In the alert stage, the path of the users is defined by three short patterns. If the pattern matches before the corner, the algorithm goes to the alert stage instead of executing the handover, in which each short pattern is compared with the signal strength. These short patterns contain the appropriate handover. This extended algorithm also works better than conventional handovers.

Prediction Based Algorithms: Mobility prediction of the users aims to reduce handover delay and unnecessary handovers and is one of the popular techniques within intelligent handover algorithms. Knowing the user's trajectory information would be useful for BS skipping; for instance, unnecessary handovers will be prevented in the densely deployed small cell environment. The study in [21] used an improved mobility prediction handover framework to assist the user equipment during the handover process to provide seamless connectivity to its users. The results show improved throughput for both homogeneous and heterogeneous networks. An adaptive handover technique for seamless mobility-based wireless networks is proposed in [22] to predict the best access point (AP) candidate, utilizing the selection metrics of RSS of candidate AP, mobile node relative direction

towards the access points in the vicinity, and AP load. Despite being more complicated than conventional handover systems, intelligent handover algorithms are much more suitable for increasing the QoS of mm-wave communication [6]. They are also capable of reducing handover delays and unnecessary handovers, as well as call blocking and call dropping probabilities. In addition to using common inputs such as signal power and SIR, intelligent algorithms use the information of the network, such as traffic and the information of UE, for instance: direction, speed, location, etc.

1.2 Mobility Management Overview

Increased demand for seamless connections has brought more attention to mobility management since mobile users tend to switch their networks and/or serving BSs, which results in service disruptions. Hence, seamless connectivity can only be provided with a proper mobility management scheme. It is reported in [23] that mobility management can be categorized as follows:

- HO management,
- resource management,
- location-based service pre-configuration and network planning (out of the scope of this thesis).

HO occurs when an active or radio resource control (RRC) connected UE -performing data transmission- alters its serving access terminal for various reasons, including receiving better signal quality from neighbouring BSs or the received signal quality from the serving BS under a certain threshold. Similar to the X2 interface in LTE, the Xn interface is the interface between next generation-radio access networks (NG-RANs) -or simply g nodeB (gNB)- is already defined in $5G$ standards [24]. According to Xn-based HO, there are HO preparation and execution phases in which certain steps are taken in order before the UE has an RRC connection (or is active). These two phases, in turn, incur some delay, resulting in service interruptions for UEs that undermine seamless connectivity. Given the limited coverage areas of mm-wave frequencies designated for $5G$ NR, the HO rates are expected to boost, making the seamless connectivity harder to sustain.

In this regard, predictive mobility management, where future locations and HOs of the users are predicted, and networks/BSs are triggered to be ready for upcoming events, such as HO requests in advance, is considered to be a promising candidate to provide the required solution for the seamless connectivity [23]. The

authors in [25] proposed a machine learning (ML) based mobility management scheme for LTE X2 HO process, where future HOs are predicted so that some of the HO preparation steps are conducted beforehand in order to reduce the HO delay.

Each BS is assigned to some certain bandwidth to provide for the users under their service, and resource management refers to using radio resources as efficiently as possible. With the ever-increasing number of users in mobile communications networks, including IoT devices [26], resource management becomes even more critical, especially for UDNs. Mobility prediction also helps provide efficient and intelligent radio resource management [23]. Upcoming HOs, for example, can be predicted for a certain BS to provide it with prior information so that it would have time to arrange the available resources accordingly. In addition to enhancing resource utilisation efficiency, HO-prediction-based resource management can also play an integral role in seamless connectivity since call droppings can be prevented by providing the target BSs with full knowledge about the upcoming HOs [3].

1.3 Research Gaps and Motivations

The rapid development of modern and smart urbanization led to more than 80% of people spending daily life in the indoor environment [27, 28]. Moreover, when emergency measures are considered, such as the Covid-19 pandemic situations, i.e. restrictions, local/national lock-downs, homeschooling, and paradigm shift to working from home, people spend more time indoors, which further increases the data demand for indoor users. However, the study of HO models, and coverage extension of an outdoor transmitter to indoor receivers, receives much more attention in the literature when compared to the indoor-related casework [29]. Thus, intelligent HO technology paves the way for new research directions in the interface between indoor and outdoor networks. The following sums up the research gaps and motivations that are addressed in this thesis, in particular.

- As the studies had pointed out that the HO failure rate in a heterogeneous macro-pico network is up to 60%, which is twice higher compared to a macro-only network [30], the research question that whether the different types of building materials have played any role on the outdoor BS's interference when the user is served by the mm-wave driven femto BS, led the work presented in Chapter 3.

- Indoor user mobility is one of the critical factors of today's system-level simulations; indoor users generate a great amount of mobile traffic. As mentioned, how to model the user's indoor movement is still being determined. To enable the seamless connection transition while the user moves from mm-wave-driven indoor small BS' coverage to outdoor macro BS coverage, prediction of mobility is notably important. Based on the social force model in [31], a human's decision-making process is divided as a product of two factors, external and internal, in which the former is represented by environment stimulus and group behaviour, whereas individual characteristics indicate the latter. Therefore, the user's mobility is stated to have

some pattern and is not entirely spontaneous. Motivated by the mentioned study, we hypothesise that a user has more regularities in their movement within an indoor environment, where degrees of freedom are lower than in an outdoor scenario. Based on the aforementioned research motivations, Chapter 4 focuses on reducing the frequency of handovers.

- Connection loss inside the coverage blind area is a significant problem if it is not properly addressed and has not received decent attention. While looking for a cost-effective solution for supplying satisfactory signal coverage to the coverage blind area and seamless connection, intelligent reflective surface, which is seen as an emerging technology and takes great attention in the literature, took our attention. However, how to integrate it into the conventional handover signalling procedure is unclear, which moved us to the study proposed in Chapter 5.

1.4 Research Aim and Objectives

Based on the aforementioned research gaps and motivations, this thesis aims to bring ultra-reliable low-latency (URLLC) communication for mm-wave indoor users by increasing indoor coverage and reducing the frequency of handovers.

The objectives of the thesis can be outlined as follow:

- Provide a literature review on mm-wave coverage, HO and mobility management.

- Analyse how the building material types react to mm-wave interference in order to provide robust indoor coverage.

- Analyse indoor mobility prediction with the utilization of Q-learning, and devise a pre-emptive HO algorithm in order to achieve seamless connection and URLLC for the UEs transitioning in the heterogeneous network.

- Analyse the mm-wave coverage in the context of IRS applied to the coverage blind areas, and devise a pre-emptive HO algorithm in order to achieve URLLC with reduced HO costs.

- Provide conclusions and future research directions on the topic of seamless connection in mm-wave.

1.5 Thesis Contributions and Organization

The remainder of this thesis with the contributions to the corresponding research objectives mentioned in Section 1.4 to each chapter follows as:

- Chapter 2 introduces the overview of mm-wave communication. Then, the benefits and drawbacks of using mm-wave for indoor coverage are explained in more detail, and the literature is examined. Our extensive survey in this area led us to produce a table that summarizes the penetration loss of materials at various frequencies, which would be useful to the researchers studying this area. According to our knowledge, this is the first table presenting most of the studies conducted in this field. Following that, more details are introduced on heterogeneous network planning. One of the main objectives of this thesis is to provide solutions for coverage and handover problems; the literature review in this chapter also includes some machine-learning techniques that could effectively achieve seamless coverage. This chapter has been published as part of a book chapter. Detailed information about the publication can be found in the publications section below.

- Chapter 3 examines the outdoor BS interference effect inside the building in the context of a heterogeneous network environment. A single building model scenario is created, and the interference analysis is performed to observe the effects of different building materials used as walls. An assessment of the results is followed by the selection of the best frequency-dependent

building material in conclusion. This chapter has been published in a conference paper. The publications section contains details of the publication.

- Chapter 4 presents two-fold contributions and provides a comprehensive study of mm-wave technology. The first study addresses the problem of modelling users' movement in the indoor environment. Therefore, a user-based indoor mobility prediction via Markov chain with an initial transition matrix is proposed, acquired from Q-learning algorithms. Based on the acquired knowledge of the user's mobility in the indoor environment, the second contribution of this chapter provides a pre-emptive handover algorithm to provide seamless connection while the user moves within the heterogeneous network. The results of the first contribution of this chapter are published at a conference, and the extended work with the second contribution is published in a journal. Publication details are provided in the publications section.

- Chapter 5 provides seamless coverage, especially for the users moving within the coverage blind area, where they lose their network connection. Following the detailed information on radio access mobility, the proposed solutions are introduced, and results are showcased. The conclusion is drawn at the end. Currently, this chapter is being prepared for submission to a conference.

- Finally, Chapter 6 concludes the thesis and provides the future direction of the research.

1.6 Publications

- Part of the Chapter 2 is published in the book chapter, details shared below.

  Muhammad A. Imran, **Aysenur Turkmen**, Metin Ozturk, Joao Nadas, Qammer H Abbasi. Seamless indoor/outdoor coverage in $5G$. Wiley 5G Ref: The Essential 5G Reference Online, 1-23 doi : 10.1002/9781119471509 URL:$https://onlinelibrary.wiley.com/doi/10.1002/9781119471509.w5GRef227$

- The study in Chapter 3 is presented in the conference. The details are given below: **Aysenur Turkmen**, Michael S. Mollel, Metin Ozturk, Sun Yao, Lei Zhang, Rami Ghannam, Muhammad A. Imran. Coverage analysis for indoor-outdoor coexistence for millimetre-wave communication 2019 UK/China Emerging Technologies (UCET), 1-4 doi : 10.1109/$UCET$.2019.8881890. URL: $https://ieeexplore.ieee.org/abstract/document/$8881890

- The initial results in Chapter 4 is presented in a conference, and the completed work is published in a journal. The details are given below:

  Aysenur Turkmen, Shuja Ansari, Paulo V. Klaine, Lei Zhang, Muhammad A. Imran. Indoor mobility prediction for mm-wave communications using Markov Chain 2021 IEEE Wireless Communications and Networking Conference (WCNC), 1-5 doi : 10.1109/$WCNC$49053.2021.9417348. URL: $https://ieeexplore.ieee.org/abstract/document/$9417348

  Aysenur Turkmen, Shuja Ansari, Paulo V. Klaine, Lei Zhang, Muhammad A. Imran. IMPRESS: Indoor Mobility Prediction Framework for Pre-Emptive Indoor-Outdoor Handover for mm-wave Networks. IEEE Open Journal of the Communications Society 2, 2714-2724 doi: 10.1109/OJ-COMS.2021.3133543. URL: https://ieeexplore.ieee.org/abstract/document/9642053

- The last contribution chapter of this thesis is in the pipeline for a journal paper submission. **Aysenur Turkmen**, Yihong Liu, Lei Zhang, Muhammad

A. Imran. IRS Assisted Handover for Next Generation Networks. IEEE Open Journal of the Communications Society is to be submitted.

Chapter 2

Literature Survey

In the next generation of cellular communications, 5G, one of the biggest technological improvements in terms of radio access network (RAN) is the use of massive MIMO (multiple-input multiple-output) and mm-wave to provide the increase in capacity [32]. However, using mm-wave has a serious issue with penetration losses due to the physical nature of high-frequency radio communications with shorter wavelengths. To resolve this issue, $5G$ will rely heavily on small cells (SCs) to provide indoor connectivity at mm-wave frequency bands [2], and this opens up new research directions regarding the interface between indoor and outdoor networks, such as intelligent handover (HO) techniques. This chapter presents an overview of mm-wave important parameters and characteristics, followed by a literature survey on recent studies that simultaneously consider outdoor and indoor coverage.

2.1 Millimeter-Wave Cellular Communication

Microwave bands, whose spectrum ranges from 300 MHz to 3 GHz, become limited due to explosive use of the sub 3 GHz band for wireless communications [33, 34]. To deal with the increased demand for traffic and capacity, $5G$ will exploit mm-wave technology, with a wavelength spectrum ranging from 1 to

100 mm [35]. This is particularly interesting as this portion of the spectrum has very large bandwidths with several unused bands. Fig. 2.1 pictures the massive spectrum availability in mm-wave, as presented in [2].

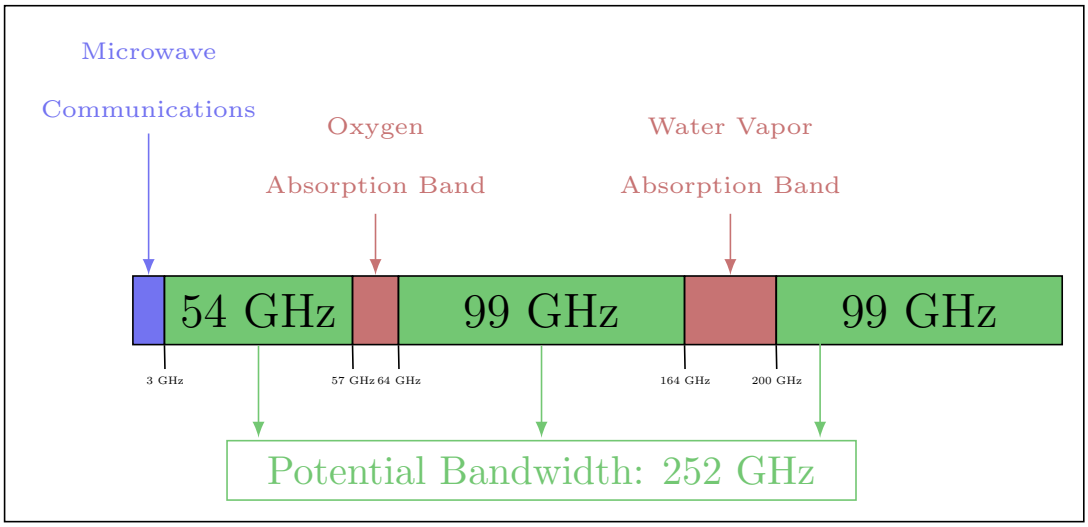

Figure 2.1: Spectrum availability of mm-wave.

Several fundamental characteristics of mm-wave are briefly discussed in the following section.

High Atmospheric Attenuation: The small wavelengths of the mm-wave spectrum are prone to serious attenuation since oxygen and water vapour in the atmosphere absorb their electromagnetic energy. Despite having two absorption spectrum bands, as shown in Fig. 2.1, mm-wave still has a much broader spectrum when compared with the microwave. From the average atmospheric attenuation of the mm-wave graph obtained in [2], the highest attenuation of oxygen absorption is around 15 dB/km for the 57–64 GHz band, and water vapour absorption has its highest attenuation between 164 and 200 GHz. This makes those frequency bands undesired for outdoor applications, resulting in a large spectrum portion, at 60 GHz, being seldom used and license-free.

Higher Propagation Losses: It has long been known that the free-space path loss line-of-sight (LOS) communication is proportional to the square of the carrier frequency, as evidenced by [36]. Thus, it is clear that mm-wave frequencies

have higher propagation losses when compared with microwave communications. For instance, the propagation loss at 60 GHz is 28 dB higher than that for 2.4 GHz [37]. For the non-line-of-sight (NLOS) cases, attenuation is also more notable when higher frequencies are deployed. For instance, the attenuation is around 17.7 dB at sub 3 GHz, whereas it reaches 175 dB at 40 GHz for concrete [38], [39]. In the presence of foliage, there is another high propagation loss, properly named foliage loss, represented by the empirical formula [40]

$$L_{\mathrm{f}} = 0.2 f^{0.3} R^{0.6}, \tag{2.1}$$

where L_{f} is the foliage loss in dB, f is the carrier frequency in MHz, and R is the foliage depth in meters, developed by Marcus and Pattan.

[2] calculated the foliage loss from Eq. (2.1) for foliage depths of less than 400 m and frequencies from 20 GHz to 95 GHz. For instance, when comparing 5 m and 30 m foliage depths at 70 GHz, L_{f} is around 15 dB and 44 dB, respectively. Therefore, it is clearly seen that foliage loss has a severe effect when the foliage depth increases.

2.2 Indoor Coverage in mm-wave

As previously mentioned, mm-wave suffers from high propagation loss as they have higher frequencies. Moreover, different materials have various effects on penetration loss. Therefore, penetration loss should also be considered depending on the material type and thickness, particularly when the mm-wave is utilized. Table 2.1 compares the penetration loss of some building materials at certain frequencies.

As mm-wave is not fully capable of penetrating through these in-building materials, mm-wave nodes should be separately specified for indoor and outdoor usage. Otherwise, propagation could suffer from huge penetration losses, negatively affecting data rates and spectral and energy efficiencies when the outdoor mm-wave base station (BS) is deployed to serve indoor and outdoor users. Since covering indoors by deploying various small outdoor BSs would be ineffective, utilizing SCs indoors is a more legitimate approach since the former costs more for mobile network operators (MNOs) instead of deploying more cells to increase the coverage and overcome the path loss issue. Some examples of SCs are pico and femto, which will be presented in the following subsection.

2.2.1 Indoor Deployment of Small Cells

The efficient deployment of mm-wave SCs for indoor management is one of the important uses of SCs, as most have a cell size with a several hundred-meter radius. They are named according to their coverage areas, ranging from smallest to largest, and some typical SCs are femtocells, picocells, and microcells.

Types of Small Cells for Indoor Coverage

Femtocells are connected to their own wired backhaul and are mostly user-deployed, low-cost, and low-power BSs to improve the quality of coverage in small sites such as a home, office or even a dead zone within a building. Some

Table 2.1: Penetration loss of materials.

Material	Thickness	Penetration Loss (dB)						
	(cm)	$\leq$ 3GHz[†]	5GHz[‡]	8.5–9GHz[††]	28GHz[‡‡]	40GHz[*]	60Ghz[**]	73GHz[***]
Brick	-	-	14.5	-	-	-	-	-
Brick	10	-	-	-	28.3	178	-	-
Brick	185.4	-	-	-	28.3	-	-	-
Drywall	2.5	5.4	-	-	6.8	-	6	-
Wood	0.9	5.4	-	-	-	3.5	-	-
Tinted glass	3.8	-	-	-	40.1	-	-	-
Clear glass	0.3	6.4	-	-	3.9	2.5	3.6	-
Clear glass	0.5	-	-	0.3	-	-	-	-
Clear glass	1	-	-	-	-	-	-	7.1
Mesh glass	0.3	7.7	-	-	-	-	10.2	-
Concrete	2.5	-	-	1	-	-	-	-
Concrete	10	17.7	-	-	34.1	175	-	-
Particleboard	1.25	-	-	0.3	-	-	-	-
Plywood	$\sim$1.25	-	-	-	2	3	-	5
Whiteboard	1.9	0.5	-	-	-	-	9.6	-
Whiteboard + wall	21.4	-	-	-	-	-	-	73.8
Closet door	7	-	-	-	-	-	-	32.3
Steel door	5.3	-	-	-	-	-	-	52.2

[†] [35, 39, 41]
[‡] [42]
[††] [43]
[‡‡] [2, 39, 44, 45]
[*] [2, 45, 46]
[**] [41]
[***] [45, 47]

benefits of using femtocells are given below:

1. Femtocells could provide better capacity than macrocells because of their proximity to the end users. Macrocells usually have coverage radii of several kilometres. They thus may incur in worse signal-to-noise ratio (SNR), as the SNR is inversely proportional to the distance between the transmitter and the receiver.

2. Offloading indoor traffic to the femtocell instead of operating them from outdoor macrocells would assure more RAN resources for mobile users since those users would not have to be served by the same portion of the spectrum as the ones connecting to the macrocells.

3. Operational expenditure and capital expenditure (OPEX/CAPEX) for MNOs will be reduced by deploying femtocells since urban macrocells have additional costs for site lease, equipment, engineering works, and electricity and backhaul cabling. Further details on OPEX and CAPEX costs for macrocells can be found in [48], where the authors compare the cost in terms of installation, site lease, equipment, Operational and Management power, and total costs.

4. Femtocells are easy to deploy, as they do not require expert knowledge and can be "commissioned" by the end user in a plug-and-play manner.

5. Femtocells are much more environmentally friendly than macrocells since they can be operated on demand, then they can be easily turned off to reduce energy consumption when there is no need to use them, such as out of hours in offices or when the user is not at home. Moreover, intelligent algorithms could be used for deciding when the femtocell should be operating, as in [49].

As mentioned above, operating femtocells for indoor traffic instead of operating them from an outdoor BS is very efficient in lowering the expenses and ease of

installation and giving mobile users more capacity and quality of service (QoS).

Picocells are the second smallest cell type with a typical cell radius ranging from 100 to 300 m. Deployment of the picocells is done by the MNOs, who are also in charge of the site rental payment and maintenance of the cell. They can enhance poor coverage in a building, such as an office floor or retail space [50]. However, their slightly higher coverage radii can cause interference in a small footprint area. Moreover, compared with femtocells, picocells would cost more because of installation, maintenance and site lease. In contrast, femtocell gives full plug-and-play features to its users, including self-configuration and no extra payment for site leasing. Since maximizing the coverage area by increasing cell radii results in a capacity reduction, femtocells would be a better choice for indoor deployment when compared with picocells, which could suffer more from shadowing effects as shown in Fig. 2.2.

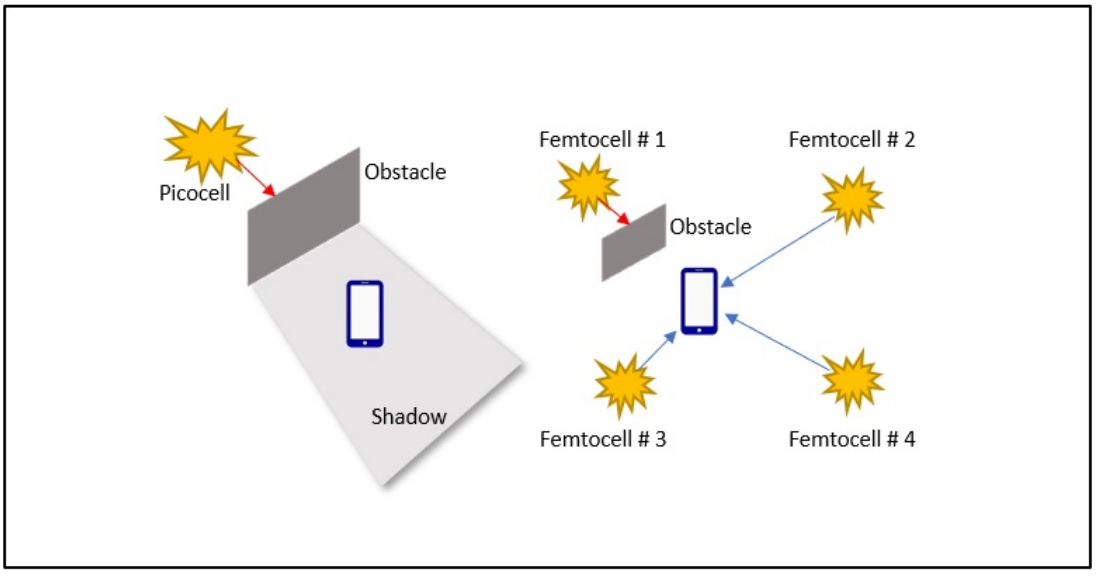

Figure 2.2: Illustration of shadowing effect on picocell and femtocells.

Macrocells will be discussed in Section 2.3.

Use-Cases of Indoor Coverage

Improving the quality of everyday life is the main driver behind today's Internet of Things (IoT) systems. Smart homes are one of the potential applications of the IoT, where home sensors such as temperature controllers, smart meters, light and security camera controllers, and high-stream multimedia services are deployed within people's dwellings. Some of these applications and services will require very high data rates. The need for higher data capacity would be enabled by deploying mm-wave SCs within buildings. In [51], the IOLITE smart kitchen scenario was given as a beyond $5G$ example to evaluate the challenges of IoT over smart home technologies, and some technological enablers were addressed to overcome the challenges.

[52] proposed improving wireless communication coverage, increasing data transfer rates, enhancing jamming and solving interference problems by the establishment of a cross-media mesh network with the help of several dual-media transceivers for wireless sensor and actuator networks (WSANs) and energy management systems (EMSs) for smart home and also smart grid applications.

The challenges and the research issues of 60 GHz networking on a system level were reviewed by [53] from the perspective of wireless local area networks for future home networks. Their study comprised use-case scenarios with cell-based and ad-hoc-based home network communication infrastructures.

To improve coverage and provide a seamless transition between home and office rooms at 60 GHz, the radio-over-fiber technique (RoF) was proposed [54], where all distributed antennas in different rooms are connected to the central station with fiber cable. However, the popularity of this topic has decreased over the years. In the IEEE database, between 2004 and 2016, there were 146 conferences, 53 journals and magazine papers. In contrast, between 2017 and 2019, there were 11 conferences and 7 journals and magazine papers about RoF home networks, meaning that the number of papers per year has decreased to less

than half for the past three years. The extended cell (EC) concept was introduced in [55] to overcome the corner effect and seamless transition and evaluate the deployment of the RoF technique.

Despite being a complementary technology to mm-wave, fiber-to-the-home has a high cost because of the expensive RF components utilized. Replacing these costly components with CMOS technology might minimize the cost. In [56], the authors designed a 40 GHz power amplifier using a 130 nm RF CMOS process for the remote antenna unit transceiver of an mm-wave RoF system to enable the feasibility of RoF by low-cost CMOS amplifier. A similar transmitter was developed for a 60 GHz by using a 90 nm CMOS process in [57].

To maintain indoor connectivity at 60 GHz, [58] employed relay nodes to improve the quality and robustness of 60 GHz links. Their simulation results showed a 33% reduction in the path loss when the relay node is deployed. Furthermore, there is also another candidate to maintain network connectivity by deploying physical reflectors, [59], who deployed mirrors as a virtual relay to forward signals for the indoor environment at 60 GHz links and, based on simulation results, their proposed scheme showed improvements on the robustness of link connectivity at 60 GHz.

The studies on enhancing mm-wave coverage using passive reflectors are also limited in the literature thus far. The robustness of 60 GHz for indoor coverage was investigated in [60] by analyzing obstacle density, the reflective surface availability and the influence of access point positions. Their simulation results show that a transmitter's average transmission loss was between 15 dB and 20 dB, including power loss on the reflective surface and the extra path loss caused by longer transmission paths. The authors claimed that 60 GHz indoor network coverage depends solely on the reflections in non-line-of-sight (NLOS) scenarios. To enhance the mm-wave coverage for an NLOS indoor scenario, passive metallic reflectors with different shapes and sizes were studied in [61]. They observed a median gain of 20 dB power gain at 28 GHz, from a square metallic reflector

compared with the no reflector scenario.

2.3 Outdoor Coverage in mm-wave

The outdoor coverage is mostly broken down into two terms, macrocells and microcells. Typically, the former is used when the focus is coverage area, while the latter is generally chosen for its capacity. *Macrocells* are designed for the immense coverage area, up to a few kilometres cell radii with a typical transmit power ranging from 20 W to 160 W [62]. *Microcells* are the second-largest BS type, having a typical cell radius between 250 m and 1 km while providing standardized interfaces over the backhaul and, simultaneously, having a transmit power lower than the macrocell BSs.

The next-generation communication concept of enabling high-capacity connection everywhere and every time to its users would not be possible with the micro-wave BSs using lower frequencies. However, as discussed before, using higher frequencies brings some problems prone to high penetration and path losses. Therefore, to bring seamless coverage in the outdoor environment, $5G$ cellular architecture will also continue to deploy heterogeneous networks since macrocell's immense coverage area would not enable the high capacities required for many users.

2.3.1 Heterogeneous Network Planning

Current macro BSs designed to provide a broad coverage area need to meet the expectations of higher data rates and outstanding quality of experience (QoE), typical of $5G$ use cases. Therefore, an integrated heterogeneous network deploying micro, pico and femto cells under the macro BS umbrella will continue to drive the next-generation cellular networks. Fig. 2.3 gives a clear image of a typical heterogeneous network deployment.

Since $5G$ will encourage the SCs to utilize mm-wave, wherein a vast amount

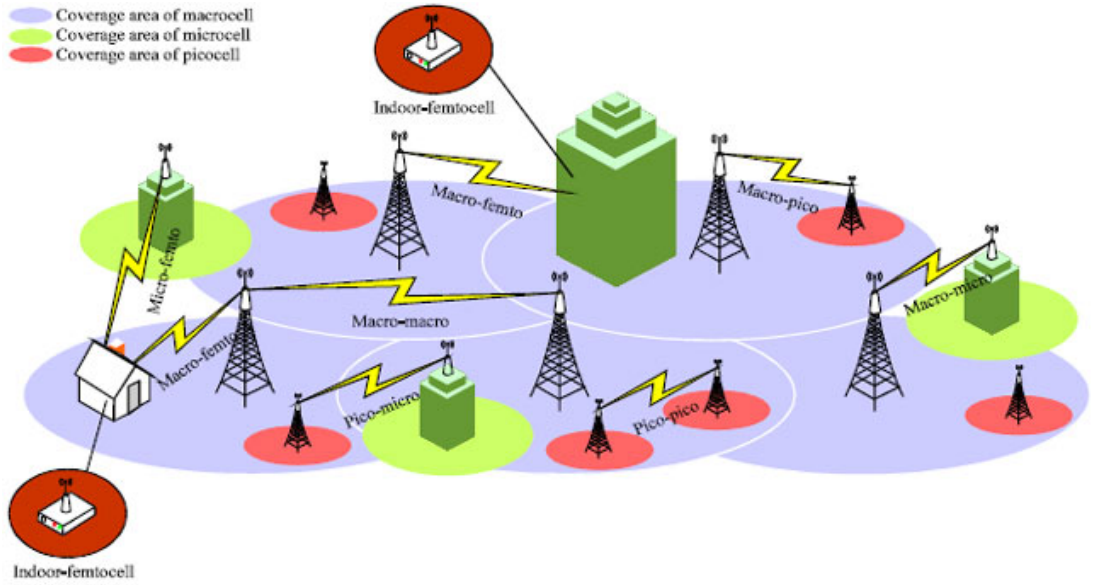

Figure 2.3: A typical heterogeneous network deployment.

of spectrum is available, the number of SCs will increase to stabilize the mm-wave coverage, which is very vulnerable to penetration losses. This may lead to some challenges in heterogeneous networks, such as green backhauling, HO strategies, on-off SC policy and several others. With $5G$, 80% of the SCs are expected to use wireless backhaul connection to reduce the cost of fiber-based backhaul in a densely deployed heterogeneous network [63]. [64] addressed the wireless backhaul problem in SCs in the mm-wave band by proposing a joint transmission scheduling scheme for the radio access by proposing the D2DMAC scheme, which enables device-to-device transmissions for performance improvement by using a path selection criterion.

Another promising approach to meet the demands of $5G$ is ultra-dense networks (UDN), which present a viable strategy to tackle the more demanding applications, such as high-definition video streaming, augmented reality, and cloud computing [65]. The idea of densely deploying SCs in hot spot areas, where more capacity and bandwidth are needed, recently became a very popular topic, as seen in the Mobile and wireless communications Enablers for Twenty-twenty (2020) Information Society (METIS) reports [65, 66].

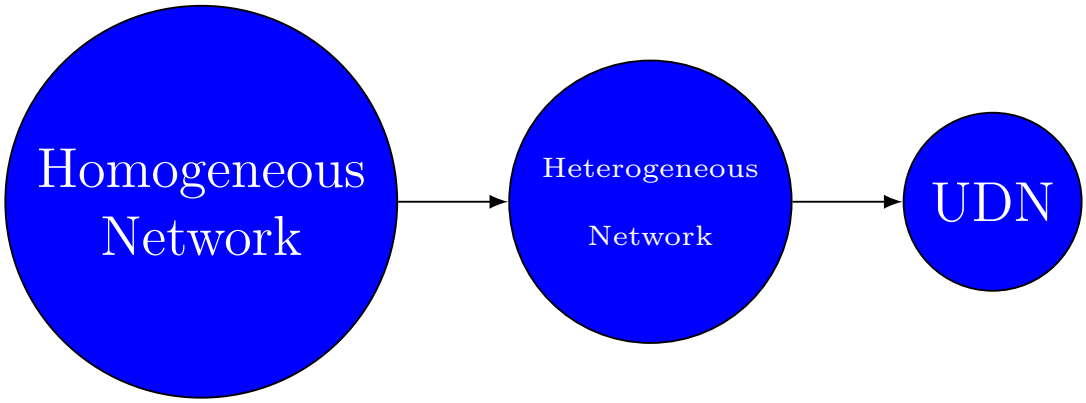

Figure 2.4: Homogeneous network evolution towards UDN.

Fig. 2.4 pictures the paradigm shift of the network towards UDNs. The radius of the circles getting smaller represents the move from very large footprints to small coverage areas. There are two common definitions of UDNs in the literature; one defines UDNs as networks whose number of cells exceeds the number of active users [67,68], while another definition provides a quantitative measurement where the cell density is greater than 10^3 cells/km^2 [69].

2.3.2 Handover in mm-wave Communication Systems

Handover management in mm-wave communication systems is an important subject, which needs to be addressed properly. As shown in Fig. 2.5, to cover the same building, the mm-wave antenna needs to be installed in nearly all rooms, since it has a smaller coverage footprint than conventional networks [6].

Users' mobility in this small size of coverage area would trigger several handovers [71], which may cause the total number of handovers to increase during a call (ping pong effect). As seen from Fig. 2.5 a), in previous networks, such as GSM, UMTS, 802.11 WLAN, and LTE, there is adequate time for the initiation and completion of a handover successfully, as overlapping areas between cells are quite large. However, with greater frequencies in mm-wave systems, the coverage size decreases rapidly. Thus, the overlapping area gets smaller. Mainly in an indoor environment, overlapping areas typically occur around open spaces

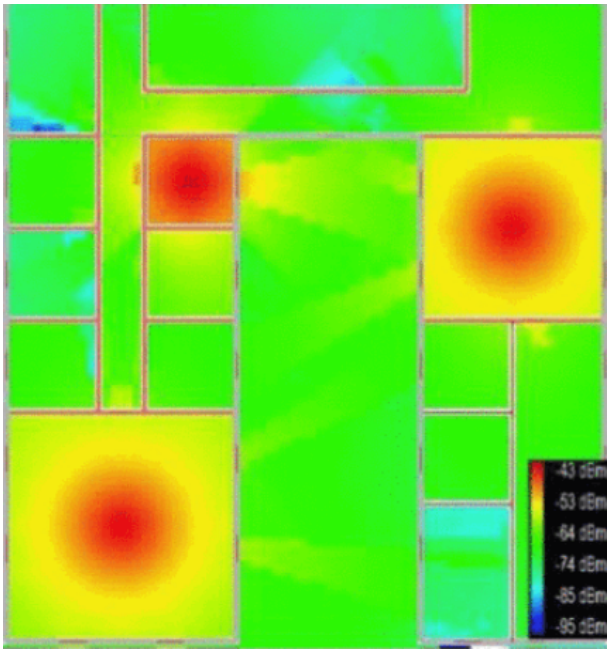

(a) 2.4 GHz

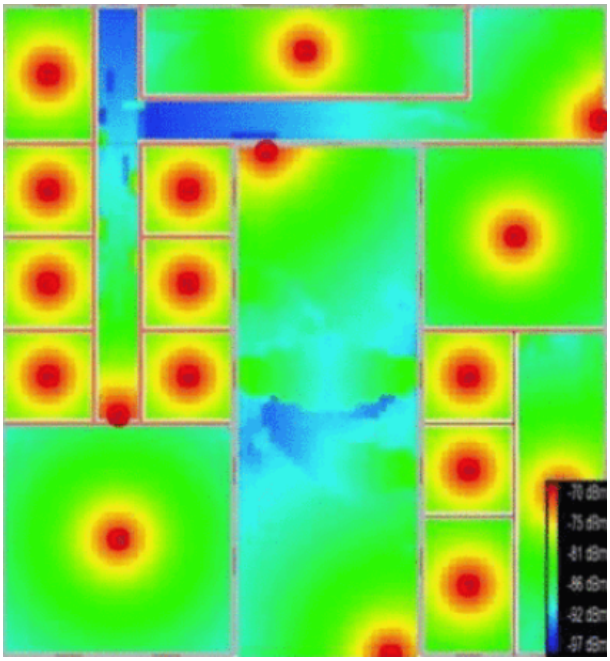

(b) 60 GHz

Figure 2.5: Coverage of the same building with 2.4 GHz and 60 GHz [70].

such as doors and windows. For instance, once a UE leaves a room through a door, the UE can make a sharp turn, turning left or right. In this case, a handover may not be completed successfully if not detected early enough since the overlapping area might be too small to allow the UE enough time to complete a handover. This phenomenon is called the corner effect, and it needs to be taken

into consideration, especially in higher frequencies.

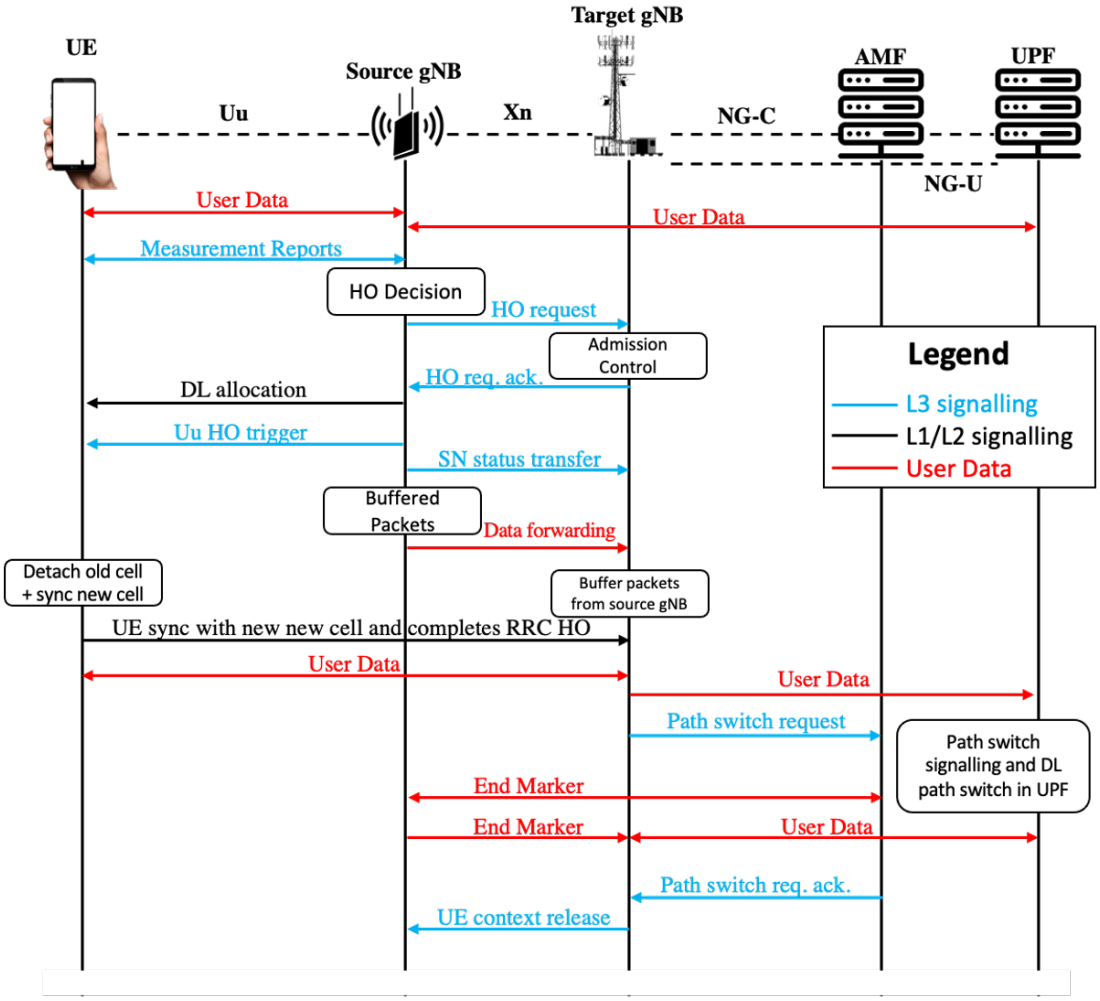

Figure 2.6: Handover in 5G NR.

Fig. 2.6 demonstrates the basic handover procedure in New Radio (NR), the latest radio access technology developed by 3GPP for the 5G mobile network [72]. There are two types of NG Radio Access Network nodes connected to the 5G core network that are gNB and ng-eNB. A gNB supports NR control-plane and user-plane protocols to the NR devices and, an ng-eNB uses the LTE control-plane and user-plane protocols to serve the LTE devices [73]. The procedure begins by checking if a UE needs a handover and follows:

1. By sending measurement reports to the source gNB.

2. The handover decision is made in the serving gNB, using RRM (Radio

Resource Management) information and the measurement report.

3. The handover request message, including the required data for preparing the HO at the target BS side, is sent from the connected gNB to the target gNB.

4. Admission Control procedure will be performed in this step if the target gNB can grant the resources.

5. The target gNB sends a handover request acknowledgement message to the serving gNB, and the forwarding of data can be initiated once the serving gNB receives it.

6. UE receives the handover command from the serving gNB.

7. The Sequence Number (SN) message is sent from the serving gNB to the target gNB to keep track of the ordering of the packets.

8. The UE disconnects from the serving gNB and synchronizes to the target gNB.

9. The target gNB informs AMF that UE has changed the cell via the Path Switch Request message.

10. NR core shifts the DL data path towards the target side.

11. The path switch request acknowledgement is sent by the AMF to the target gNB.

12. The serving gNB receives successful handover information from the target gNB, and activates the release of resources via UE context release message.

The radio resources related to the UE are released eventually by the serving gNB [74].

2.3.3 Cell Range Extension

The RSRP plays an essential role in determining a handover (connected mode) and conventional cell selection (idle mode) since the decisions are based on it [75]. The mobility modes will be discussed more in detail in the following Section 2.3.4. In a heterogeneous network environment, macro cells have higher transmit power up to 16 dB than SCs [76]; therefore users inherently choose macro cells over SCs, when assessing the downlink reception. However, this situation would make SC implementation redundant, and the resources of SCs would not be fully exploited, which may cause overloading on the macro cells. In order to cope with the problem, a cell range extension, CRE, is presented in [77], where a bias value is added to the received signal of SC. Thus, SC coverage is increased virtually, and more UEs can make a connection to the picocells, resulting in offloading on macro BSs [78], as described by

$$({w_p}^{pilot})_{dB} + (\Delta_{\text{bias}})_{\text{dB}} > \ ({w_m}^{pilot})_{dB}, \tag{2.2}$$

where $(\text{w}_p^{pilot})_{dB}$, $(\text{w}_m^{pilot})_{dB}$, and $(\Delta_{bias})_{dB}$, are the decibel value of the pilot signal from pico and macro BSs, and bias value respectively, [79].

2.3.4 Radio Access Mobility in mm-wave

The UE is not engaged in an active data connection in Idle mode, but it must still be reachable via signalling (paging) through an appropriate cell. Paging is a method of broadcasting a brief message across the entire service area, typically in a multicast fashion by multiple BSs at the same time [80]. The paging channel is monitored by the UE for incoming service requests as well as the cell (re-) selection process. To check and synchronize the network's paging messages, the UEs 'wake up' periodically. When a paging message is received, the UE connects to the BS operating the cell where the UE is camped. The UE changes to a Connected

state after a successful connection using a random access technique [81]. Cell (re-)selection occurs only when the UE is in Idle mode. It is a way of changing to camp on a more appropriate cell than the currently selected cell to receive future paging messages successfully. Idle mode and cell selection criteria help the UE to determine the suitable cells whose measured attribute meets the SS/quality selection criteria (coined as s-criteria) for the cell selection procedure. In case there is not a suitable cell available, an *acceptable* cell will be identified. In this case, the UE will camp on that acceptable cell and begin the cell reselection procedure. Furthermore, a UE in Idle mode will try to reduce battery power consumption. This is accomplished through a technique known as Discontinuous Reception (DRX), in which the terminal disconnects its receiver and enters a low-power state. To be able to receive the paging indications, the terminal will 'wake up' periodically with wake-up intervals, also known as DRX cycles, such as 0.32s, 0.64s, 1.28s and 2.56s in LTE [82]. The purpose is to minimise paging reception interruptions during the cell reselection operation. Notably, unlike in Connected mode, the UE can decide on cell reselection independently, and it is not necessary to report measurements or events to the network. When camping on a cell, the UE must regularly look for a better cell using the cell reselection criteria.

The centralized entities keep the UE's approximate location information (MME in LTE, AMF in NR) in Idle mode. This location is identified for each collection of cells designated as a tracking area (TA). A TA list (TAL) was introduced in 3GPP Release 8 to minimize the frequent registration during the ping-pong effect and lower the signalling overheads of location management. In this design, each UE may contain a list of TAs rather than a single TA. Until it goes to a cell that the TAL does not cover, the UE keeps the TAL [83].

In addition to the aforementioned mobility states of a UE, a new mode that falls between Idle and Connected modes is introduced by NR, called Inactive_mode. Once the UE is turned on, it goes into Disconnected mode/Idle

mode, and it can move to Connected mode with initial attach or connection establishment. Whenever there is no activity from the UE for a brief period, it can suspend its session by switching to Inactive_mode and resume its session by switching to Connected mode. The goal of this state is to shorten the time it takes to bring the UE into the Connected state while minimizing signalling overheads and enhancing the UE battery life [84].

In contrast to cell (re-)selection, HO occurs when a user switches from one BS to another while actively engaged in a data session or phone call. The user switches its serving cell during an active connection. High signalling overheads among BSs and small cells are the cost of seamless communication [85]. As a result, mobility directly impacts data session performance since data transmission may be interrupted owing to a change in serving BS and high signalling overheads, reducing throughput, latency, and so on.

One of the most difficult challenges in NR is ensuring mobility robustness while reducing service disruption. As the cell size gets smaller, there are three key challenges raised in NR. Frequent handover is the first, which causes an increase in the handover failure rate. The second one which lowers the mobile user's battery life is an increased number of intra/inter-frequency measurements. The third is increased overheads caused by frequent HO at mm-wave/microwave frequencies, which might limit frequency resources for static users.

The entities and interfaces involved in the NR network architecture shown in Fig. 2.7 are the following: *gNodeB (5G NodeB)*: To service NR UEs, the gNB uses NR user-/control-plane protocols and is connected to the 5G Core Network (5GC) via the NG interface and to other gNBs via the Xn interface. Some aspects of the user mobility in the connected mode are handled at the gNBs; such as receiving the measurement report sent by the UE, deciding whether a HO is needed, requesting the target gNB/eNB for admission control, and others. The 5GC has a service-based architecture, allows network slicing, and divides the user and control planes. The *User Plane Function (UPF)* serves as a gateway between

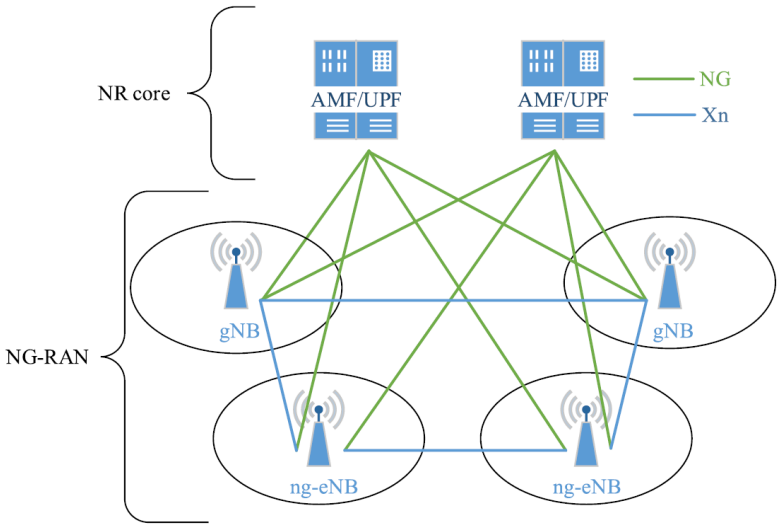

Figure 2.7: Overall Architecture of NR [84, 86].

the RAN and external networks. It is in charge of packet routing, forwarding, and inspection, as well as handling QoS and maintaining traffic measures. The following are the *Control Plane Functions (CPF)*. The *Session Management Function (SMF)* manages and establishes sessions, assigns IP addresses to UEs, supports roaming, and regulates the UPF. The *Access and Mobility Management Function (AMF)* handles reachability, location services, mobility, connection and registration. The *Xn* interface interconnects gNBs and ng-eNBs and carries control information messages. HO preparation and HO signalling messages between the target and source gNBs/ng-eNBs are carried by this interface during Xn-based HO. The connection between gNBs and ng-eNBs to the NR core network is done by using *NG* interface. More particularly, the *NG-U* interface connects gNBs and ng-eNBs to the User Plane Function (UPF), while the *NG-C* interface links gNBs and ng-eNBs to the Access and Mobility Management Function (AMF).

The HO cases in NR mobility architecture with the correspondent interfaces as specified in [87] are depicted in Fig. 2.8, which can be defined as:

- **Intra-gNB HO:** As shown in Fig. 2.8, this HO occurs when both the target and source cells belong to the same g-NB.

- **Inter-gNB HO:** This HO occurs when the target and source cells are

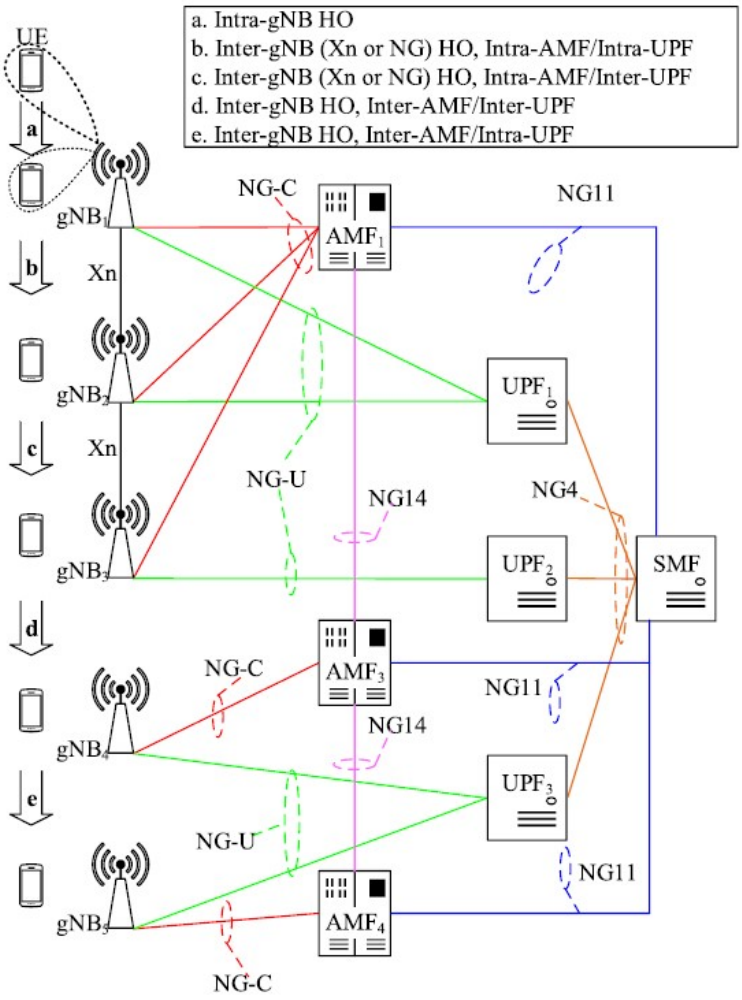

Figure 2.8: NR mobility architecture along with relevant interfaces and HO use cases [84, 86].

different gNBs. In this HO, AMF is assumed to not change (i.e. intra-AMF). Furthermore, the UPF might (intra-UPF) or it may not (inter-UPF) be migrated, depending on the established physical deployment, as shown in Fig. 2.8 (c) and Fig. 2.8 (b), respectively.

- **Inter-gNB HO with AMF Change:** In this HO occurs with the change of AMF. In this event, only the NG interface (not Xn) will be used. Furthermore, the UPF may (intra-UPF) or may not (inter-UPF) be migrated, depending on the established physical deployment, as shown in Fig. 2.8 (e) and Fig. 2.8 (d), respectively.

2.4 Self Organized Seamless Coverage

Indoor and outdoor coverage characteristics of mm-wave communication were discussed in Section 2.2 and Section 2.3, respectively. This section will introduce how the concept of self-organized networks (SON) can help in providing indoor-outdoor seamless coverage, where users do not experience any service disruptions during the switch between different networks and/or BSs/access points.

2.4.1 Self-Organized Networks

SON is a concept that helps wireless communication networks be more agile, dynamic, and efficient. It offers network automation, where the networks become capable of taking action to adapt themselves to an environment-of-interest [88]. Eliminating human intervention lies at the heart of the SON concept owing to the fact that the more human intervention networks include, the more cumbersome, costly, and time-consuming they become. As such, in SON, the networks can decide and act according to the current conditions and/or past experiences, making them intelligent and adaptive [89]. Given the stringent requirements of $5G$ networks, including peak data rates, end-to-end latency, and spectral efficiency [90], it has been a self-evident truth that intelligence is no more a luxury for wireless communication networks, but a necessity. Even though the peak data rate targets of $5G$, for instance, are addressed by designating mm-wave frequencies in $5G$ new radio (NR) [91], new challenges arise, such as mobility and power consumptions [92], that are quite difficult to be dealt with inefficient conventional methods employed in the legacy networks. Therefore, self-organization seeks not only a higher level of QoS but also sustainable businesses for mobile network operators since their capital and operational costs can be significantly cut down with the help of self-organization [88].

It is reported in [88] that three integral characteristics constitute the SON concept: 1) scalability, where the prospective SON-based solution should result

in minimal complexity; 2) stability, where the proposed solution converges/adapts to the final/intended state in a reasonable period; 3) agility, where the solution is reactive to the environmental alterations. Furthermore, based on the objectives of the developed solutions, SON can be investigated in three main subcategories, namely self-configuration, self-optimization, and self-healing [88, 89]. In self-configuration, system parameters, such as frequency allocations and neighbour lists, are configured for new BS deployments and/or changing conditions, including network upgrades and failures. Once the self-configuration phase gets the system working, the self-optimization phase ensures that the network is continuously optimized regarding mobility, resources, energy consumption, coverage, etc. Although self-configuration is essential in having a network operational, self-optimization is vital in making the entire process efficient and sustainable. Lastly, the self-healing phase takes the stage when the system has a fault. In this regard, the system is continuously monitored to automatically detect outages/failures. In addition to detecting, self-healing should also diagnose and take care of the problem to revert the system to its operational condition [89].

2.4.2 Seamless Indoor and Outdoor Coverage

In the previous sections, indoor and outdoor coverage were discussed separately. From this section onwards, outdoor-to-indoor (O_2I) and indoor-to-outdoor (I_2O) papers will be surveyed to address the seamless transaction between two environments. Several works in the literature rely on ML techniques to provide better performance in the context of O_2I or I_2O systems. Thus, for the reader's benefit, a brief summary of some important ML techniques is included before the O_2I and I_2O literature discussion.

Machine Learning in Mobility Prediction

Several ML techniques used in mobility prediction are introduced in the following subsections. These techniques are used to improve prediction accuracy as well as enhance network performance.

The techniques below are almost always used for outdoor mobility management; however, they could be tweaked and adapted to particular indoor/outdoor seamless HO constraints and solve problems from that particular use case.

Markov Models Markov models are a stochastic process mainly used in randomly changed systems. The Markov property refers to the memoryless property of a stochastic process, which means the probability of future states depends on the current state rather than the previous state [23]. In cellular networks, Markov chains and Hidden Markov Models (HMM) are the most common ones used among the various different Markov models. The former one is mainly chosen when the observability of the system states is fully visible; the latter one is preferred when system states are not fully visible [89]. From the mobility prediction perspective, HMM enables better predictions since the number of lost information is lesser than the Markov chain. Moreover, deploying HMM in a mobile node would enable the system to learn the environment and then update the information. However, computation complexity caused by hidden states should also be considered in the case of deploying HMM [23].

Artificial Neural Networks Artificial Neural Network (ANN) models are inspired by the human brain, which could resemble a complex machine, constantly performing non-linear and parallel computations. The model can handle the functions that have a large number of inputs [93]. ANN is popular for its flexible and self-organization characteristics. In [94], the user's next location predicted a simple road model built to predict the user's next BS connection by employing RSS distribution, where the results gave an accuracy of over 98%.

Bayesian Networks Bayesian networks are a family of probabilistic graphical models that a set of random variables, and their conditional dependencies are represented by a directed acyclic graph [95]. Its great ability to resolve uncertainty and make correlations between different variables in a complex environment makes Bayesian networks applicable in many fields, such as from user movement historical data; the probability of a user's presence at a specific place can be computed using Bayesian networks. This model can be incorporated with other models to boost its prediction performance. In [96], Bayesian networks combined with the neural networks for predicting locations on cellular networks, in which results show that the hybrid Bayesian neural network model outperformed compared to other standard neural networks. In a complicated cell environment such as UDN, constructing Bayesian networks would cause difficulties since the system models conditional dependence by edges in a directed graph [23].

Outdoor to Indoor

O_2I coverage and measurements are important for developing a suitable propagation model, measuring possible indoor coverage achieved by outdoor nodes and addressing its interference effect on indoor nodes. O_2I coverage relies on penetration and reflection of mm-wave signals through different materials situated in the office/residential buildings, for instance, wood, glass, and concrete [97]. An extensive study of the O_2I interface, including the effects of the different materials, was given in [98]. To evaluate the feasibility of O_2I coverage in mm-wave, measurements were performed in [97] for 29 and 61 GHz bands, where authors stated that penetration loss and reflection response are functions of frequency, material property, polarization and incident angle in the O_2I coverage scenario.

Moreover, in [99], an experimental study was performed at 28 GHz for O_2I propagation. To attain narrow-band measurements, a transmitter (TX) was placed within an office on the top of a neighbouring building 70 m above the receiver (RX). The study examined path loss through both coated glass and stan-

dard window glass. Results indicated that coated glass has significant penetration loss, and from obtained measurements O_2I coverage loss varies between 3 dB and 60 dB, depending on the location of RX as well as the material type constructed in the building. In [100], narrow-band building penetration measurements at 28 GHz were conducted in New Jersey suburban residential area deploying fixed wireless access technology. To differ building penetration loss from outdoor path loss, a *common-slope cross-comparison* approach was proposed, and measured building penetration loss was found to vary from 9 dB to 17 dB, depending on the building type. Similarly, [101] studied a fixed wireless access scenario at 28 GHz to examine the effects of O_2I penetration on the wireless propagation channel characteristics in an urban area. The measurements were executed using a real-time channel sounder and reported a mean average loss of 22.7 dB for the multi-story brick building and 10.6 for the wood-frame single-family home. Penetration loss measurements for internal and external walls at various carrier frequencies ranging from 0.8 GHz to 28 GHz with narrow-band signals were performed, and an empirical multi-frequency O_2I path loss model was presented in [102]. The authors in [103] proposed that the effects of O_2I propagation on the direction of arrival and delay spread statistics are progressively influenced by the floor plan and the relative area of the building with respect to the structures in lieu of its building materials.

Although the trend in most of the present literature on O_2I coverage focuses on measurements at 28 GHz, other studies also explore various mm-wave frequencies for O_2I propagation. The O_2I transmissions at 10, 30, and 60 GHz were analyzed in [104] for two types of building scenarios, namely *old* and *new* which were presumed as consisting of 70% concrete walls and 30% glass windows in the former scenario, and for latter one assumed to made up 30% concrete wall and 70% infrared-reflective glass, which is a common insulation material in modern dwellings. Delay and angular statistics in the O_2I propagation scenario at 20 GHz were provided in [105] for one office building on different floors using a channel

sounder. [106] modeled O_2I path loss characteristics based on measurements conducted for 0.8-3.7 GHz in an urban microcell scenario. [107] studied 3, 10, 17, and 60 GHz frequencies for an O_2I scenario and measurements for channel delay spread and path loss have been taken for different RX positions in various rooms. The results show that signal attenuation varies between 5 dB and 40 dB based on the room window material compound, where penetration loss is smaller, and thus the strongest signal component can get through. A measurement-based analysis of O_2I propagation at 3.5 GHz and its comparison were given in [108]. Similarly, [109] studied characteristics of mm-wave at 38 GHz-also in an O_2I measurement-based setup-, where line-of-sight propagation, transmission, reflection, diffraction, scattering, as well as polarization effects are in place. By its turn, [110] observed a significant increase in propagation path loss in the O_2I scenario while the frequency increased from 2 GHz to 60 GHz. An O_2I propagation measurement at 4.9 GHz was conducted in [111] using the unmanned aerial vehicle to observe building entry loss measurements in a high building. $5G$ channel models for bands up to 100 GHz and O_2I penetration loss comparison depending on materials constructed in the building were presented in [112]. More detailed information on mm-wave propagation models can be found in [113]. Important elements regarding $5G$ deployments of O_2I scenarios were reported in [114].

Indoor to Outdoor

The rapid development of modern and smart urbanisation led to more than 80% of people spending daily life in the indoor environment [27]. However, the study of O_2I propagation models, aiming at coverage extension of an outdoor transmitter to indoor receivers, receives much more attention in the literature when compared to the I_2O casework [29]. The work in [115] analysed I_2O wave propagation characteristics for a WLAN access point installed in an office, where computational simulation results showed that the path loss at 5.2 GHz was smaller than at 2.4 GHz. Measurement-based studies in [116, 117] stated that path loss and

transmission power mainly rely on the number of concrete walls the signal penetrates before the transmitted signal reaches the receiver. Additionally, indoor obstacles have shown notable effects on path loss based on the measurements conducted in [118] and [116]. [116] focused on the 3.5 GHz band and performed field measurements for I_2O propagation characteristics in residential areas where traditional houses are arranged in a line and I_2O propagation considering houses built out of wood. An empirical I_2O propagation model for residential areas was proposed in [119]. In-site measurements of reflection coefficients and penetration losses were conducted at 28 GHz in [120] for common building materials such as tinted glass, clear glass, brick, concrete, and drywall with the goal of designing the future mm-wave communication networks. Results revealed that I_2O penetration would be quite difficult at 28 GHz, because of the higher penetration losses of the strong reflectivity of external building materials. Furthermore, it was stated that interference could be reduced for frequency reuse by combining the lower penetration loss of indoor materials with reflective outdoor materials and highly lossy external glass and walls.

Knowing user localisations is extremely useful to provide a seamless transition from the I_2O environment. Global positioning system (GPS) is mostly used in outdoor localisation systems; however, performing indoor localisation by GPS is not a proper option since the satellite signals need LOS propagation and are blocked easily in the presence of obstacles. Therefore, localisation for an indoor environment is becoming a hot topic. [121] presented a comparison between the power consumption and accuracy of WiFi, Bluetooth low energy (BLE), Zigbee, and LoRaWAN for use in an indoor localisation system through trilateration and the Received Signal Strength Indicator (RSSI) values from each modality were used. An intelligent mobile terminal indoor positioning system based on Building Information Model (BIM) was proposed in [27]. [122] used the magnetic sensor, the light sensor, and the satellite signal integrated to navigate indoor/outdoor status. Their experimental results showed an improvement in indoor/outdoor

seamless position accuracy. Besides, detailed information on indoor tracking can be found in [123], in which indoor wireless tracking and mapping problems and solutions were surveyed.

The I_2O path loss model is crucial for the heterogeneous network simulations which cover indoor and outdoor environments. Path loss and shadow fading models in residential I_2O scenarios were proposed by [119]. The measurements were conducted for frequencies between 0.9 and 3.5 GHz from the two rooms of the house. The number of walls between the transmitter and receiver was also considered in the proposed frequency-dependent model. Despite the proposed work's uniqueness, the practicality of this study is limited since the case where the transmitter is further from the outer walls was not modelled. [124] used the same data set proposed in [119]; however, they extended the work by employing a different methodology called singular value decomposition (SVD) to determine empirical path loss models for the femtocell I_2O scenario. Two different I_2O path loss models were proposed in [125] using ray tracing alongside an analytic parametric model. The indirect propagation path loss was assessed in [126] to provide NLOS coverage at 60 GHz. Their path loss measurements showed that non-direct paths have a notable effect and could be deployed to extend the mm-wave coverage in the neighbouring room around the access point. In [127], the authors proposed a statistical model for the I_2O path loss. The work was conducted by simulating a large number of floor plans with a random first, then that plan was used to analyse the interference around the house, which was caused by the signal from femto BS inside the floor plan. Their approach consisted of choosing the optimal placement of the femto BS inside the created floor plan, showing that proper placement of the femto BS could reduce the mean interference by about 23 dB around the house.

Interference is one of the critical issues that should be addressed when the SCs are deployed under macrocells or microcells to increase the coverage and capacity. In [128], we studied the coverage probability of an indoor mm-wave

femtocell in the presence of interference from an outdoor mm-wave BS. The effects of different building materials, such as brick, concrete, glass, and wood, were also taken into consideration in a detailed system-level simulation. Moreover, we have also considered in our modelling the distance between the BS and the building and the BS transmit power. Given the emerging applications of mm-wave technology in wireless communication, especially in providing indoor coverage, such a study will provide useful insights into its expected performance trends. [62] proposed an empirical I_2O path loss model to assess the femtocell BS interference impact on macrocell users. Exhaustive measurements were performed in [118] to investigate I_2O signal propagation and analyse the interference in future $5G$ networks with femtocell overlaying microcells. [29] presented a generalised I_2O propagation model in order to achieve a unified model for the interference in $5G$ networks with femtocells underlying macrocells.

Studies in the direction of self-organised HO from I_2O environments are very scarce despite the growing trend of indoor communications. Moreover, in UDN, the number of indoor femtocells is expected to grow, increasing the need for seamless HO techniques. In this context, ML approaches, wherein the HO and resource allocation is determined using intelligent solutions, are prominent solutions to offer the desired QoE.

In the context of I_2O seamless transition, several works have explored using ML techniques, as mentioned before. For instance, [129] presented an ML for reducing redundant HO occurrences specifically for indoor-outdoor HO management in 4G femtocells. The authors used kernel methods, and their self-optimising algorithm results indicated that unnecessary HOs could be reduced by 65% in the case of detecting where unnecessary HOs were likely to happen. ML algorithms with convolutional neural networks were used in [130] for predicting massive MIMO indoor channel characteristics. Authors in [131] had applied the self-organising map (SOM) technique to develop their work in [129] in the interest of making the system fully plug-and-play, as required by the SON paradigm.

Table 2.2: Classification of Surveys on O_2I and I_2O.

Ref.	Frequencies	Research Topic
[79]	29 & 61 GHz	O_2I
[81-84]	28 GHz	O_2I
[86]	10 & 30 & 60 GHz	O_2I
[87]	20 GHz	O_2I
[89]	3 & 10 & 17 & 60 GHz	O_2I
[90]	3.5 GHz	O_2I
[91]	38 GHz	O_2I
[92]	2 - 60 GHz	O_2I
[93]	4.9 GHz	O_2I
[97]	2.4 & 5.2 GHz	I_2O
[98]	3.5 GHz	I_2O
[102]	28 GHz	I_2O
[101]	0.9 - 3.5 GHz	I_2O
[108]	60 GHz	I_2O

Their modified version of SOM allows a femtocell to learn indoor locations where unnecessary HOs may occur. Based on previous experience, it can decide whether to execute these HOs or not. Their results reveal that the updated algorithm can reduce unnecessary HOs by up to 70% in an LTE system. [132] presented an indoor path loss calculation model to predict the wireless signal attenuation by indoor obstacles using a combination of the Okumura-Hata model and an ANN, called a hybrid-empirical model. As we mentioned the importance of indoor navigation above, detailed information on data mining techniques used in indoor navigation systems can be found in survey study [133].

Table 2.2 presents the frequency classification on O_2I and I_2O studies introduced in this chapter so far.

2.5 Conclusions

A survey-style study on indoor and outdoor mm-wave propagation was presented in this chapter. We began the survey with an overview of mm-wave, then continued with its deployment in mm-wave for indoor and outdoor coverage, where related papers and methods on the area were reviewed. Subsequently, this survey emphasised self-organized seamless coverage that would help reduce the number of call drops when a user moves in a different direction between network environments, such as moving from indoor femtocell to outdoor macrocell. To enable the seamless transaction, useful ML techniques were provided to make the system smart enough when performing preemptive HO predictions. Moreover, papers focusing on seamless coverage between indoor and outdoor; O_2I; and I_2O were surveyed. Moreover, our extensive survey in this area led us to produce a table that summarizes the penetration loss of materials at various frequencies, which would be useful to the researchers studying this area. According to our knowledge, this is the first table presenting the most studies that have been conducted in this field.

Chapter 3

Coverage Analysis for Indoor-Outdoor Coexistence for Millimetre-Wave Communication

3.1 Introduction

The fifth generation of mobile communication networks (5G) has been standardized to exploit mm-wave frequencies to provide high data rate connection, seamless connection, and robust coverage to indoor and outdoor users. However, using mm-wave comes with new and peculiar challenges, such as limited coverage, since the penetration loss is proportional to the carrier frequency of the electromagnetic signal [2], [134].

As such, providing high data rates to indoor users could be challenging by solely deploying outdoor BSs since the mm-wave signals attenuate greatly depending on the material type and the thickness of the wall [127]. To overcome this issue, deploying local base stations, such as femto BSs inside the building, could effectively deliver high-quality broadband service to indoor users.

Femtocells can share the spectrum with the existing network or work in assigned channels based on the availability of spectrum [135]. In the former case,

operating femtocells under the coverage of outdoor BS may degrade the performance of femto users because of the outdoor BS interference inside the building. To satisfy indoor users' demands for a higher quality of service (QoS), received signal-to-interference-plus-noise-ratio (SINR) should be sufficient anywhere inside the building. Meanwhile, signal leakage from the femto BS deployed building to the outdoors should also be considered and kept minimum; otherwise, the QoS of outdoor users near the building might be affected negatively because of indoor interference on outside. Adjusting the transmitter power of BSs is one way of mitigating the impact of mutual interference. However, this method would decrease the QoS of users when the transmit power is lessened. Therefore, signal attenuation caused by the propagation through walls and other building materials would be the critical parameter to achieve mutual interference reduction. In other words, building walls could play a role as shielding mutual interference between the indoor femto BS and outdoor BS. Since thickness and the type of material used in the building changes wall attenuation in order of 5 dB to 20 dB or more, the signal attenuation through doors or windows is around 3 dB [127]. The approach of using buildings as shielding would help to reuse the same frequencies in the area where small cells are deployed close to each other.

In the literature, many studies concentrated on outdoor-to-indoor propagation to increase outdoor coverage to serve indoor users, whereas a few research focused on the indoor-to-outdoor case. In [127], a sample floor plan model was built to investigate the interference effect between macro and indoor femto BS. The authors in [136] examined the mutual interference between macro and femto BS, i.e., impacts of the interference caused by femtocell on the users served by macro cell and the interference caused by macro cell on the users served by femtocell. Their results show that the interference between macro and femtocell affects the system's throughput; therefore, it should be considered while configuring the system. The study conducted in [104] analyzed in the indoor coverage by deploying a single building scenario with an outdoor deployed BS utilizing

high frequencies, e.g., 10, 30, and 60 GHz. Their results also highlighted that the building type and materials are important parameters, especially at high frequencies. However, since the nature of high frequencies, such as mm-waves, are highly susceptible to penetration losses, covering indoor users with outdoor BS, operating at high-frequencies would not be feasible in terms of users' QoE. The majority of the present literature at 28 GHz focuses on measurements from indoor to indoor (I_2I) or outdoor to outdoor (O_2O).There are also studies on propagation loss at 28 GHz; however, the majority of them focus on measurements from indoor to indoor (I_2I) or outdoor to outdoor (O_2O), such as [137–140]. One exception to this trend was in [141] on O_2I measurements at 28 GHz using a rotating horn antenna channel sounder, which measures the absolute delay and the angle of arrival. Compared to similar outdoor locations, the paper found more clusters, larger excess delays, and larger angular spreads indoors. However, there were just a few indoor receivers (RX) locations, and only one kind of building was examined. According to [142], O_2I penetration losses varied from 3 dB to 60 dB depending on RX location and construction material types in an office building. The observations, however, were made for highly directed receivers and did not take into account how indoor settings with significant scattering affect the angular spectrum. The authors of [143] report penetration loss and reflection coefficient measurements for several building materials. For instance, clear glass has a penetration loss of 3.9 dB, whereas tinted glass has a penetration loss of 40 dB. However, the O_2I measurements indicate a device-to-device use case rather than a cellular deployment. Chapter 2 compiled the works in the literature on the penetration loss of some building materials at certain frequencies and presented them in Table 2.1.

This chapter investigates the effects of the interference caused by the outdoor mm-wave BS inside the femtocell deployed building. Of all the factors affecting the interference experienced by indoor users, three integral ones are identified:

1. The transmit power of the outdoor BS.

2. The distance between the outdoor BS and the building of interest.

3. The material type used for constructing the walls of the building.

The rest of the chapter is organized as follows. Section 4.2 presents the simulation environment. Section 3.3 analyzes the simulation results. Finally, the chapter is concluded in Section 4.4.

3.1.1 Electrical properties of materials

Radiowaves that hit a building will enter the building by a variety of methods. Each mechanism is affected by building materials' electrical characteristics differently. Line of Sight (LOS) and Non-LOS (NLOS) propagation are engaged in outdoor to indoor propagation in a small cell environment and comprise path loss computation, determination of reflection and diffraction loss, penetration loss, and other indoor losses. The majority of common building materials are non-ionized and non-magnetic. Thus, all that needs to be considered while choosing building materials is their dielectric qualities. Most construction materials exhibit lossy dielectric behaviour. Even metals can be described in this fashion, despite metal having very large RF losses [144]. A radio wave travelling through the atmosphere will be refracted when it collides with a dielectric medium, like a wall or window. A portion will be reflected, and another will be transmitted into the structure through the material. The well-known Fresnel reflection and transmission coefficients determine the magnitude and phase of the reflected and transmitted components. These, in turn, are influenced by a material's dielectric qualities and the angle at which a radio wave incident on it. The wave reflected by the exterior wall appears to a receiver inside the structure as a loss. However, because the building material is lossy, there is an extra (usually more significant) loss. As a result of absorption, the transmitted wave is attenuated as it moves through the substance. The attenuation in decibels is merely proportional to the thickness of the substance the signal travels through. As a result, while the

rate of attenuation (in dB per metre, for example) is an inherent property of the material and is independent of the incidence angle, the total attenuation will rely on the angle of incidence of the radio wave to the building (through a secant dependence of material depth on incidence angle) [144]. Since building materials are typically not simply homogeneous substances, calculating and measuring reflection and absorption losses becomes more challenging. The underlying physics of material permittivity is briefly discussed in the following section.

3.1.2 Electromagnetic Wave Propagation

Communications over wireless networks are based on electromagnetic waves, and the rapid development of wireless communication technology has continued since the discovery of electromagnetic waves in the 19th century. Any indoor or outdoor propagation model must be evaluated and designed using knowledge of wave propagation. A suitable source generates electromagnetic waves by varying electric and magnetic fields. It is possible to transmit information from one antenna to another using guided media, such as transmission lines, coaxial cables, or free space. The Maxwell's equations describe how electromagnetic (EM) waves interact with other materials. The Maxwell equations are obtained from the following four quantities: electric flux density D, magnetic field strength H, electric field strength vector E, and magnetic flux density B. The Maxwell's equations are given as follows in differential form:

$$\nabla . D = \rho \tag{3.1}$$

$$\nabla . B = 0 \tag{3.2}$$

$$\nabla \times E = -\frac{\partial B}{\partial t} \tag{3.3}$$

$$\nabla \times H = J + \frac{\partial B}{\partial t} \tag{3.4}$$

Equations 3.1, 3.3, and 3.4, respectively, reflect the Gauss law, the Faraday law, and the Ampere law with Maxwell's addition. According to the electric and magnetic characteristics of various media, the relationship between field strengths and flux densities is as follows:

$$D = \varepsilon E \tag{3.5}$$

$$B = \mu H \tag{3.6}$$

where ε is the permittivity and $\mu$is the permeability of the medium. 10 11 14 The power density attenuates by $\frac{1}{r^2}$ as electromagnetic waves move through free space from the transmit antenna to the receive antenna. The atmospheric conditions and system abnormalities are not taken into consideration by this reducing factor. The Friis free-space equation, thus, provides the received power at the receiver in free space:

$$P_r = P_t G_t G_r (\frac{\lambda}{4\pi r})^2 \tag{3.7}$$

where P_r stands for received power, P_t for transmitted power, G_t for transmitter gain, G_r for receiver gain, λ for wavelength, and r for distance between transmitter and receiver. Power transmitted will never exceed power supplied to the transmit antenna, and power received will never exceed transmitted power. Similarly, the antenna's received power will always be lower than the antenna's supply power. Various factors can contribute to this, including impedance mismatches, polarization mismatches, antenna orientation (if the antennas are pointed incorrectly), multipath fading, scattering, and reflections [145].

Due to widespread wireless technology use, radio wave propagation has been extensively studied in various environments. There are several propagation effects when designing wireless communication systems in heavily populated urban areas. Several obstacles can hinder the propagation of waves, including buildings and building walls made from various materials. Various mechanisms can explain propagation, including reflection, refraction, and transmission. Further-

more, different materials have different electrical and magnetic properties, so the EM fields change when interacting. Permittivity and permeability define the materials' electric and magnetic properties, respectively. Material's permittivity determines how much energy is stored, and its permeability determines how much magnetic field it can generate. By definition, absolute permeability is $\mu = \mu_r \mu_o$ where the permeability of vacuum is $\mu_o = 4\pi x 10^7$ H/m. This study only considers non-magnetic materials with close to unity relative permeability. Thus, we will focus only on permittivity here. EM waves interact differently with different materials due to their EM properties. Wireless communication systems use dielectric materials to interact with the radiated waves. In contact with a dielectric medium, electromagnetic waves undergo changes in wavelength, attenuation, and wave impedance. It is mostly due to differences in permittivity and permeability (for magnetic materials) between the two media. The complex permittivity can be calculated as follows:

$$\varepsilon^* = \varepsilon_o \varepsilon_r \tag{3.8}$$

where the permittivity of free-space ε_o is 8.845×10^{12} F/m and the complex relative permittivity of the material is ε_r, defined as:

$$\varepsilon_r = \acute{\varepsilon_r} - j\varepsilon'' \tag{3.9}$$

where the dielectric constant, $\acute{\varepsilon_r}$, indicates how much electric energy is stored in the material as the real part of complex relative permittivity. The imaginary part of complex permittivity ε'', also known as the loss factor, represents the energy dissipated by the medium [146]. In the case of a lossless medium, the loss factor is zero, and the relative permittivity is real. A loss factor is usually much lower than a dielectric constant, and most materials have a dielectric constant greater than 1. A material's dielectric constant is not constant; it depends on the frequency and nature of the material, as well as temperature and humidity.

3.2 Methodology

3.2.1 Ray Tracing Simulation Set-Up

In order to estimate the interference caused by the outdoor BS and to perform an indoor coverage analysis inside a building served by femtocell, a simulation environment is created in Wireless Insite™ software by placing 1600 points of the receiver set inside the building, which is neighbour to an mm-wave small cell outdoor BS, as depicted in Fig. 3.1. To observe the effects of different material

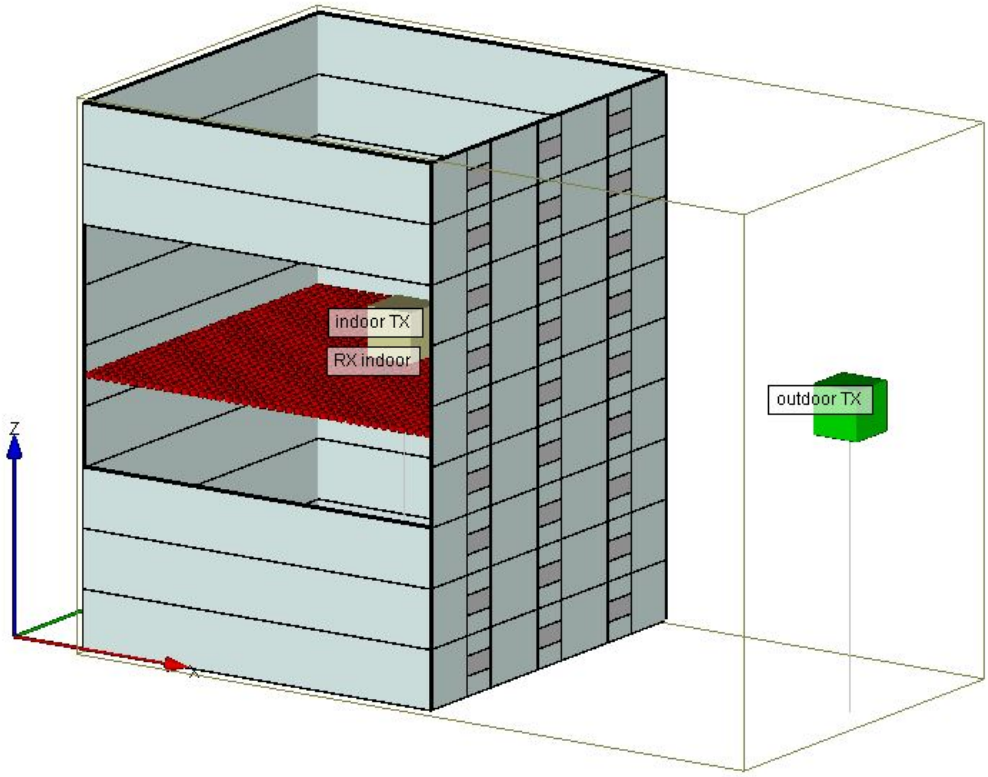

Figure 3.1: Simulation environment including a multi-storey building with, indoor and outdoor transmitters, and receiver points inside the building.

types on the experienced indoor interference, building scenarios with four different materials used in the walls of the building are developed. In the first scenario, walls are built up using one-layer brick. Based on the ITU recommendations, the

Table 3.1: Dielectric parameters and thickness of the material used in simulated building.

Material type used in the simulated building	Permittivity, ϵ_r	Conductivity, σ (S/m)	Thickness, d (m)
Brick (one layer)	4.440	0.0010	0.125
ITU Concrete 28 GHz	5.310	0.4838	0.125
ITU Wood 28 GHz	1.990	0.1672	0.125
ITU Glass 28 GHz (full glass building)	6.270	0.2287	0.125

following scenarios change walls to frequency-sensitive materials whose dielectric parameters are specified in Wireless Insite™ database. In the second scenario, ITU 28 GHz concrete is used for the building's walls, while in the third scenario, walls are changed to ITU 28 GHz wood. The windows in the first, second, and third scenarios are built up by deploying ITU 28 GHz glass with a thickness of 0.003 m. In the last scenario, the full building is created by using ITU 28 GHz glass with a thickness of 0.125 m. Table 3.1 shows the dielectric parameters of the materials used in the building. Simulations are conducted for different power values of outdoor small cell BS, such as 0 dBm is selected by considering outdoor BS is in sleep mode, whereas 30 dBm for regular transmitted power for mm-wave BS [147] and 50 dBm in case of outdoor BS which act as backhaul [148] BS introduce interference to inside the building. Furthermore, to account for the distance effect on interference due to ultra-dense deployment of mm-wave BSs, the distances of 25 m, 50 m, and 100 m are selected to illustrate the general trends of how coverage probability alters across the distance range. Table 4.2 shows the deployment and simulation parameters used in this study. Our system model uses the through-wall ray propagation model in [149]. It combines the two different propagation models for the case of outdoor mm-wave frequency propagation through the wall and the Friis equation for free space

Table 3.2: Simulations and deployment parameters.

Simulations Parameters	Parameter Value
Carrier frequency (GHz)	28
Number of buildings	1
Building size (m)	20x20x27
Number of floors	9
Number of outdoor base stations	1
Number of indoor base stations (femtocells)	1
Distance between outdoor BS and the building (m)	{25, 50, 100}
Bandwidth (MHz)	100
Outdoor BS height (m)	15
Indoor BS height (m)	15
Indoor receiver height (m)	13.5
Number of indoor receiver points	1600
Indoor transmit power (dBm)	30
Outdoor transmit powers (dBm)	{0, 30, 50}
Antenna type (indoor/outdoor)	Half-wave dipole

wireless propagation. The combination of these models expressed as [149]

$$\begin{aligned} P_r(\text{dBm}) =& P_t(\text{dBm}) + \sum_{i \in antenna} G_i(\text{dB}) + 20\log_{10} T \\ & - 20\log_{10} f(\text{MHz}) - 20\log_{10} d(\text{m}) + 27.6, \end{aligned} \tag{3.10}$$

where P_r and P_t are the received and transmit power, respectively; G_i represents all the gains associated with antenna and channel link; d is the distance between receiver node and transmitting antenna; f is the frequency of communication; T is the gain affiliated with Fresnel reflection and transmission coefficient [149] during propagation of mm-wave. Reflection coefficients which depend on material permittivity and polarization, play an important role in our system model, which is based on ray tracing simulations. Reflection coefficients for perpendicular ($|\Gamma_\perp|$) and parallel ($|\Gamma_\parallel|$) polarizations are given as

$$|\Gamma_\perp| = \frac{\sin(\beta) - \sqrt{\varepsilon_\text{r} - \cos^2(\beta)}}{\sin(\beta) + \sqrt{\varepsilon_\text{r} - \cos^2(\beta)}}, \tag{3.11a}$$

$$|\Gamma_\parallel| = \frac{-\varepsilon_\text{r}\sin(\beta) + \sqrt{\varepsilon_\text{r} - \cos^2(\beta)}}{\varepsilon_\text{r}\sin(\beta) + \sqrt{\varepsilon_\text{r} - \cos^2(\beta)}} \tag{3.11b}$$

where ε_{r} is the material permittivity of the reflecting surface and β is the angle between the incident ray and the reflected surface [150].

3.3 Simulation Results

The results are based on simulations performed in Wireless Insite™ X3D model, suitable for indoor or outdoor scenes by providing high fidelity, GPU accelerated, 3D ray tracing, and accounting atmospheric attenuation, the effect of the reflection and transmission on mm-wave frequency.

The effects of materials are analyzed by incorporating the coverage probability of the signal in the area of interest. The coverage probability is the probability that the SINR received by the arbitrary user exceeds a certain SINR threshold $\bar{\gamma}$. Mathematically the coverage probability is given by

$$\mathcal{P}_c = \mathbb{P}\left\{\frac{P_{r(in)}}{\sum_{i\epsilon\setminus BS_{in}} P_{r(out)} + \sigma^2} = \bar{\gamma} > \gamma_{\mathrm{th}}\right\}, \tag{3.12}$$

where any other indoor BS, denoted as BS_{in}, is removed from the interfering serving indoor BS because of a small contribution to the interference, we assume frequency reuse for indoor BS. $\mathcal{P}_c$ is the coverage probability; $P_{r(in)}$ and $P_{r(out)}$ are received power from indoor and outdoor BSs respectively; σ^2 is the noise; $\bar{\gamma}$ is the experience SINR for any arbitrary receiver, and γ_{th} is the set threshold SINR.

We first study the effect of the varying power on the same distance for different materials. Fig. 3.2 and Fig. 3.3 show coverage probability for four different materials, brick & ITU 28 GHz concrete and ITU 28 GHz glass & ITU 28 GHz wood with variable outdoor transmitting powers at 25 m distance away from the building, respectively.

When the transmitter power is 50 dBm, it can be seen that brick has a high transmission gain for mm-wave frequencies compared with other materials. The trend shows that even at lower transmit power; brick demonstrates the same behaviour of higher negative slope as seen in ITU 28 GHz glass. When the

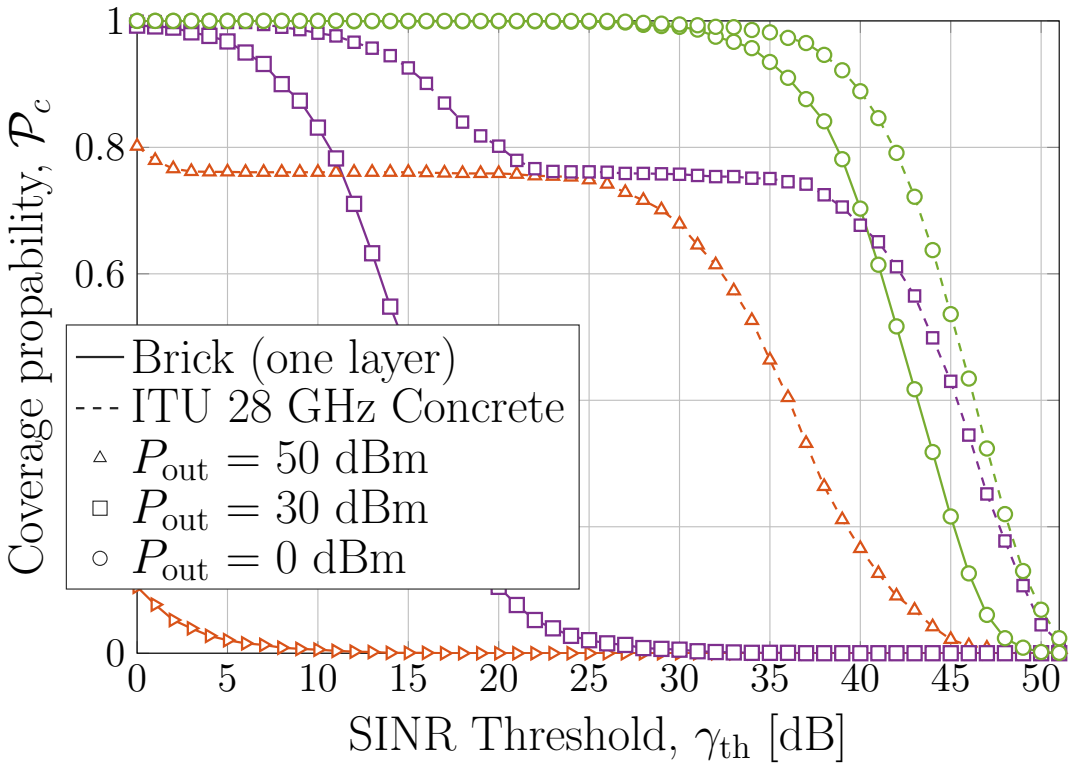

Figure 3.2: Coverage probability vs. SINR threshold for brick and concrete for different TX Power at 25 meters.

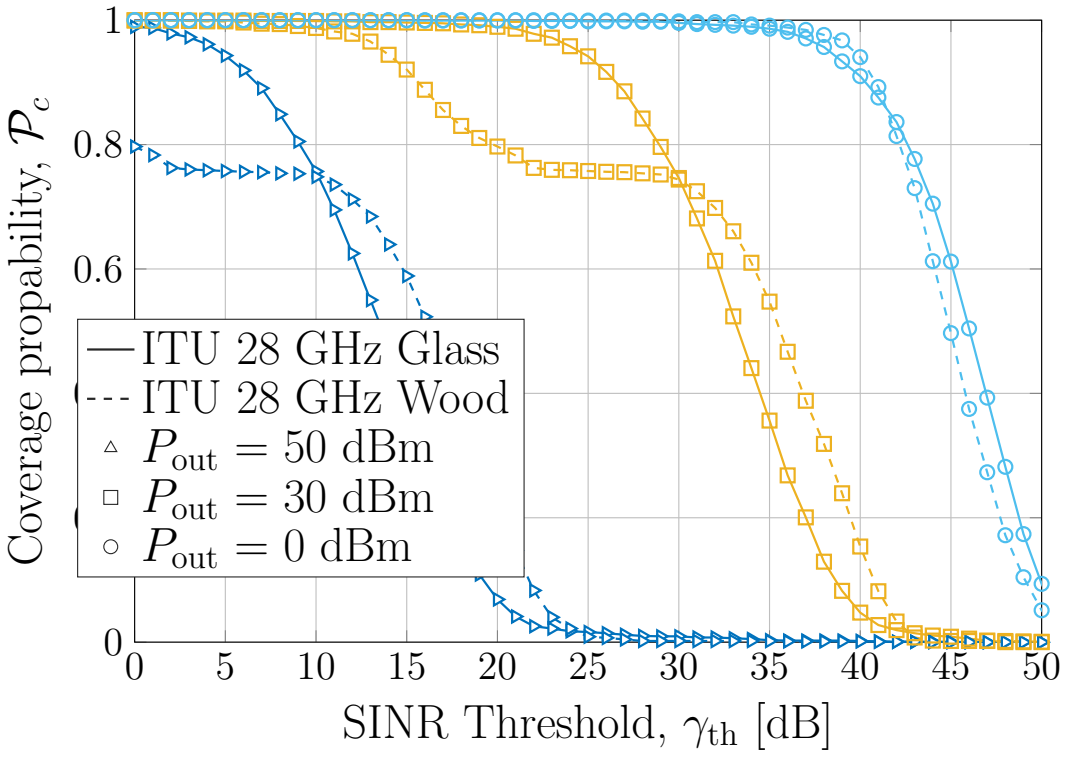

Figure 3.3: Coverage probability vs. SINR threshold for glass and wood for different TX Power at 25 meter.

distance is changed to 50 m as shown in Fig. 3.4 and Fig. 3.5, the coverage probability for brick increases noticeably, nearly 30% at $\bar{\gamma}$=0 for 50 dBm, while the coverage probability of other materials increases slightly compared to when the distance is 25 m, such as increase in glass is around 14% at $\bar{\gamma}$= 10 for 50 dBm.

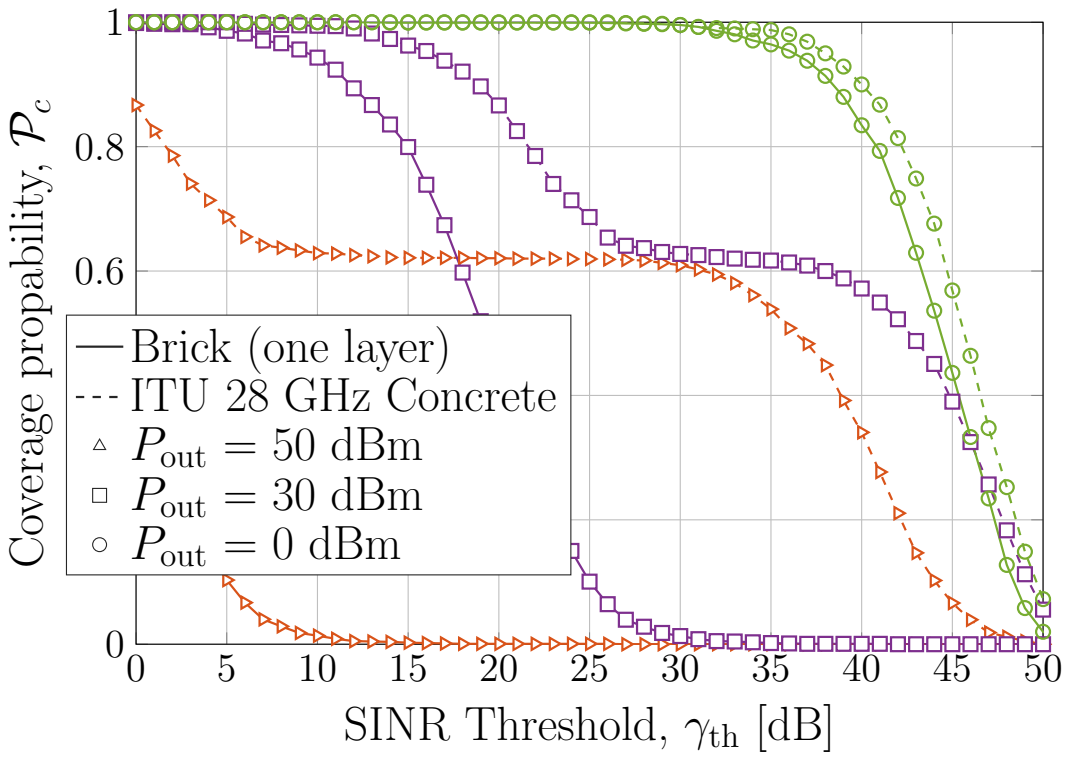

Figure 3.4: Coverage probability vs. SINR threshold for brick and concrete for different TX Power at 50 meters.

Figs. 3.6 and 3.7 illustrate simulation results when distance is 100m, where brick has a higher coverage probability even with the higher outdoor transmit power; however, its coverage probability remains lower with respect to other materials.

Overall, the coverage probability of concrete is higher than the brick at different distances while outdoor transmit power is changed. For an environment highly populated with outdoor mm-wave BSs, utilizing frequency dependant concrete would benefit indoor users by blocking the outdoor signal. Compared to ITU 28 GHz glass and ITU 28 GHz wood, the coverage probability for both materials looks quite similar for higher SINR thresholds; however, the difference in

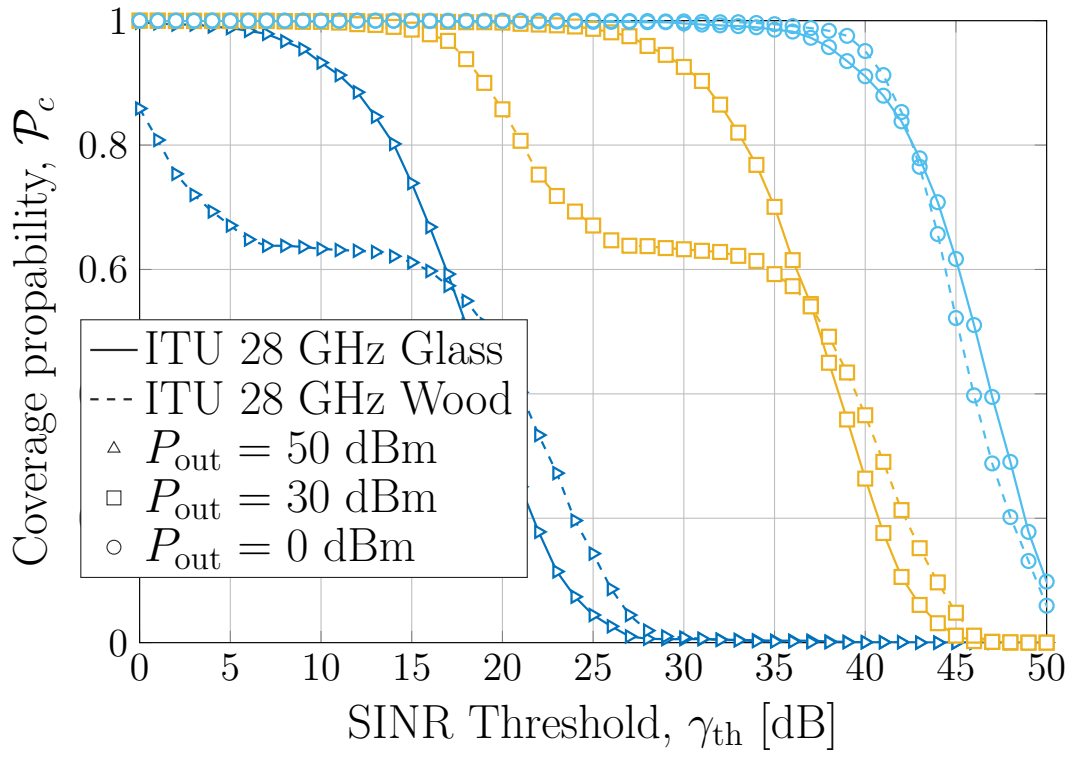

Figure 3.5: Coverage probability vs. SINR threshold for glass and wood for different TX Power at 50 meters.

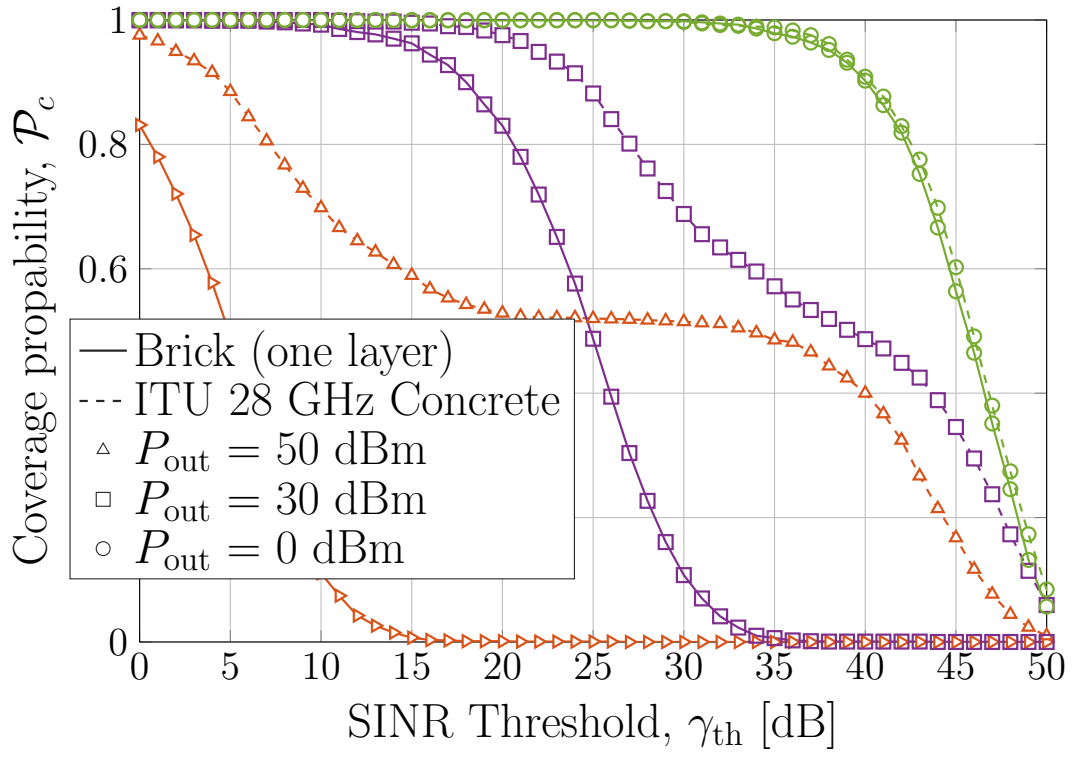

Figure 3.6: Coverage probability vs. SINR threshold for brick and concrete for different TX Power at 100 meters.

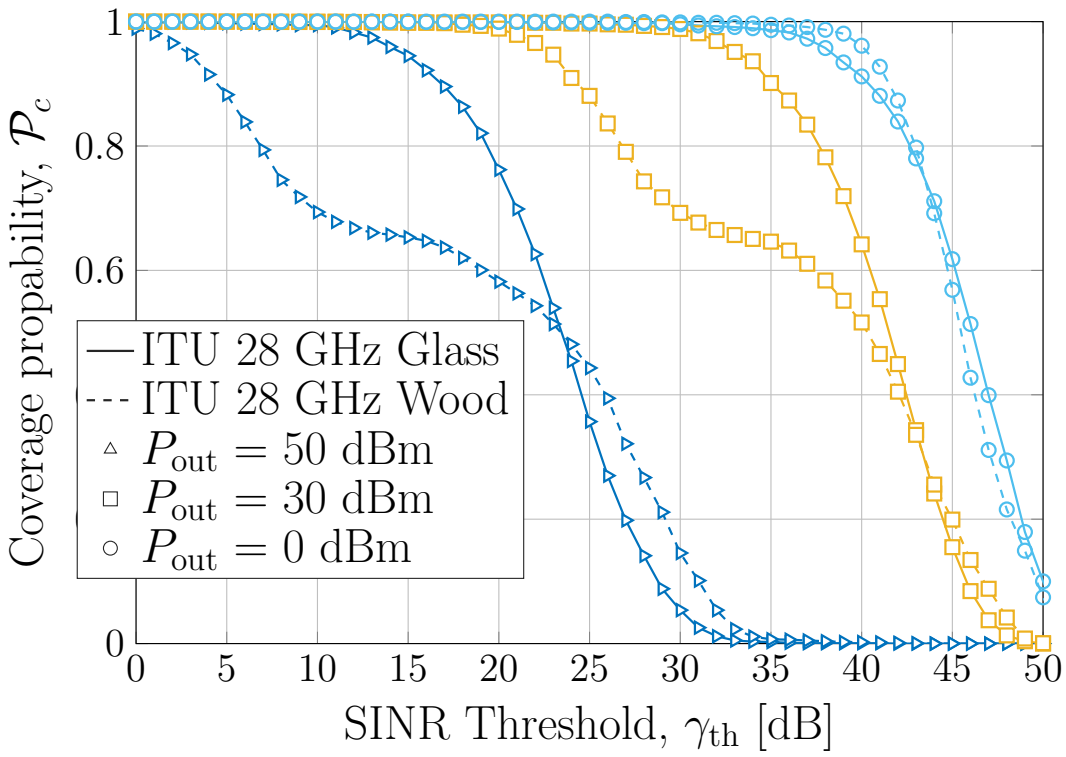

Figure 3.7: Coverage probability vs. SINR threshold for glass and wood for different TX Power at 100 meters.

coverage probability becomes particularly noticeable for lower SINR threshold in all power and all distances. The non-linearity behavior shown between the materials is attributed to the fact that the building is a non-homogeneous structure, and throughout the simulation, the building is comprised of glass windows.

3.4 Conclusion

This chapter analyses the outdoor BS interference effect inside the building when different types of materials are used in the walls of a building. We developed a single-building model and analyzed the coverage probability and effects of varying outdoor BS transmit power with the fixed indoor BS transmit power. The results reveal the importance of choosing the material type when outdoor BS is close to the building. Moreover, the outdoor BS interference effect should be minimized when the frequency re-use technique is deployed in very short insite distances. Therefore in the following chapters, the experience gained in this chapter is used as a base when the single-building model scenario is applied.

Chapter 4

IMPRESS: Indoor Mobility Prediction Framework for Pre-emptive Indoor-Outdoor Handover for mm-wave Networks

4.1 Introduction

The Fifth Generation (5G) of the mobile network is a game-changer technology since it promises to meet the significant data demand of the 21st century. The first phase of 5G's practical implementations has already begun at a global scale, and its second phase (mm-wave 5G) plans are moving forward [151]. Countries around the world, such as the U.K. and China for instance, have already deployed 5G in their major cities, promising low latency in high data rate communications [1].

The high-frequency spectrum range of the mm-wave band is the main factor of the 5G's achievement for enabling high data rates with minimum latency. Moreover, the mm-wave bandwidth provides almost ten times the capacity of its predecessor cellular networks [152, 153]. Although mm-wave bandwidth is an excellent feature for the next generation of wireless communications, they come

with a severe loss of penetration problem. The coverage footprint of mm-waves is relatively smaller than the previous generations, as the wavelength gets smaller while frequency increases because of the physical nature of radio communications.

Ultra-dense small network (UDN) is one the practical solution to this issue, in which mm-wave frequency driven small cells (SCs) are densely deployed over an area, to increase the network coverage [2]. However, careful management and regulations are needed in UDN; otherwise, the number of handovers would increase wherein SCs are densely deployed. In the presence of frequent handover occurrences, two essential parameters of a network: Quality of Experience (QoE) and the Quality of Service (QoS) of users are affected negatively. Furthermore, studies conducted by the 3GPP show that the HO failure rate in a heterogeneous macro-pico network is up to 60%, which is twice higher compared to a macro-only network [30]. Additionally, frequency sharing, energy efficiency, resource management, user association, interference management, and the economics of this ultra-dense network are some of the challenging areas that have yet to be addressed [2]. The high number of plug-and-play SCs placements especially in the residential areas may notably degenerate the QoS because of the severe inter-cell interference (ICI) [154]. Network slicing in the mm-wave could be one of the feasible solutions to the aforementioned challenges by establishing the framework of air-interface heterogeneous signal orchestration and efficient resource allocation. To ensure the best mm-wave coverage for indoor users, mm-wave driven femto base station, FBS, need to be deployed inside the building. Therefore indoor users would reach the high data rate communications provided by mm-wave frequencies. However, mm-wave's great exposure to the penetration loss creates coverage holes between indoor and outdoor environments served by mm-wave SCs. Hence, the user will receive an abrupt drop in RSS when moving out from indoor FBS coverage to outdoor SC coverage.

As a promising approach to ensure seamless connectivity, predictive mobility management can predict future locations of user equipment (UE) as well as the

HO requests of UE, hence the next network BSs could be prepared for incoming HO requests. It is essential to consider the environment and network for predictive mobility management, as it needs some input that can be useful for machine learning algorithms, for example. The importance of mobility prediction in wireless communications has prompted numerous studies to investigate the subject. In [155], the authors used Markov chains to predict user movement and highlight the impact of the transition probability matrix, which was built based on their assumptions. As part of their work in [156], the authors used the users' mobility history to input a transition probability matrix, which was used to uncover the most frequently visited base stations. To reduce the HO delay in 4G X2 HO, [157] proposes a machine learning model for managing the mobility of the part of the HO process to improve the prediction of future HOs. In order to solve the path dependency problems arising from classical Markov chains, which occur when users access the same cell repeatedly, the authors introduced a 3D transition matrix. A mobility prediction model using Markov Chains has been developed in [158] for 4G data plane networks. They introduced a trajectory dependency parameter, therefore, their proposed model's reaction to less frequent and random movements could be controlled by a trajectories dependency parameter.

Despite the fact that indoor users generate nearly 80% of the mobile traffic [28], however, the majority of the studies mainly focused on mobility prediction in outdoor environments. Moreover, when the Covid-19 pandemic situations are considered, i.e. restrictions such as local/national lock-downs, homeschooling and paradigm shift to working from home, led to people spending more time indoors, which further increases the data demand for indoor users. For instance, Vodafone reported that internet usage by their contractors is already seen up to 50% in some European countries as the impact of Covid-19, and the demand is expected to be even higher depending on rules that governments implement, such as working from home [159].

The handover management of users from indoors to outdoors has not received

Table 4.1: Literature comparison.

Ref.	Technology		Environment		Management	
	LTE	5G	Indoor	Outdoor	Handover	Mobility
[155]	✓					✓
[156]	✓					✓
[157]	✓			✓	✓	
[158]	✓			✓	✓	✓
[160]	✓		✓		✓	
[161]	✓		✓		✓	
[162]	✓		✓		✓	
This work		✓	✓	✓	✓	✓

the necessary attention, even though most of the traffic demand is created from indoor users [128]. The authors of [160] used Kernel methods to reduce the ping-pong handover occurrences when an indoor UE moves close to areas where the outdoor macro BS's signal strength increases, such as the corner of a window or a door. Yet, the study only focuses on when the user is indoors. In [161], handover delay optimization for femtocell users are done by predicting the next cell. In [162], a dual handover triggering scheme is proposed for indoor users, where some additional event parameters are introduced. Even though the mentioned studies approach a common problem of reducing the ping-pong handovers and the handovers when the UE moves from indoor to outdoor (I_2O) [161, 162]; the studies are conducted in a 4G-LTE environment whose coverage size of macro BSs can be of several kilometres. Table 4.1 gives a brief insight of the difference between our work and the surveyed studies above.

According to real-world measurements of 28 GHz and 73 GHz in [152], the coverage size of mm-waves will have a small footprint of around 100–200 meters, which brings us to the necessity of an intelligent and seamless I_2O handover management scheme. Considering the fact that SCs will be deployed both indoors and outdoors, with a much higher density, it is crucial that they are deployed efficiently, and are supported by mobility predictions. Even more so, high penetration losses would create mm-wave-driven indoor environments isolated from

the outdoors [128]. As such, due to this isolation and sharp change of RSS, when a UE passes through a door; call drops would be inevitable.

The aforementioned studies and the work we have presented so far in the previous chapters are the basis of our motivation to present the following twofold contributions in this chapter:

- First, an Indoor Mobility Prediction model for mm-wave CommunicationS using Markov ChainS (IMPRESS) is introduced, in which Markov chains are utilized in favor of preemptive handovers for a user-centric indoor mobility prediction.

- Based on the results from the previous Chapter 3 on the interference effect of outdoor BS, a pre-emptive I_2O handover algorithm is presented as the second contribution in order to reduce the latency within the indoor and outdoor multi-tier network, while a user transitions among them.

The remainder of this chapter is organized as follows. Section 4.2.1, introduces the IMPRESS algorithm, while Section 4.2.4 presents the preemptive I_2O handover algorithm. The results are presented in Section 4.3. Finally, Section 4.4 concludes this chapter and its contributions.

4.2 Methodology

As this study provides a twofold contribution, the methodology used for Indoor Mobility PREdiction for mm-wave CommunicationS using Markov ChainS -IMPRESS- is presented first, along with the proposed solution for the defined problem in Section 4.2.1. Secondly, the proposed pre-emptive Indoor-to-Outdoor (I_2O) mm-wave handover algorithm is presented and its results are evaluated.

4.2.1 Indoor Mobility Prediction and Proposed Solution for IMPRESS Framework

Indoor user mobility is one of the critical factors of today's system-level simulations; as stated in [28], indoor users generate almost 80% of mobile traffic. Based on the studies in [163–166], the user's mobility is stated to have some pattern and is not entirely spontaneous. On the contrary, it is target-oriented [165], as humans do not walk around erratically but rather aim for a particular goal, for instance, leaving home to go to a train station or heading to the kitchen from the living room. Using human decision-making process in [31], [166] modelled user mobility in a non-random manner. The authors in [31] evaluated this decision-making process as a product of two factors; external and internal, in which the former is represented by environment stimulus and group behaviour, whereas individual characteristics indicate the latter. Motivated by the above-mentioned studies, our hypothesis is that a user has more regularities in their movement within an indoor environment, where degrees of freedom are lower as compared to an outdoor scenario. Considering these regularities, we designate a special area in our indoor model, called the cloakroom, where users usually visit to take his/her coat, shoes, keys, umbrellas etc., before going outdoor, or vice-versa. Therefore, we model an indoor environment segmenting indoor regions (IR) into Markov Chain states as shown in Fig. 4.1, and prediction algorithms are implemented to track the probabilities of a user following the given scenario trajectory [167]. Moreover,

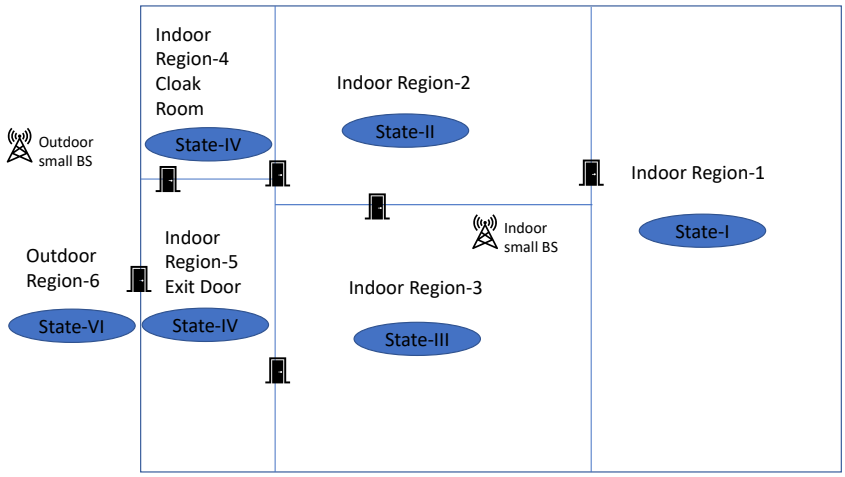

Figure 4.1: System Model showing Indoor Regions as Markov Chain states.

we consider this environment with a single small BS and a macro BS located in the outdoor environment, positioned at a distance of d from the left wall of the user's building. Regarding the indoor environment, a building with an area of A is considered, with a single small cell providing coverage for the entire region.

4.2.2 Markov Chain for Mobility Prediction

Markov chain is a stochastic process and is referred to as memory-less since the next state relies on the current state rather than the previous state [156]. A Markov chain consists of a set of states, which in our scenario are S=$\{IR_1, IR_2,..IR_n\}$, where being the states' indices $\mathbb{I} = \{1, 2, ..., n\}$ and transitions, $t_{i,j}$, represent the movement probabilities from one state to another, as illustrated in Fig. 4.2. Markov chains are mainly used for predictions in a randomly changing system, and mathematically model the probabilities of transitions to the next states, as:

$$\mathbb{P}(S_{n+1} = s_{n+1}|S_n = s_n, ..., S_1 = s_1) = \mathbb{P}(S_{n+1} = s_{n+1}|S_n = s_n). \quad (4.1)$$

Contrary to the studies mentioned in Section 4.1 where the states are defined as base stations; our proposed scheme defines the Markov chain states as indoor regions (IR) within an indoor environment. Received signal strength (RSS) approach which is one of the simplest and broadly used techniques for indoor localization [168] is utilized to determine in which state UE is.

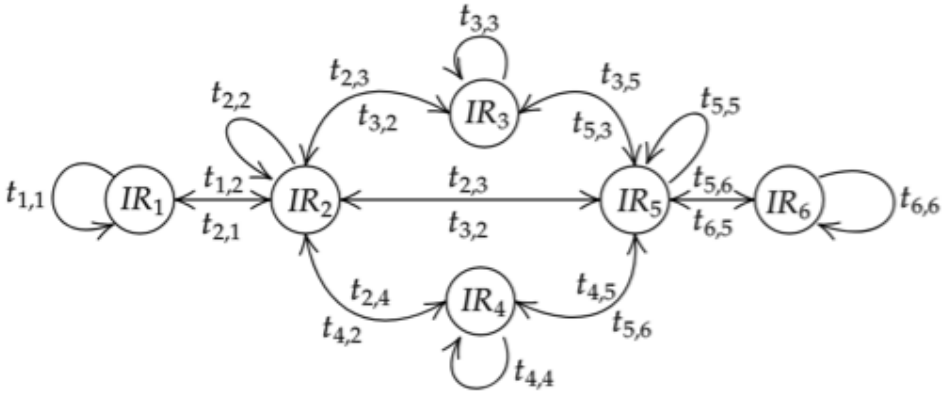

Figure 4.2: Discrete-time Markov Chain with 6 finite state spaces (i.e., IRs).

The probability distribution is derived from:

$$\mathbf{p}_k = \mathbf{p}_0 \mathbf{T}^k, \tag{4.2}$$

$$\mathbf{T} = \begin{bmatrix} t_{1,1} & t_{1,2} & \cdots & t_{1,n} \\ t_{2,1} & t_{2,2} & \cdots & t_{2,n} \\ \vdots & \vdots & \vdots & \vdots \\ t_{n,1} & t_{n,2} & \cdots & t_{n,n} \end{bmatrix}, \tag{4.3}$$

where $\mathbf{p}_k$ is the k$^{\text{th}}$ transition probability vector, $\mathbf{p}_0$ is the initial distribution vector and $\mathbf{T}$ is the transition probability matrix.

4.2.3 Proposed Solution

Given that user movements are goal-oriented, in this section, we propose a novel concept for initialising the transition matrix of a Markov chain and evaluate its impact on indoor mobility prediction. However, before presenting the proposed solution, it is important to give an overview of how Markov chains can be used for mobility prediction.

Online Learning Transition Matrix

There are some steps needed to be set before initializing the transition matrix such as; 1) A transition from any state to itself is prohibited, making the transition matrix hollow, such that $t_{i,i} = 0, \forall i \in \mathbb{I}$; and 2) The transition matrix should be a right stochastic matrix, satisfying the condition $\sum_{j=1}^{n} t_{i,j} = 1, \forall i \in \mathbb{I}$.

Since the UE initiates the HO transition, we assume that the transition matrix $\mathbf{T}$ is updated according to the user's tracked movement. The idea is to assign higher probabilities to the most common routes followed by the user as compared to the other routes. A trajectory dependency parameter R_d is used to control the model's learning rate and reaction to random or less frequent movements as proposed by [158], where $0 \leq R_d \leq 1$. Consequently, small values of R_d update the transition matrix more slowly, giving more weight to the overall path of a user (minimizing the randomness). In the case of $R_d = 0$, $\mathbf{T}$ is not updated making the prediction independent of the past movement, whereas, in the case of $R_d = 1$, the prediction is biased towards the most recent trajectory.

To further explain the update procedure of $\mathbf{T}$, let us consider an example where a user follows the path: $IR_1 \longrightarrow IR_2 \longrightarrow IR_3$. For each movement between a region, e.g., from IR_1 to IR_2 the UE will update the probabilities of outbound movements from IR_1 to all neighbouring IRs in a game scheme of several stages. In the first stage, the outbound movement probability of UE from IR_1 to IR_2 is increased by an amount controlled by R_d, while the probabilities

of direct movement of UE from IR_1 towards all playing IRs are decreased. This is expressed as:

$$t_{1,2} = t_{1,2} + \sum_j t_{1,j} R_d, j \in \mathbb{N}_{IR_1}, \tag{4.4}$$

$$t_{1,j} = t_{1,j} - \frac{\sum_j t_{1,j} R_d}{|\mathbb{N}_{IR_1}| - 1}, j \in \mathbb{N}_{IR_1}, \tag{4.5}$$

where $|\mathbb{N}_{IR_1}|$ is the cardinality of the set of neighbouring IRs for IR_1 which are taking part in the game. To satisfy the condition of inclusivity ($0 \leq t_{i,j} \leq 1$), a lower bound of 0 and an upper bound of 1 is set for each entry in $\mathbf{T}$. This brings in the challenge of satisfying the condition of the right stochastic matrix. This is solved by adding additional stages that approach equilibrium without violating the conditions of transition matrix [158].

Q-Learning Initialization of the Transition Matrix

Based on the model proposed by [158] and the fact that user mobility is not totally random, but rather goal-oriented, in this chapter we propose to initialize the transition matrix $\mathbf{T}$ according to a Q-learning algorithm. Q-learning is a reinforcement learning technique that learns an action-value function that gives the expected utility of taking a given action in a given state and following a fixed policy thereafter [169]. Since reinforcement learning algorithms are goal-oriented by nature, it is deemed a suitable fit for this problem.

Considering our Markov chain model with finite state spaces represented by S, a finite set of possible actions $U(i)$ where $i \in S$ and transition probabilities represented by $t_{i,j}$ such that $\sum_{i,j} t_{i,j} = 1$ for all $j \in S$. It is assumed that before using the Markov chain for mobility prediction, the user would gather some data based on its movement. As such, in this context, we have trained a Q-learning model according to the scenario from Fig. 4.1, where a user could start in any state and its goal was to reach the outside region (state 6). Based on that,

Q-learning is able to update its function according to

$$Q(s_t, a_t) \leftarrow Q(s_t, a_t) + \alpha[r_{t+1} + \phi \max_a Q(s_{t+1}, a) - Q(s_t, a_t)] \tag{4.6}$$

where $Q(s_t, a_t)$ is the current action-value function, α, is the learning rate, r_{t+1} is the expected reward at the next time step, ϕ is the discount factor and $\max_a Q(s_{t+1}, a)$ is an estimate of the optimal future action-value function at the next state over all possible actions.

Based on this model, given any starting state, Q-learning learns the next action of a user in order for it to reach the outside (the goal). Thus, by training this model and counting how many times each state-action pair were visited, a transition matrix can be built, given by $t_{i,j} = N_i / \sum_j N_j$.

4.2.4 Preemptive I_2O Handover Framework

The rapid drop in SINR due to the penetration loss, especially when a UE moves from the door of a building, is verified by the field measurements conducted in [162]. However, the mentioned study above is conducted by utilizing LTE frequencies. Since mm-wave driven networks are far greater prone to penetration losses than LTE, we present a preemptive I_2O handover scheme for a UE transitioning from indoor to outdoor under a heterogeneous network environment. The proposed scheme aims to perform the HO process beforehand the out-of-synchronization (out-of-sync) happens; to avoid a rapid decline in communication quality.

Proposed Scheme to I_2O Handover

Mobility is the most important parameter for handover management. When its proper configurations are done, it can lower the number of handovers. Thus the handover signalling cost, which can be expressed in terms of the delay required to transmit and process the HO messages, could be reduced. Therefore in the

IMPRESS algorithm, the information about the user's indoor trajectory on the most visited rooms (states) before the user goes out are considered *(MVSBGO)*. In the second contribution of this study, *I_2O handover*, we build a realistic simulation scenario of a multi-tier heterogeneous network, where mm-wave driven femto and picocell BSs are deployed in the presence of a macro BS. The UE's trajectory information before going out is obtained in Section 4.2.1, which is in this scenario, the user mostly visits the state-IV (also can be called cloakroom in here), then follows the state-V and state-VI to go out. After acquiring this information, we designated a particular area in the state-V called *HO spot area*, which is 0.5 meters away from the exit door of the building. When the user comes to the *HO spot area* while being in the active state, our pre-emptive *I_2O handover algorithm* checks the trajectory history of the user to obtain the information of whether this history contains the coordinates of the state-IV or not. If the user's mobility trajectory history contains the coordinate of the state-IV, the *I_2O handover algorithm* initiates the handover signalling, similar to the A3 event in the LTE. But with the only difference is that in the LTE A3 event, handover is triggered, and the measurement report is sent from the UE when the received RSRP of the serving cell goes below the RSRP of the neighbouring cell over a pre-defined period named time-to-trigger (TTT), which is defined as in [162]:

$$RSRP_n - RSRP_s > A3offset_s - CIO_{n,s}, \tag{4.7}$$

where RSRP_n and RSRP_s the RSRP of the neighbouring and the serving base stations, respectively. A3offset_s is the offset of the serving cell, and $\text{CIO}_{n,s}$ is the cell individual offset between the neighbouring and serving cells. However, in our case, the RSRP of the serving cell -femtocell here- only goes below the threshold or the RSRP of neighbouring cells when the UE goes out of the exit door and leaves the building. Instead of starting the handover signalling after the UE leaves the building, we propose initiating the handover signalling before

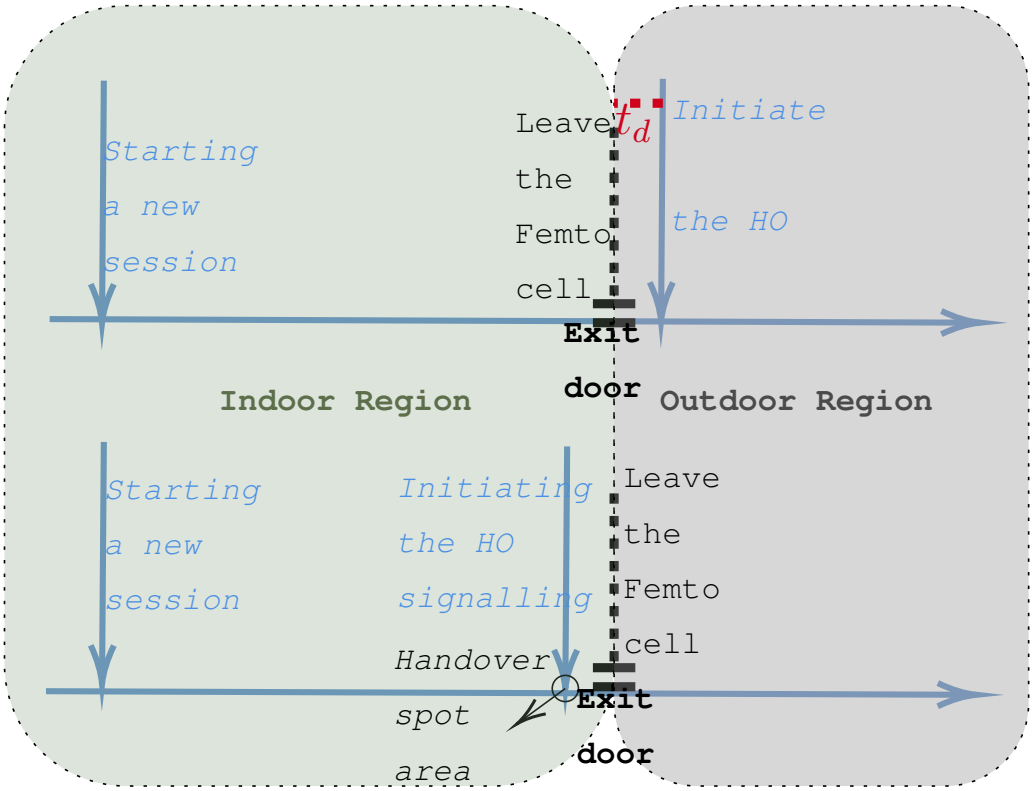

Figure 4.3: The timing diagram of proposed I_2O handover.

the UE leaves the building. More precisely, the HO process will be initiated at the *HO spot area*, as it is illustrated in Fig. 4.3 to maintain the continuity of the user's ongoing active session. Otherwise, because of the high penetration losses for mm-waves, the user would face an abrupt drop in the received power when they move out from the serving BS's coverage. A call drop would happen eventually, resulting in a reduction of the QoE.

The RSRP plays an essential role in a conventional cell selection (idle mode) and handover (connected mode) as the decisions depend on it [75]. Therefore, to enable the proposed scheme, an additional offset value (CREO) is added to the RSRP of the closest outdoor small BS to extend its cell range. Thus, the handover process should be initiated preemptively to prevent out-of-synchronization (out-of-sync) when the UE leaves the building. The detailed pseudo code of the proposed handover algorithm for the I_2O is explained in Fig. 4.4.

Algorithm 1 Pre-emptive I_2O Handover Algorithm

Inputs: SINR, UE location, UE trajectory history, HO spot area, CREO.
Mobility Management: Initialization of the UE transition matrix to find probabilities of visited states of the indoor environment.
Output: Probability of the most visited state, $MVSBGO$, before going out.
HO preemption:
if $UE_{currentlocation} = HO_{spotarea}$ **then**
    check the UE trajectory history
    if $UE_{trajectoryhistory} = MVSBGO$ **then**
        $SNR\_outBS = SNR\_outBS + offset$
        $SNR\_FBS = SNR\_FBS + offset$
        $reward = 1$
    else
        $reward = 0$
    end if
end if

Figure 4.4: Pre-emptive I_2O Handover Algorithm

Propagation Model for I_2O Handover

The surrounding environment and the maximum radius of the cell, which have a substantial impact on the received signal, are two of the most critical characteristics that affect wireless coverage. The received signal parameters are principally affected by three factors: multipath (small-scale) fading, shadow (large-scale) fading, and, path loss propagation. A zero-mean Gaussian random variable with a logarithmic variance is used to simulate the features of fading. Thus, a radio propagation model based on the well-known log-distance path loss model in [170] has been adapted and implemented as:

$$PL_{in} = P0_{in} + 10\gamma_{in}\log_{10}(d/d0_{in}) + \delta + \rho_{drywall} + \varrho, \tag{4.8}$$

$$PL_{out} = P0_{out} + 10\gamma_{out}\log_{10}(d/d0_{out}) + \delta + \rho_{concrete} + \varrho, \tag{4.9}$$

Table 4.2: Simulations and deployment parameters.

Simulations Parameters	Parameter Value
Carrier frequency for FBS and SBS (GHz) [171]	28
Carrier frequency for MBS (GHz) [172]	3
Bandwidth of FBS and SBS (MHz) [173]	100
Bandwidth of MBS (MHz) [174]	20
Transmit power of FBS (dBm) [175]	30
Transmit power of SBS (dBm) [176]	35
Transmit power of MBS (dBm) [175]	46
Concrete ρ at 28 GHz [128]	34.1
Concrete ρ at 3 GHz [128]	17.7
Drywall ρ at 28 GHz [128]	6.8
γ_{in} [177]	1.6
γ_{out} [177]	3
Number of outdoor base stations	2
Number of indoor base stations (femtocells)	1
Antenna type (indoor/outdoor) [128]	Half-wave dipole

where PL is the total path loss in decibel (dB) at a distance d in meters, and $P0$ is the free-space path loss at the reference distance $d0$. γ is the path loss exponent, δ is the Gaussian random variable with zero mean, $\rho_{drywall}$ and $\rho_{concrete}$ are the penetration loss exponents for each specific material. Lastly, ϱ is the shadow fading of the channel.

As it can be seen in (4.8) and (4.9), the path loss is calculated separately for both mm-wave indoor and outdoor small BSs and macro BS. These calculations are done by denoting the parameters into the specified frequency values for indoor and outdoor for the equations mentioned above. The specifications for the simulation parameters are stated in Table 4.2. The SINR of the system is calculated as:

$$SINR = \frac{P_r}{\sigma^2 + I}, \tag{4.10}$$

where Pr is the received power in Watt, derived by subtracting the path loss from the transmit power of relevant BS. σ^2 is the noise power density and I is the interference of the neighboring cells.

4.3 Simulation Results

4.3.1 IMPRESS Simulation Results

The simulation environment contains six Markov states, the states from one to five belong to the indoor environment and state six represents the outdoor environment, as illustrated in Fig. 4.1. The transition between the states is evaluated to examine the accuracy of the initial values of the transition matrix. The system checks the probabilities for a sequence of 100 days with 6 transitions each day. Four different mobility scenarios are applied for each day for a single user: 0% of random data, where users follow predefined routes every day; 10%, 20% and 50% random data, in which random routes are followed with the given percentages and evenly distributed across the 100 days. The proposed solution with Q-learning initialization is compared to the solution in [158] in terms of prediction accuracy, identified as the ratio between the number of correct and total number of predictions. For the Q-learning, a learning rate of $\alpha = 1$, a discount factor of $\phi = 0.8$ and an ϵ-greedy policy with ϵ decaying from 1 to 0.3 are assumed. A total of 500 episodes are simulated, with varying numbers of iterations (the algorithm would stop when the outside region is reached). In terms of the reward, a reward of 0 is assumed for every step the user would take, as the user's movement within the states is not the main argument here; except in states 5 (*HO spot area*) and 6 (outside) where a reward of 25 and 100 is given as going outside is the main goal for the user when the user is in the *HO spot area*.

Fig.4.5 illustrates the average prediction accuracy values w.r.t different R_d values for the solution from [158] and our proposed Q-learning method. In the first scenario, shown in the solid lines, since the transition matrix is initialized with equiprobable values over all possible states, it can be seen that for low values of R_d, the prediction accuracy is very low, with accuracy ranging from 25% to 40% for the different mobility models when $R_d = 0$. This occurs because the Markov chain model does not assume any prior knowledge of user mobility,

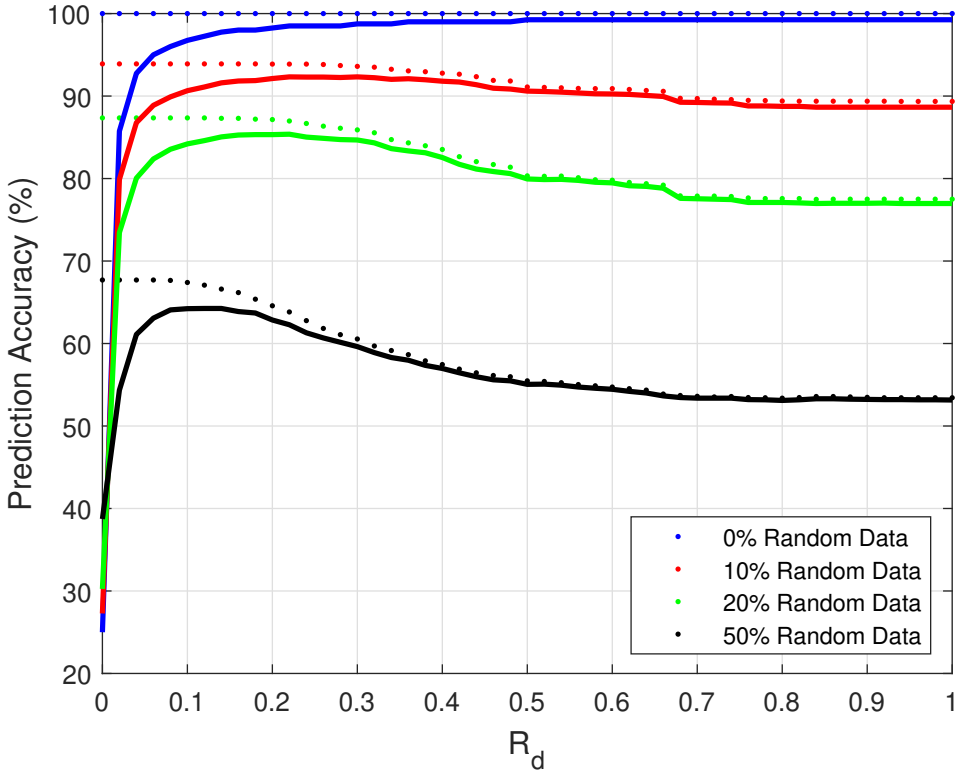

Figure 4.5: Accuracy for different values of R_d for Online Learning and Q Learning Initialization of the TM.

which results in an initial learning time, in which the algorithm makes wrong predictions more often than correct ones. However, as R_d increases, we can see that the prediction accuracy reaches values of 98 - 99% when no randomness is considered and declines for higher values of R_d for the other mobility models. This occurs because when R_d is higher the transition matrix updates faster, thus when randomness is introduced, it is less reliable [158].

For the proposed scenario, shown in the dashed line, it can be seen that the prediction accuracy without any randomness, has the maximum accuracy of 100% as the system already had the initial transition matrix value, which is derived from the Q-Learning method. In addition, this method gives more robust estimate of the accuracy with respect to lower R_d values. However, the increment in the random data, reduces the accuracy comparatively with the higher values in R_d, for the same reasons as mentioned above.

Table 4.3: Accuracy gain in percentage.

R_d Values	0	0.2	0.4	0.6	0.8	1
0% Random Data	3	1.78	1.01	0.75	0.75	0.75
10% Random Data	2.44	1.89	1.06	0.72	0.73	0.78
20% Random Data	1.88	2.13	1.18	0.40	0.61	0.68
50% Random Data	0.74	2.74	0.83	0.50	0.51	0.51

Table 4.3 shows the gain in terms of accuracy between the proposed solution and the solution in [158], for different values of R_d. It can be seen that, initializing the Markov transition matrix with values from Q-learning yields higher gains when R_d is smaller, with gains over 1% for values of $R_d \leq 0.4$ whereas when R_d is larger, the two solutions converge to each other. This occurs when R_d is larger as the values in the transition matrix are updated more quickly, therefore only the most recent paths are considered more important than the previous one. Therefore, the initialization is not as effective as when smaller values of R_d are considered. Lastly, Fig. 4.6a demonstrates a heatmap of the path that the user follows according to the Q-learning mobility pattern, which is then used to initialize the transition matrix in the Markov chain algorithm. On the other hand, Fig. 4.6b shows a heatmap of what the proposed solution has learned, for a value of $R_d = 0.2$ and a 50% randomness in user mobility.

4.3.2 Preemptive I_2O Handover Results

The measured SINR values for the simulation environment with three scenarios are presented in Fig. 4.7. At first, we began our simulations by deploying only small cells at 28 GHz to imitate the UDN environment; however, in real life, these environments are mostly underlaid by the macro BSs. Therefore we improved our simulations by adding macro BS serving at 3GHz, and the interference between these frequencies is shown in Fig. 4.7. The first scenario in Fig. 4.7a shows the SINR measurements, in which the handover algorithm is not applied. As it is seen, the FBS has the highest SINR value of 20 dBm compared with the other two

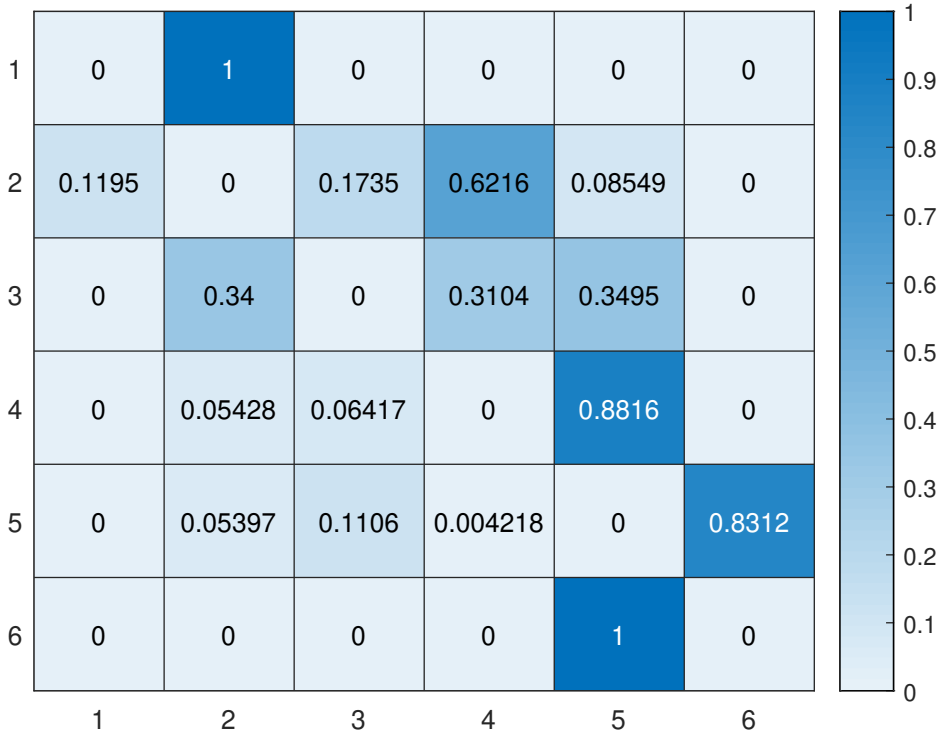

(a) Initial transition matrix acquired from Q-Learning

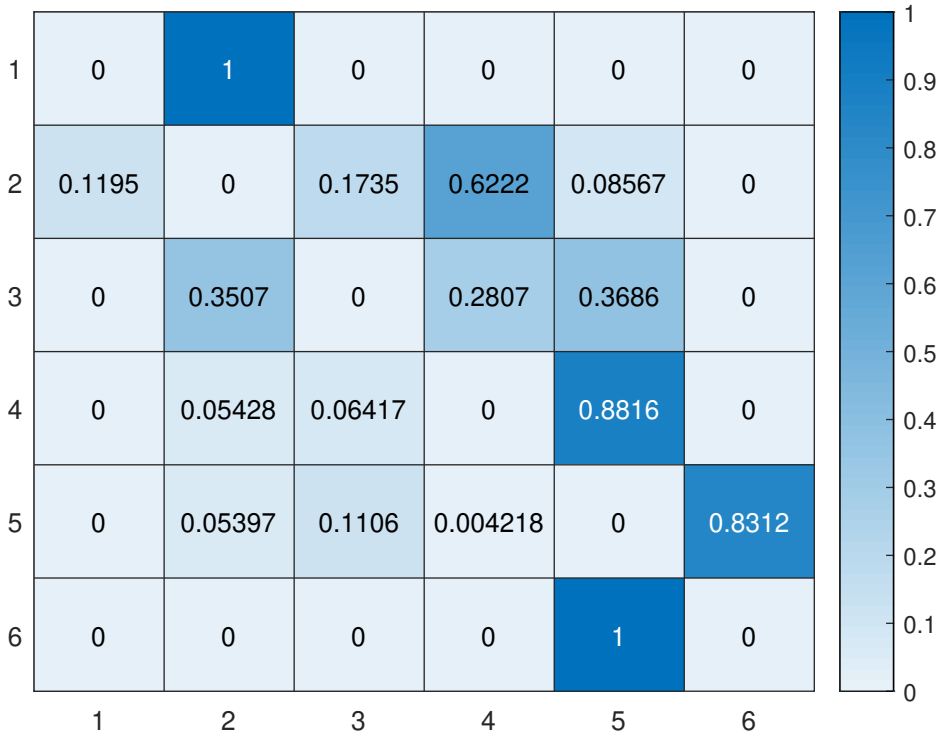

(b) Transition matrix after learning, when $R_d = 0.2$.

Figure 4.6: Markov Chain Transition Matrix.

outdoor BSs having SINR of -20 dBm and -55 dBm. However, when the UE moves to outdoor, there is an abrupt drop in the SINR of the FBS dropping to below

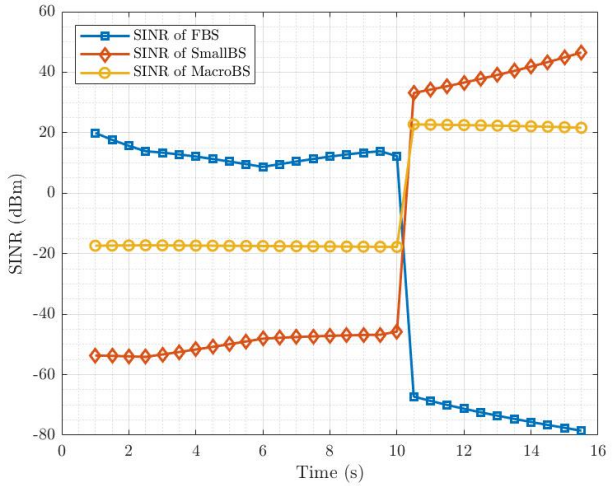

(a) Measured $SINR$ result without any algorithm is applied, Scenario 1.

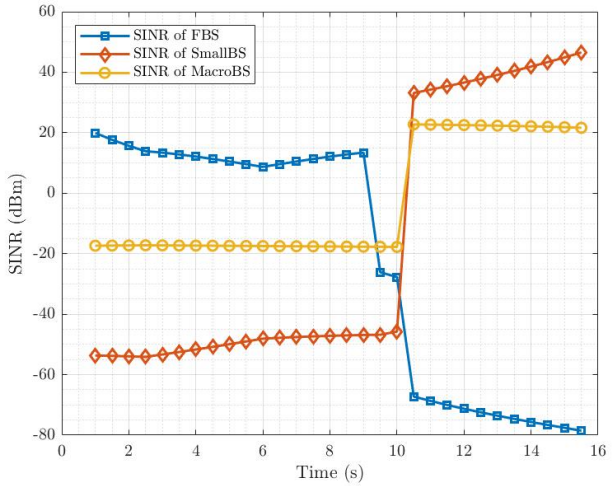

(b) Negative offset value is added to the FBS received power, Scenario 2.

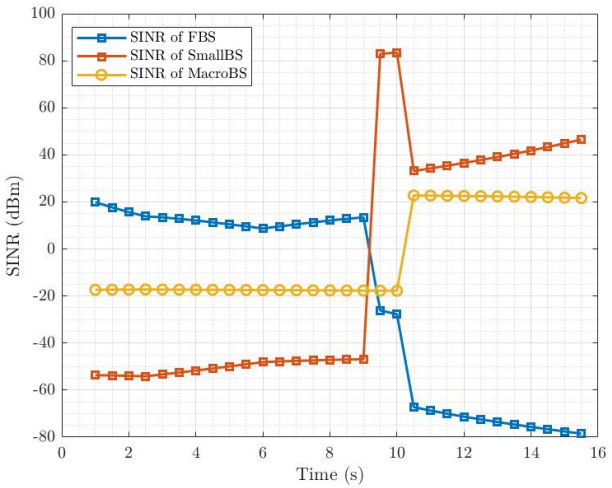

(c) Presented algorithm is applied to the received power of FBS and SC BS, Scenario 3.

Figure 4.7: Measured SINR values for the simulation environment.

-60 dBm, while the SINR of outdoor BSs increases swiftly. This result proves our hypothesis about the need for a proper handover algorithm for indoor users while transitioning to the outdoors. Otherwise, because of these abrupt changes seen in Fig. 4.7a, it is inevitable to avoid connection losses, which will reduce the QoS of the communication network. Fig. 4.7b shows where the negative offset value is added to the FBS' received power when UE is at the handover spot area. In this case, the UE will preemptively connect to the macro BS, as it has the highest SINR value at that point. However, there will be another handover in a very short time when UE moves outside, as SC BS has a higher SINR than the macro BS. The extra loading on the macro BS and the unnecessary handover occurrence in this scenario show that this scenario is not feasible. Hence, we propose adding a positive offset value to the closest small BS' SINR value, as shown in Fig. 4.7c; this way, the UE can connect pre-emptively to the SC BS before moving outdoors. Therefore, the positive offset is added to the closest small BS's SINR value as we proposed in Algorithm 1 Step 8 ($2 \times SINR_{outdoorBS}$). Thanks to this rapid increase from the offset value shown in Fig. 4.7c the user can accommodate the closest small BS preemptively, avoiding the ping pong between macro and small outdoor BSs. Thus, transitioning between these two BSs becomes seamless while maintaining the QoS, as we aim to reduce the latency [1] by initiating advance preparation of the HO procedure.

4.3.3 I_2O Handover Signalling Cost

To evaluate the performance of the proposed I_2O handover algorithm, HO signalling cost is employed. The required time for delivering and processing the signalling messages is stated as the transmission cost, and processing cost in [178]. The one-way transfer delay between a pair of nodes is the transmission cost; the delay in processing one message in one node is the processing cost. Despite the lengths of handover messages are varied, we use the assumption made in [158] for

[1] in mm-wave driven UDN whose coverage is isolated because of the high penetration losses

simplicity, i.e., transmission cost for different messages among the same pair of nodes is the same regardless of the message size. A similar assumption goes with the processing time, i.e., the processing time is the same for the different messages at the same node. Moreover, we follow [158] by assuming that the mobility management entity (MME) and the serving gateway (S-GW) are located in the same location. Therefore the transmission delay among these nodes is constant and can be neglected. The HO signalling cost, C_{HO} provided in Fig. 4.8 for the

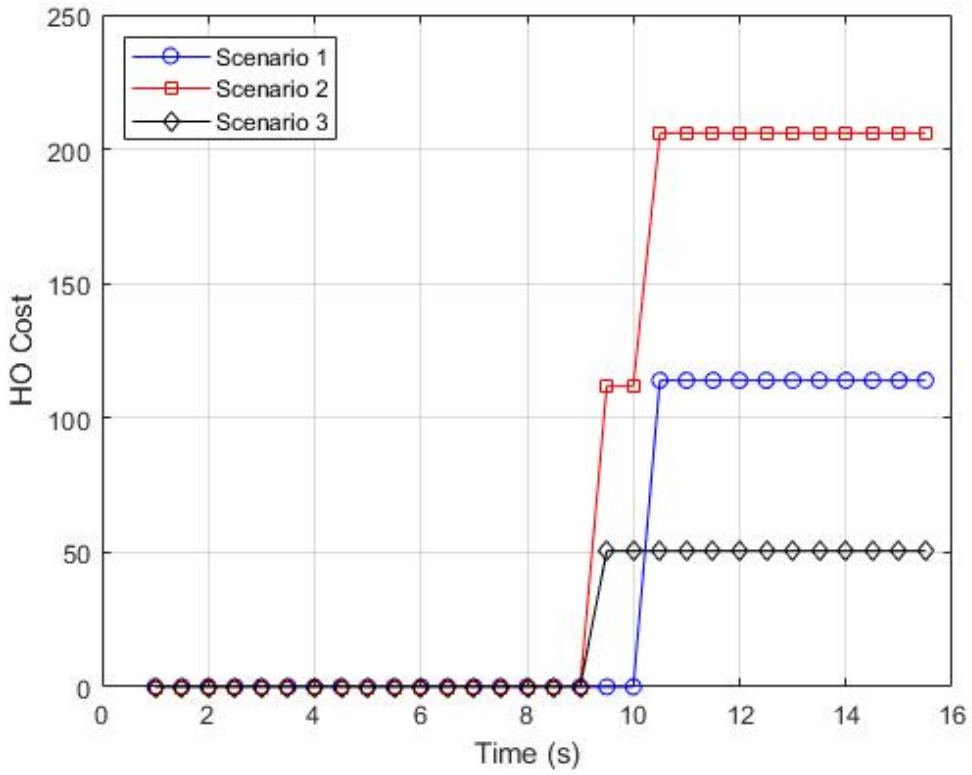

Figure 4.8: HO signalling cost for the proposed scenarios.

three different scenarios discussed in previous sections, is calculated by [179]:

$$C_{HO} = \sum \psi_{i,j} + \sum \gamma_i, \tag{4.11}$$

where $\psi_{i,j}$ is denoted as the one way transmission cost among nodes i and j, and γ_i is the processing cost in node i. Scenario 1 is the regular case where a traditional handover algorithm is implemented. In scenario 2, the SINR of

the FBS is decreased by an offset value to enable the comparison observations between scenario 3. Finally, scenario 3 is where the proposed I_2O algorithm is implemented by adding a positive offset value to the nearest small BS in the outdoor. As it is clearly seen that the proposed algorithm applied in scenario 3 outperforms the other two scenarios by more than 50%, bringing the signalling costs from 115 in scenario 1 to only 50 in scenario 3.

4.4 Conclusions

This chapter has a two-fold contribution with a comprehensive study on mm-wave handovers. First, a user-based indoor mobility prediction via Markov chain with an initial transition matrix is proposed, acquired from Q-learning algorithms. Results show that the model using an initial transition matrix has slightly higher accuracy, with a price of more complexity, as the system needs prior training based on historical data. Therefore, we propose an online learning method for the transition matrix when no user mobility data is available. Based on this acquired knowledge of the user's mobility in the indoor environment, among other functionalities, preemptive handovers for mm-wave communications can be applied to reduce handover latency in densely deployed SC networks. In the second step, depending on the user's indoor mobility history acquired from the first step, we propose a pre-emptive indoor-to-outdoor handover algorithm to maintain the high QoS for indoor users transitioning between indoor and outdoor regions in a heterogeneous network environment. The implementation and evaluation of our proposed algorithm show a reduction in the handover signalling costs by more than 50%, outperforming conventional handover algorithms. Since mm-wave networks are now being commercially deployed in indoor environments, as future work, the proposed IMPRESS framework and the proposed handover algorithm will be applied to scale up dense femto-cell deployments in order to analyse the performance in a more comprehensive and real-life scenario.

Chapter 5

IRS Assisted Handover for Next Generation Networks

5.1 Introduction

The 5G and beyond mobile network is anticipated to bring a boost in low latency communication, spectral efficiency and user connection density [180]. Ultra-reliable low latency communications (URLLC), massive machine-type communications (MMTC) and enhanced mobile broadband (eMBB) are the main use cases that are encompassed by the 5G vision [181]. Wireless communications are currently conducted in sub-6 GHz channels [182]. The millimetre wave spectrum, between 10 GHz to 70 GHz, has been certified by the International Telecommunication Union (ITU) to maximise the possibilities for 5G and beyond [182, 183]. By raising the frequencies for transmission to the millimetre wave (mm-wave) spectrum, a 100-fold improvement in bandwidth can be achieved [182, 184, 185]. Due to its unfavourable propagation characteristics, including path loss, atmospheric and rain absorption, low diffraction and object penetration, significant phase noise, and expensive cost, mm-wave was previously considered unsuitable for mobile communications [128, 186]. One strategy for combating the radio environment's poor propagation effects, notably in the mm-wave band, is the utilisa-

tion of massive antenna arrays with narrow beams to coherently steer the beam energy [182, 183]. The massive multiple input and multiple output (mMIMO) beamforming approaches have been utilised to address the significant free space path loss in the mm-wave frequency [187]. The outdoor-to-indoor coverage in mm-wave bands is severely constrained, even with beamforming. Thanks to recent developments in the technology of metamaterials, a newer technology known as intelligent reflecting surface (IRS) is quickly becoming a household name in academia and within the industry, as it has the ability to overcome the poor propagation effects of the wireless channel [188]. IRS is a cutting-edge hardware innovation that has the potential to improve signal coverage and save energy consumption at a cheaper deployment cost [188]. As a result of advancements in artificial electromagnetic materials, it is now possible to use digital, programmable, and reconfigurable techniques to manage the communication environment using the IRS [189]. More detailed information on IRS fundamentals is presented in 5.1.2. To meet the rising data traffic demands, ultra-cell densification is a critical strategy backed by mm-wave communications. Reduced base station (BS) coverage could lead to fewer customers being served by each BS, increasing frequency reuse and spectral efficiency of the mm-wave network. Nevertheless, an increased handover (HO) rate is an obvious result of densification planning, i.e. the successive change of handling BS for a moving user. The increase in capacity is attained with this method, albeit at the expense of increased HO rates and higher signalling overheads imposed by the HO technique. Signalling overheads disrupt data flow and degrade user throughput [84,190]. Future cellular networks must be able to accommodate data-intensive applications with higher data rates, possibly through cell densification (small cells). In addition to offering high data rates, it is crucial to offer secure HO mechanisms since these directly impact the end-perceived user's quality of experience (QoE).

Fewer works are devoted to HO management regarding small cell investigations, with the bulk focusing entirely on capacity and throughput analysis. How-

ever, a real obstacle still exists in the form of dependable HO systems that offer high data rates for users with moderate to high speeds in metropolitan settings. Cellular network mobility mechanisms allow users to move anywhere within the coverage area while still being serviced. In general, we can divide radio access mobility into two distinct procedures: cell (re-)selection and HO. Cell (re-)selection occurs when the UE is in Idle mode, i.e. there is no active transmission/reception and the need to choose a suitable cell to camp on to be reachable when incoming data is available (then transitioning to active or Connected mode). Cell reselection will be initiated whenever a new camping cell is assessed to be superior to the present one. Unlike cell (re-)selection, HO occurs when the UE is in Connected mode, and a better-serving cell is considered preferable to the current cell.

Coverage blind areas, wherein there is no direct line-of-sight connection between a user and a BS, are one of the problems that reduce the user's QoE because of the aforementioned coverage footprint drawbacks in mm-wave communication systems. This chapter introduces the IRS-assisted HO algorithm for the users in coverage blind areas, providing seamless coverage to the users in these coverage blind areas.

The remainder of this chapter is organized as follows. As this chapter proposes utilizing IRS to reduce the latency of HO, the following sections are split into giving introductions to IRS and the reference signals that are used as a key role in the HO management of this chapter. Section 5.1.1 summarizes reference signals in NR. Section 5.1.2 gives the introduction to IRS fundamentals. Section 5.2.1 introduces the methodology used in IRS, and Section 5.2.2 presents the HO model with IRS. The results are presented in Section 5.3. Finally, Section 5.4 concludes this chapter and its contributions.

5.1.1 Reference Signals in NR

Only if necessary, reference signals are transmitted in NR. Following is a list of them:

- *Positioning Reference Signal (PRS)*: This new reference signal supports DL-based positioning. The UE records the arrival timings of PRSs provided by several base stations, allowing the location server to identify the UE position.
- *Sounding Reference Signal (SRS)* helps the gNB estimate the CSI by transmitting SRS from the UE. As part of massive MIMO and UL beam management, SRS is also used for reciprocity.
- *Demodulation Reference Signal (DMRS)* measures the radio channel specific to each UE, as part of MIMO multi-layer transmission and low latency applications.
- *Channel-State Information Reference Signal (CSI-RS)*: As part of its channel evaluation, the UE receives the CSI-RS, which is then transferred to the gNB along with the channel quality information.
- *Phase-Tracking Reference Signal (PTRS)*: In an OFDM signal, PTRS mitigates phase noise caused by subcarrier rotation caused by mm-wave frequencies. Oscillator phase noise is compensated by PTRS.
- *Primary synchronization signal (PSS)*: helps the UE to identify the cell identity and determine the radio frame boundary, and is a physical layer-specific signal.
- *Secondary synchronization signal (SSS)*: Additionally to the PSS, SSS helps the UE identify the cell ID group at the physical layer.

Fig. 5.1 illustrates the UE's positioning with PRS. It is possible to see each beam as a resource, and the measurements can be collected across one or more

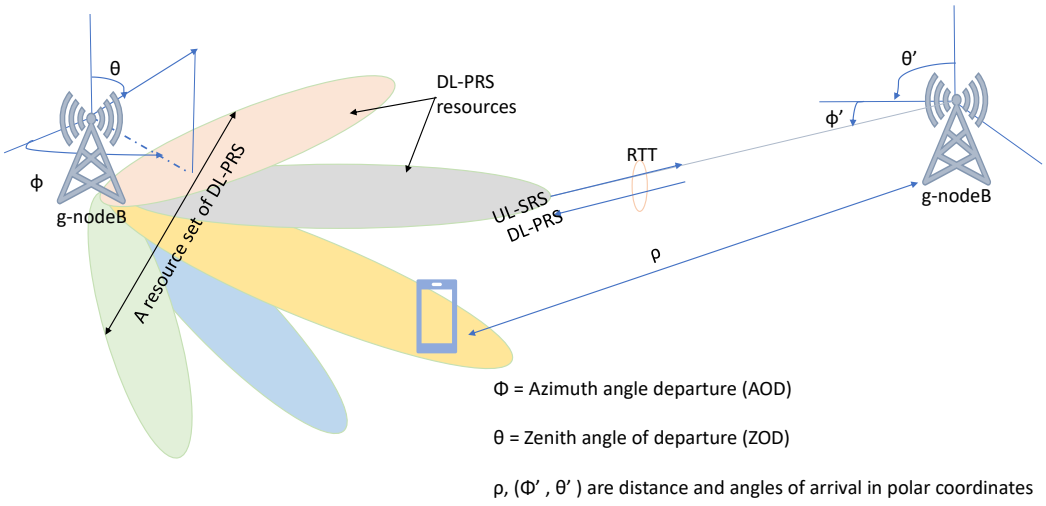

Figure 5.1: llustration of the UE positining with PSR [191].

resources. A variety of positioning methods may require different measurements, and measurements may be collected over a variety of resources or resource sets. Among the new methods supported by 5G is round trip time (RTT) and angle-based positioning. For several applications of 5G, this includes the addition of new positioning methods and the enhancement of existing positioning methods.

5.1.2 IRS Fundamentals

Intelligent reflective surfaces (IRS), also known as software-controlled metasurfaces, are man-made electromagnetic surfaces, consisting of a wide array of passive scattering devices with the ability to regulate how the waves that reach them are reflected. The IRS provides an alternative to relaying and backscattering communications. The IRS consists of many small, reconfigurable, low-cost passive reflecting elements, which, by controlling the phase shift of the impinging electromagnetic wave, can optimize signal strength and mitigate interference by modifying the propagation characteristics between the transmitter and receiver. With the IRS elements, electromagnetic waves are reflected independently, with

a phase shift that can be adjusted. Moreover, as the IRS is passive, there is no dedicated energy source for RF processing, encoding, or decoding the incident signal. Due to its only reflection of incident signals without any transmission modulation, IRSs are an energy-saving alternative to amplify-and-forward (AF) relays [182, 192]. Therefore, IRS enables controlling the propagation environment by simply placing them in between the transmitter and receiver [193, 194]. The following is a list of some advantages of wireless communications supported by the IRS.

Simple installation and sustainable operation: An IRS composed of low-cost passive elements that allow many reflecting elements to be embedded on a single metasurface, allowing it to be easily deployed on buildings, walls, ceilings, and underground tunnels with a clear line of sight (LoS) to the base station (BS). Furthermore, the absence of RF chains induces an IRS to consume very little power.

Flexible reconfiguration through beamforming: Passive beamforming can be accomplished by optimising the phase shift of each scattering element simultaneously. The incident signal could be easily and effectively directed towards the user and cancelled in other directions by deploying the significant number of reflecting elements, hence the overall performance gain of the wireless network is enhanced.

Reduction in cell edge outage: Users receive lower signal power and higher interference at the cell edge. In this case, an IRS can improve overall signal quality for cell-edge users by suppressing interference.

Applications: An IRS will be required to meet the very high data rate specifications of emerging technologies such as virtual reality (VR), holographic communication, and other IoT applications. The IRS is used to intelligently control signal propagation in areas such as non-line-of-sight (NLoS) trans-

mission and blockages, smart wireless power transfer, enhanced security, interference cancellation, and so on [182].

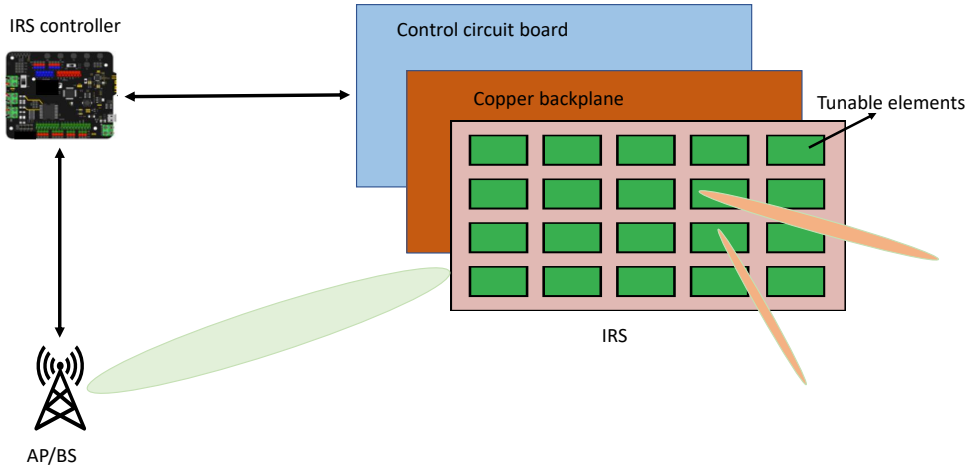

Figure 5.2: Architecture of an IRS [182].

In Fig. 5.2 a typical architecture of IRS that consists of three layers and a smart controller is depicted. To directly modify incident signals, a large number of tunable/reconfigurable metallic patches are printed on a dielectric substrate in the first/outside layer. A copper plate is typically used in the second or intermediate layer to reduce signal energy leakage during IRS reflection. The third/inner layer is made up of a control circuit board with real-time steering capabilities for the reflection's phase and amplitude. Additionally, a smart controller which can be constructed using a field-programmable gate array (FPGA), is attached to each IRS to trigger and regulate the reflection adaptations [195]. Moreover, the IRS controller serves as a communication gateway for other network elements (such as BSs/APs and user terminals) via wired or wireless backhaul/control lines.

5.2 Methodology

Connection loss inside coverage blind areas is a significant problem if the coverage inside this area is not properly addressed, as we mentioned previously. In this section, we provide a smart solution for maintaining the user's connection inside the coverage blind area by deploying IRS, as well as present a pre-emptive handover algorithm for the user moving from one BS's coverage to another BS's coverage. Fig. 5.3 illustrates the simulation scenario, in which a user has to pass through the coverage blind area while moving from source BS's coverage to target BS's coverage. Since there is no direct link between the user and the source BS due to the blockage between them, an IRS is mounted on the wall where a direct line of sight is available, to maintain the communication between the source BS and the UE.

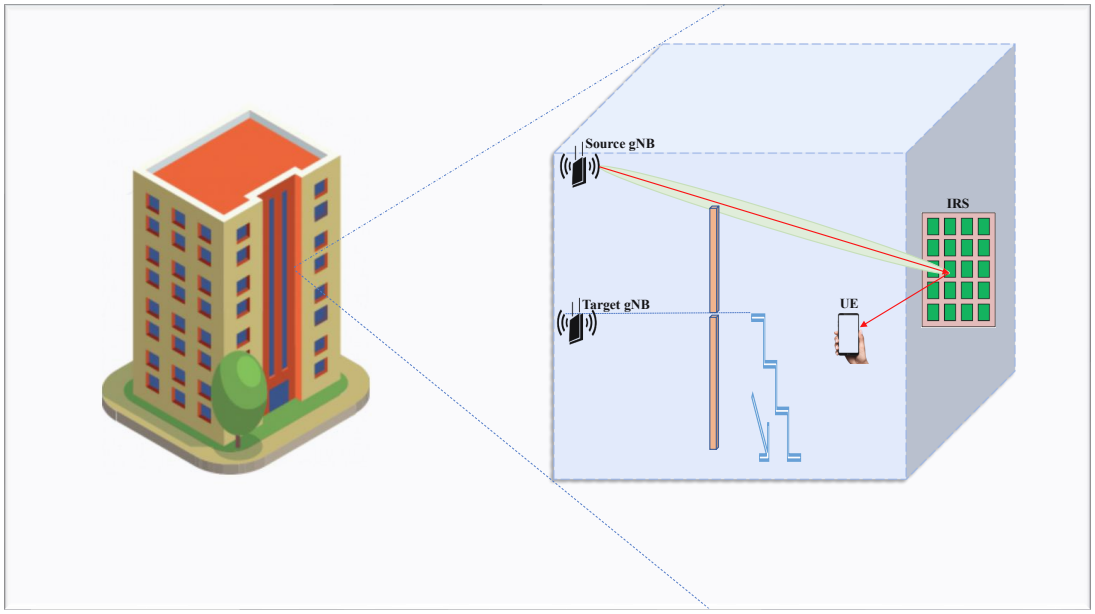

Figure 5.3: Simulation scenario with the IRS in coverage blind area.

The simulations in this chapter are conducted by using MATLAB™ software. The following sections introduce the IRS system model that is used to provide coverage in the coverage blind area, then present the HO system model with the proposed HO algorithm.

5.2.1 IRS System Model

The system model of IRS here consists of M elements shaping a uniform linear array (ULA). Since there is no direct link communication between the UE and FBS because of the blockage in-between as shown in Fig. 5.4, We consider the communication is provided by narrowband line-of-sight (LOS) transmission in the far field between the UE and the source BSs. The received signal at the UE

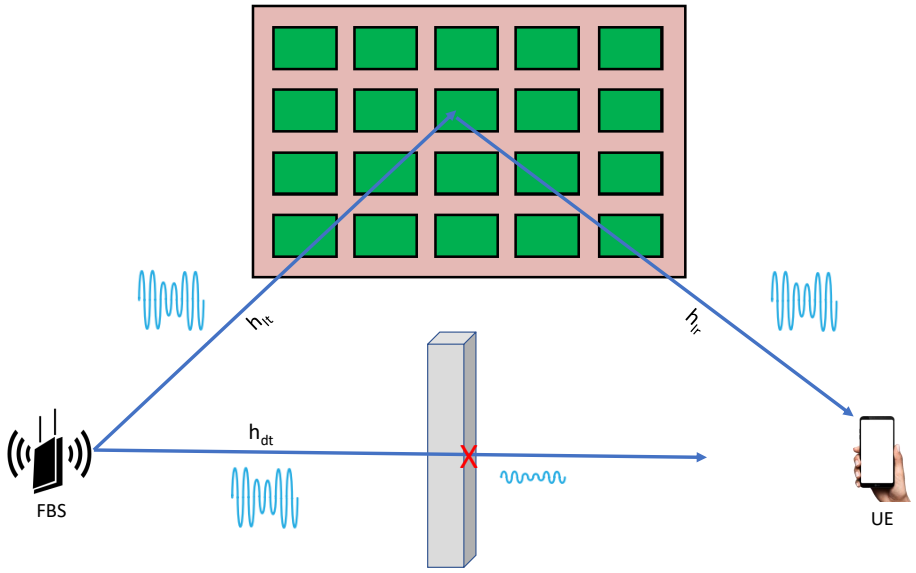

Figure 5.4: IRS communication channel representation.

end can be stated as

$$y = (h_{dt} + \mathbf{h_{Ir}^H W h_{It}})s + n, \tag{5.1}$$

where $h_{dt} \epsilon C^{1*1}$, $\mathbf{h}_{It} \epsilon \mathbb{C}^{M*1}$, $\mathbf{h}_{Ir} \epsilon \mathbb{C}^{M*1}$ correspond the direct channel between the source BS, FBS, and the UE, FBS to IRS, and IRS to UE, respectively. The weight matrix W $\epsilon \mathbb{C}^{M*M}$ is a diagonal matrix that contains the RIS weights of each surface element for each entity on the diagonal [196]. The s is the source signal from the FBS, and n is the noise of the channel. As there is no direct line-of-sight between the source FBS and the UE by virtue of the blockage, the reflection channel, $\check{H}$=$\mathbf{h_{Ir}^H W h_{It}}$ becomes the major source of the communication. Therefore, we concentrate on $\check{H}$ which may be represented as follows using

steering vectors and weight vector [197]

$$\check{H} = \mathbf{w}^H \cdot [b(\Omega_i) \odot b(\Omega_o)], \tag{5.2}$$

where $\mathbf{w}$ is a column vector whose elements are $\mathbf{W}$'s primary diagonal elements. It is important to note that $\mathbf{w}$ is the single weight vector used on the surface to concurrently accomplish the required signal response and mutual interference reduction for the transceiver pair. Additionally, the steering vectors of the channels between the source FBS and IRS, and IRS and UE are

$$b(\Omega_i) = [b(\Omega_{i,1}), ..., b(\Omega_{i,m}), ..., b(\Omega_{i,M})]^T, \tag{5.3}$$

$$b(\Omega_o) = [b(\Omega_{o,1}), ..., b(\Omega_{o,m}), ..., b(\Omega_{o,M})]^T, \tag{5.4}$$

where Ω_i and Ω_o are the terms describing, correspondingly, the spatial information incident from the source FBS at IRS m-th element and the spatial information reflected from m-th element to UE.

Note: Notations that are used in this section represent respectively; scalar values are denoted by lightfaced letters, whereas matrix or column vectors are denoted by boldfaced letters. The transpose, conjugate, and conjugate transpose operations are denoted by the superscripts $(\cdot)^{\mathbb{T}}$, $(\cdot)^*$, and $(\cdot)^{\mathbb{H}}$, accordingly. The $\odot$ represents point-wise multiplication.

5.2.2 HO System Model

The basic NR handover signalling procedure in [86] is updated in this work with the employment of IRS technology. The aim is to eliminate the coverage holes/gaps within the indoor environments by simply deploying the IRS, where there is no direct link between the UE and the base stations.

There are two types of NG Radio Access Network nodes connected to the 5G core network that are gNB and ng-eNB. A gNB supports NR control-plane and

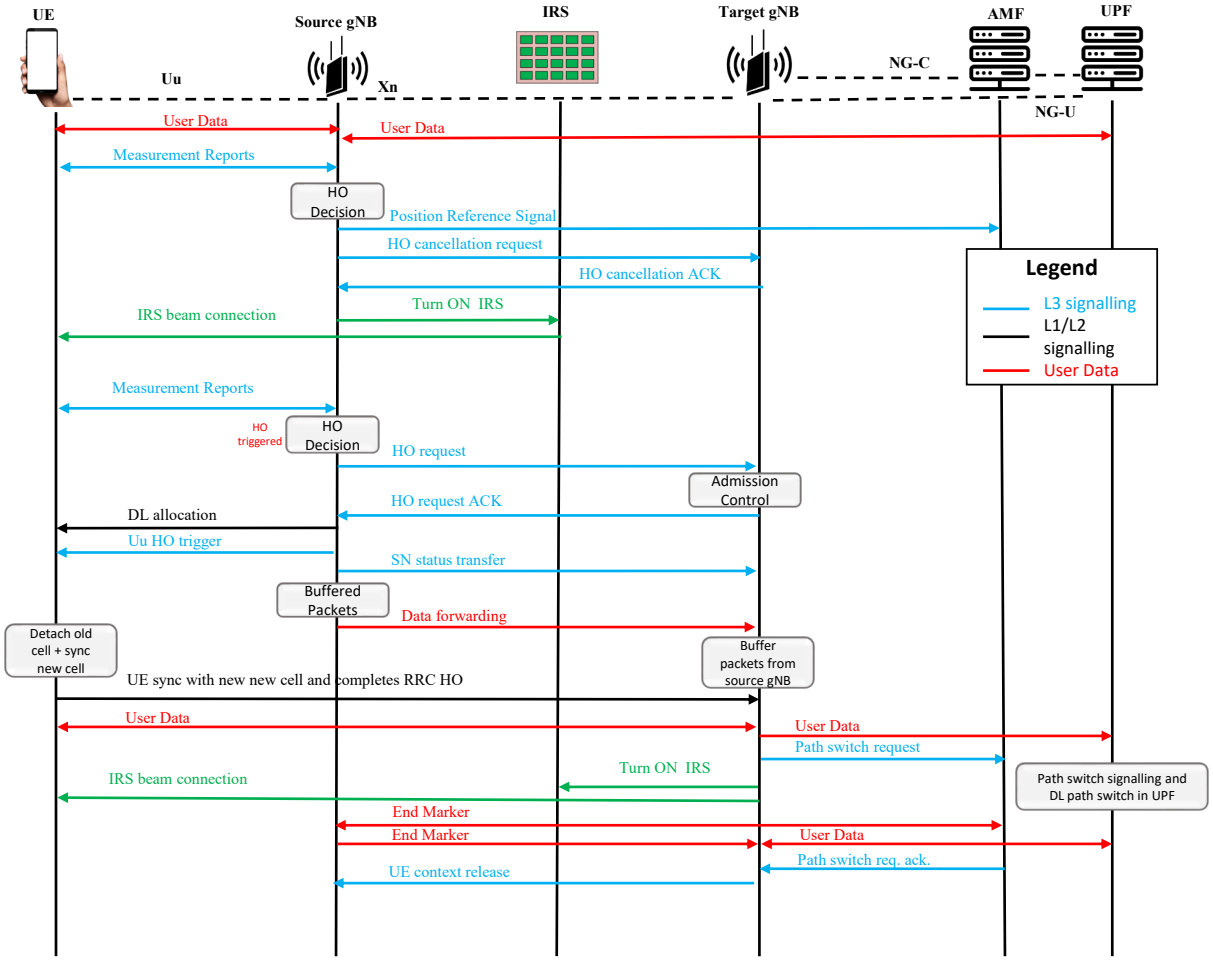

Figure 5.5: Handover signalling in 5G NR with IRS.

user-plane protocols to the NR devices and, an ng-eNB uses the LTE control-plane and user-plane protocols to serve the LTE devices [73]. The proposed HO signalling procedure with IRS, shown in Fig. 5.5, and the detailed flowchart shown in Fig. 5.6 begins by checking if a UE needs a handover:

1. By sending measurement reports to the source gNB, next-generation Node B in 5G.

2. The source gNB receives the measurement report indicating that a HO is required, and process this report by checking PRS.

3. After the UE's position is confirmed by the PRS report, the HO request is cancelled, as the position of the UE could be served by IRS.

4. IRS is turned on by source gNB and a beam is created to connect the link between the UE and the IRS.

5. Measurement report sent and a handover decision is made in the serving gNB, using RRM (Radio Resource Management) information and the measurement report.

6. The handover request message, including the required data for preparing the HO at the target BS side, is sent from the connected gNB to the target gNB.

7. Admission Control procedure will be performed in this step if the target gNB can grant the resources.

8. The target gNB sends a handover request acknowledgement message to the serving gNB, and the forwarding of data can be initiated once the serving gNB receives it.

9. UE receives the handover command from the serving gNB.

10. The Sequence Number (SN) message is sent from the serving gNB to the target gNB to keep track of the ordering of the packets.

11. The UE disconnects from the serving gNB and synchronizes to the target gNB.

12. IRS is turned on by the target gNB and a beam is created to connect the link between the UE and the IRS at the coverage blind area.

13. The target gNB informs AMF that UE has changed the cell via the Path Switch Request message.

14. NR core shifts the DL data path towards the target side.

15. The path switch request acknowledgement is sent by the AMF to the target gNB.

16. The serving gNB receives successful handover information from the target gNB, and activates the release of resources via UE context release message.

The radio resources related to the UE are released eventually by the serving gNB [74].

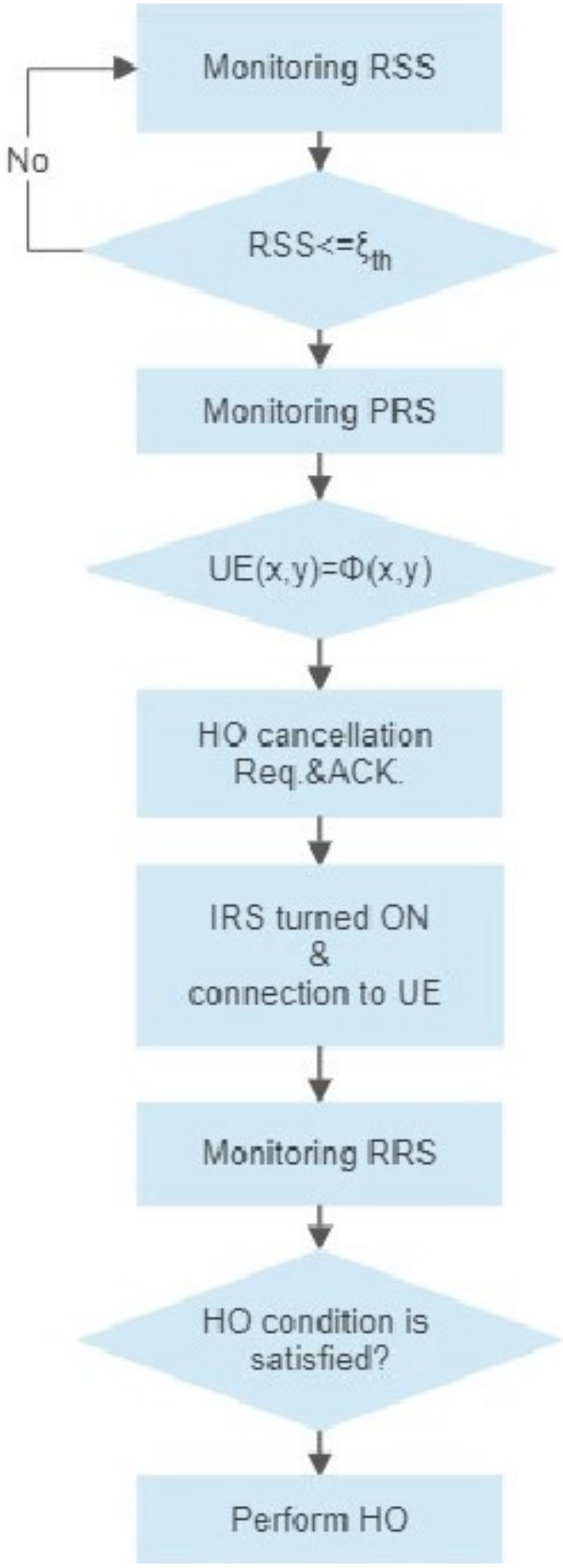

Figure 5.6: Flowchart of the proposed algorithm.

5.3 Simulation Results

5.3.1 IRS Beam Coverage

In this section, we provide the continuation of the communication within the coverage blind area by placing IRS to the wall, as it is shown in Fig 5.3. The path-loss $P_{IRS,uv}$ is presented by [193]

$$P_{IRS,uv} = \frac{G_t G_r}{(4\pi)^2}\left(\frac{S}{d_{tx} d_{rx}}\right)^2 \cos^2(\Omega_{in,u}) \tag{5.5}$$

where the transmitting and receiving antenna gains are Gt and Gr, respectively. The distances from transmitter to IRS, and from IRS to receiver, correspondingly, are d_{tx}, and d_{rx}, and S is the effective area of a single IRS element.

The beampattern presented in Fig. 5.7 shows the max gain on the amplitude to cover the coverage blind area. The transmitter and receiver pair is located at $\Omega_i = (45°, 110°)$, to maintain users' connection to the source BS in the coverage blind area. The beam perfectly covers the coverage blind area, with a maximum peak at the received power of 36.12 dB. Thus, the result provides that the coverage in the blind area can be supported by utilizing IRS.

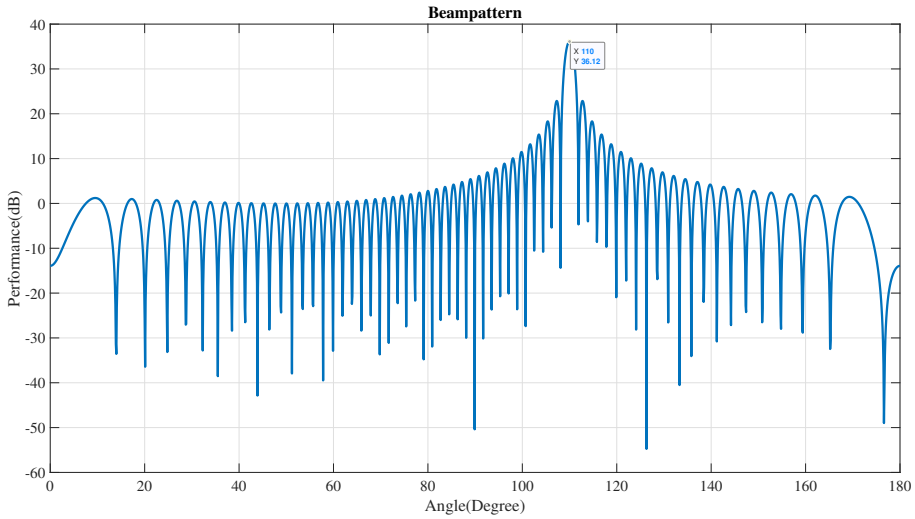

Figure 5.7: IRS beam pattern in coverage blind area.

5.3.2 HO Signalling Cost

In this section, the HO signalling cost is used to assess the performance of the suggested pre-emptive handover method. The cost of HO signalling can be defined in terms of the time delay that is necessary to send and process HO messages [178].

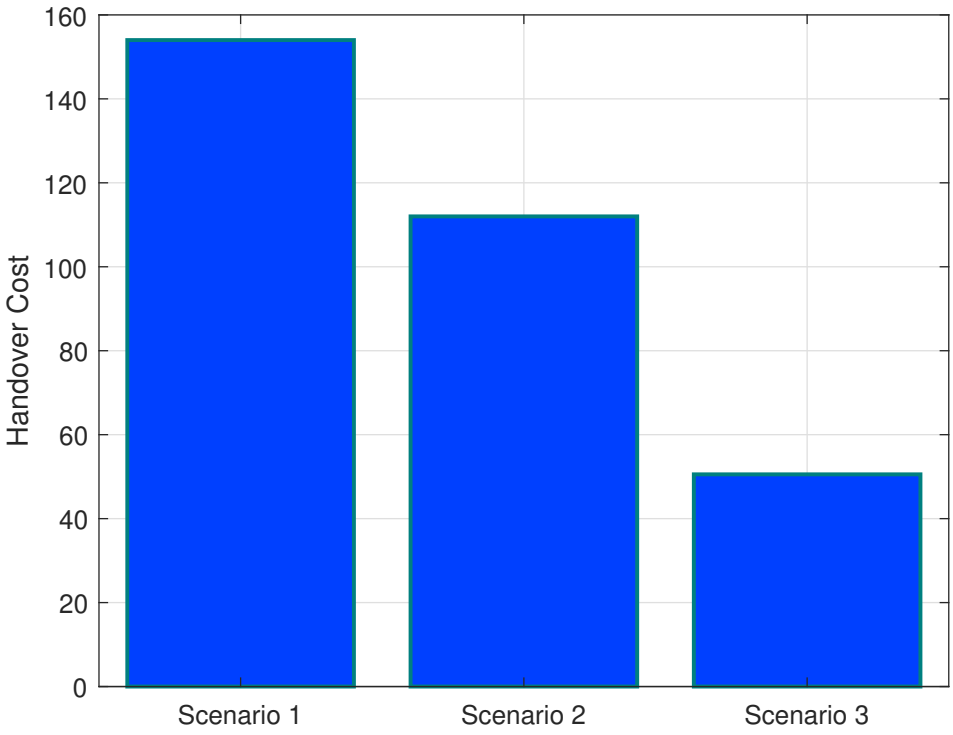

Figure 5.8: HO cost comparison.

Despite the lengths of handover messages are varied, we use the assumption made in [178] for simplicity, i.e., transmission cost for different messages among the same pair of nodes are the same regardless of the message size. A similar assumption goes with the processing time, i.e., the processing time is the same for the different messages at the same node. Moreover, we follow [158] by assuming that the mobility management entity (MME) and the serving gateway (S-GW) are located in the same location. Therefore the transmission delay among these nodes is constant and can be neglected. The HO signalling cost, C_{HO} provided in Fig. 5.8 for the three different scenarios discussed in previous sections, is cal-

culated by [179]:

$$C_{HO} = \sum \psi_{i,j} + \sum \gamma_i, \tag{5.6}$$

where $\psi_{i,j}$ is denoted as the one way transmission cost among nodes i and j, and γ_i is the processing cost in node i.

To evaluate the HO costs, three different scenarios are created. In Scenario 1, we calculated the HO cost when IRS is not deployed in the coverage blind area. In Scenario 2, the HO cost is calculated when IRS is deployed in the coverage blind area. In Scenario 3, the HO cost is calculated when the pre-emptive HO algorithm is used with the help of the IRS in the coverage blind area.

5.4 Conclusions

In this chapter, we provided a solution for seamless coverage and handover to the users who are moving from one BS's coverage to the next BS however, has to pass through a coverage blind area, where there is no direct LOS between the user and the source BS because of the blockage between them. To provide robust coverage for the users in Connected mode within these coverage blind areas, we propose implementing IRS, which is a more cost-effective solution than the deployment of APs. The results show that the users can maintain their connection to the serving BS, thanks to the IRS which is implemented in the coverage blind area. Secondly, this chapter provides a pre-emptive handover algorithm in which the handover is initiated at the IRS. The results show that when the proposed pre-emptive handover algorithm at the IRS is applied; the handover cost is reduced by nearly around 33% compared to the case when IRS is not utilized in the coverage blind area. Therefore, the proposed pre-emptive handover algorithm supports seamless transitioning and reduces handover cost, in return the QoE system is increased.

Chapter 6

Conclusion and Future Work

This chapter draws conclusions and discusses possible extensions of the previous chapters.

6.1 Conclusions

Densely deployment of the small cells in $5G$ networks will bring high-quality service to the end users as well as will solve the small footprint coverage problem of mm-waves. The increase in the number of small cells will require self-organized systems to enable the seamless transaction between heterogeneous network environments. Therefore, a survey-style study on self-organized seamless coverage in $5G$, covering mm-wave features and its indoor and outdoor coverage along with some machine learning techniques, handover and mobility management in mm-wave are presented in Chapter 2.

In an mm-wave-driven small cell environment, outdoor base stations will get closer to the buildings, in which users are covered and served by indoor small cells that in turn degrade the user's QoE owing to the increased interference caused by the outdoor BSs. In Chapter 3, indoor coverage analysis is conducted by considering a scenario, which includes a multi-storey building and two identical indoor femtocell and outdoor BS operating at 28 GHz. Throughout the simulations, the

impacts of frequency-sensitive materials used in the building wall are investigated for indoor coverage in the context of the outdoor BS's transmit power and the distance from the building. The results show the importance of choosing a proper material type when outdoor BS is close to the building.

Providing a seamless connection to mm-wave users, transitioning between indoor and outdoor in a heterogeneous network environment particularly, is a significant issue that needs to be addressed. Therefore, a two-fold contribution with a comprehensive study on mm-wave handovers is proposed in Chapter 4. A user-based indoor mobility prediction via a Markov chain with an initial transition matrix is proposed in the first step. Based on this acquired knowledge of the user's movement pattern in the indoor environment, a pre-emptive handover algorithm is presented in the second step. This algorithm aims to keep the QoS high for indoor users when transitioning between indoor and outdoor in a heterogeneous network environment. The proposed algorithm shows a reduction in the handover signalling cost by more than 50%, outperforming conventional handover algorithms.

Chapter 5, proposes a solution for seamless coverage and handover to the users who are moving from one BS's coverage to the next BS, however, has to pass through a coverage blind area, where there is no direct LOS between the user and the source BS because of the blockage between them. To provide robust coverage for the users in Connected mode within these coverage blind areas, this chapter proposes implementing IRSs, a more cost-effective solution than deploying APs. Moreover, a pre-emptive handover algorithm is proposed to support seamless transitioning and reduces handover cost by nearly %33; in return, the QoE system is increased.

6.2 Future Work

The potential extensions to each chapter in this thesis follow as:

- The work proposed in Chapter 3 is planned to be extended by studying the interference effect under the multiple base stations. Also, one of the plans is to create the interference heatmap of our office inside the James Watt South Building by using TSMA6 as the office is currently operating under a heterogeneous network environment. Thus, a data set would be available for the future research area.

- Since mm-wave networks are now being commercially deployed in indoor environments, as future work of Chapter 4, the proposed IMPRESS framework and the proposed handover algorithm will be applied to scale up dense femtocell deployments in order to analyse the performance in a more comprehensive scenario.

  Moreover, different AI models could be explored as indoor localization of the UE and predicting the UE's next movement in the indoor environment.

- The work presented in Chapter 5 portrays a real-life problem in a simulation environment, however for future work, this algorithm could be implemented where the IRSs is deployed in a real system, and the simulation system results could be evaluated within this system, in which more constraints of the system needs to be taken into account.

  Additionally, the IRS model could be extended to more sophisticated beamforming algorithms to enable multi-user case system scenarios.

Bibliography

[1] BBC News, "China rolls out 'one of the world's largest' 5G networks," https://www.bbc.co.uk/news/business-50258287, 2019, Accessed: 2020-06-24.

[2] N. Al-Falahy and O. Y. Alani, "Millimetre wave frequency band as a candidate spectrum for 5G network architecture: A survey," *Physical Communication*, vol. 32, pp. 120–144, feb 2019.

[3] P. Fazio, F. De Rango, and M. Tropea, "Prediction and qos enhancement in new generation cellular networks with mobile hosts: A survey on different protocols and conventional/unconventional approaches," *IEEE Communications Surveys Tutorials*, vol. 19, no. 3, pp. 1822–1841, thirdquarter 2017.

[4] I. Stojmenovic, *Handbook of wireless networks and mobile computing*. Wiley Online Library, 2002.

[5] M. Mamman, "Call admission control algorithm with efficient handoff for both 4G and 5G networks," *International Journal of Wireless & Mobile Networks (IJWMN) Vol*, vol. 13, 2021.

[6] B. V. Quang, R. V. Prasad, and I. Niemegeers, "A survey on handoffs — lessons for 60 GHz based wireless systems," *IEEE Communications Surveys Tutorials*, vol. 14, no. 1, pp. 64–86, 2012.

[7] Z. Xiao, H. Liu, V. Havyarimana, T. Li, and D. Wang, "Analytical study on multi-tier 5g heterogeneous small cell networks: Coverage performance and energy efficiency," *Sensors*, vol. 16, no. 11, p. 1854, 2016.

[8] J. Zander, S.-L. Kim, M. Almgren, and O. Queseth, *Radio resource management for wireless networks*. Artech House, Inc., 2001.

[9] N. D. Tripathi, "Generic adaptive handoff algorithms using fuzzy logic and neural networks," Ph.D. dissertation, Virginia Tech, 1997.

[10] J. P. Mkel, "Effects of handoff algorithms on the performance of multimedia wireless networks," Ph.D. dissertation, Faculty of Tech. of the Univ. of Oulu, 2008.

[11] M. D. Austin and G. L. Stuber, "Velocity adaptive handoff algorithms for microcellular systems," *IEEE Transactions on Vehicular Technology*, vol. 43, no. 3, pp. 549–561, 1994.

[12] G. Azemi, B. Senadji, and B. Boashash, "Mobile unit velocity estimation based on the instantaneous frequency of the received signal," *IEEE Transactions on Vehicular Technology*, vol. 53, no. 3, pp. 716–724, 2004.

[13] M. D. Austin and G. L. Stüber, "Direction biased handoff algorithms for urban microcells," *Wireless Personal Communications*, vol. 3, no. 3, pp. 287–298, 1996.

[14] Chen-Nee Chuah and R. D. Yates, "Evaluation of a minimum power handoff algorithm," in *Proceedings of 6th International Symposium on Personal, Indoor and Mobile Radio Communications*, vol. 2, 1995, pp. 814–818 vol.2.

[15] P. Israt, N. Chakma, and M. M. A. Hashem, "A fuzzy logic-based adaptive handoff management protocol for next-generation wireless systems," in *2008 11th International Conference on Computer and Information Technology*, 2008, pp. 288–293.

[16] T. Coqueiro, J. Jailton, T. Carvalho, and R. Francês, "A fuzzy logic system for vertical handover and maximizing battery lifetime in heterogeneous wireless multimedia networks," *Wireless Communications and Mobile Computing*, vol. 2019, 2019.

[17] A. Çalhan and C. Çeken, "Artificial neural network based vertical handoff algorithm for reducing handoff latency," *Wireless Personal Communications*, vol. 71, no. 4, pp. 2399–2415, nov 2012.

[18] A. Aibinu, A. Onumanyi, A. Adedigba, M. Ipinyomi, T. Folorunso, and M. Salami, "Development of hybrid artificial intelligent based handover decision algorithm," *Engineering Science and Technology, an International Journal*, vol. 20, no. 2, pp. 381–390, apr 2017.

[19] K. D. Wong and D. C. Cox, "A pattern recognition system for handoff algorithms," *IEEE Journal on Selected Areas in Communications*, vol. 18, no. 7, pp. 1301–1312, 2000.

[20] K. D. Wong and D. C. Cox, "Two-state pattern-recognition handoffs for corner-turning situations," *IEEE Transactions on Vehicular Technology*, vol. 50, no. 2, pp. 354–363, 2001.

[21] K.-L. Yap, Y.-W. Chong, and W. Liu, "Enhanced handover mechanism using mobility prediction in wireless networks," *PLOS ONE*, vol. 15, no. 1, p. e0227982, jan 2020.

[22] A. S. Sadiq, N. B. Fisal, K. Z. Ghafoor, and J. Lloret, "An adaptive handover prediction scheme for seamless mobility based wireless networks," *The Scientific World Journal*, vol. 2014, pp. 1–17, 2014.

[23] H. Zhang and L. Dai, "Mobility prediction: A survey on state-of-the-art schemes and future applications," *IEEE Access*, vol. 7, pp. 802–822, 2019.

[24] 3GPP, "5G; Procedures for the 5G System ," 3rd Generation Partnership Project (3GPP), TS 23.502, June 2018.

[25] M. Ozturk, M. Gogate, O. Onireti, A. Adeel, A. Hussain, and M. A. Imran, "A novel deep learning driven, low-cost mobility prediction approach for 5G cellular networks: The case of the control/data separation architecture (cdsa)," *Neurocomputing*, vol. 358, pp. 479 – 489, 2019. [Online]. Available: http://www.sciencedirect.com/science/article/pii/S0925231219300438

[26] Ericsson, "Ericsson mobility report," Ericsson, Tech. Rep., June 2019. [Online]. Available: https://www.ericsson.com/49d1d9/assets/local/mobility-report/documents/2019/ericsson-mobility-report-june-2019.pdf

[27] G. Xiaodong, H. Jiwei, L. Siyu, L. Jianhua, and D. Mingyi, "Indoor localization method of intelligent mobile terminal based on bim," in *2018 Ubiquitous Positioning, Indoor Navigation and Location-Based Services (UPINLBS)*, March 2018, pp. 1–9.

[28] E. Perez, K.-J. Friederichs, A. Lobinger, B. Wegmann, and I. Viering, "Erratum to: Utilization of licensed shared access resources in indoor small cells scenarios," in *Cognitive Radio Oriented Wireless Networks*, D. Noguet, K. Moessner, and J. Palicot, Eds. Cham: Springer International Publishing, 2016, pp. E1–E1.

[29] S. Hamid, A. J. Al-Dweik, M. Mirahmadi, K. Mubarak, and A. Shami, "Inside-out propagation: Developing a unified model for the interference in 5G networks," *IEEE Vehicular Technology Magazine*, vol. 10, no. 2, pp. 47–54, June 2015.

[30] J. G. Andrews, "Seven ways that hetnets are a cellular paradigm shift," *IEEE Communications Magazine*, vol. 51, no. 3, pp. 136–144, 2013.

[31] D. Helbing and P. Molnar, "Social force model for pedestrian dynamics," *Physical review E*, vol. 51, no. 5, p. 4282, 1995.

[32] A. V. Lopez, A. Chervyakov, G. Chance, S. Verma, and Y. Tang, "Opportunities and challenges of mmWave NR," *IEEE Wireless Communications*, vol. 26, no. 2, pp. 4–6, apr 2019.

[33] T. S. Rappaport, W. Roh, and K. Cheun, "Wireless engineers long considered high frequencies worthless for cellular systems. they couldn't be more wrong," *IEEE SPECTRUM*, vol. 51, no. 9, pp. 34–+, 2014.

[34] J. G. Andrews, S. Buzzi, W. Choi, S. V. Hanly, A. Lozano, A. C. Soong, and J. C. Zhang, "What will 5G be?" *IEEE Journal on selected areas in communications*, vol. 32, no. 6, pp. 1065–1082, 2014.

[35] Z. Pi and F. Khan, "An introduction to millimeter-wave mobile broadband systems," *IEEE Communications Magazine*, vol. 49, no. 6, pp. 101–107, June 2011.

[36] H. T. Friis, "A note on a simple transmission formula," *Proceedings of the IRE*, vol. 34, no. 5, pp. 254–256, 1946.

[37] A. Maltsev, R. Maslennikov, A. Sevastyanov, A. Khoryaev, and A. Lomayev, "Experimental investigations of 60 GHz WLAN systems in office environment," *IEEE Journal on Selected Areas in Communications*, vol. 27, no. 8, pp. 1488–1499, October 2009.

[38] C. R. Anderson and T. S. Rappaort, "In-building wideband partition loss measurements at 2.5 GHz and 60 GHz," *arXiv preprint arXiv:1701.03415*, 2016.

[39] K. Allen, N. DeMinco, J. Hoffman, Y. Lo, and P. Papazian, "Building penetration loss measurements at 900 MHz, 11.4 GHz, and 28.8 GHz," *US*

Department of Commerce, National Telecommunications and Information Administration Rep, pp. 94–306, 1994.

[40] M. Marcus and B. Pattan, "Millimeter wave propagation: spectrum management implications," *IEEE Microwave Magazine*, vol. 6, no. 2, pp. 54–62, 2005.

[41] C. R. Anderson and T. S. Rappaport, "In-building wideband partition loss measurements at 2.5 and 60 GHz," *IEEE Transactions on Wireless Communications*, vol. 3, no. 3, pp. 922–928, May 2004.

[42] G. Durgin, T. S. Rappaport, and Hao Xu, "Measurements and models for radio path loss and penetration loss in and around homes and trees at 5.85 GHz," *IEEE Transactions on Communications*, vol. 46, no. 11, pp. 1484–1496, Nov 1998.

[43] M. Tanvir Kawser, *Determination of penetration losses of various building materials to help design a building with better wireless services.* Department of Architecture, BUET, 2018.

[44] H. Zhao, R. Mayzus, S. Sun, M. Samimi, J. K. Schulz, Y. Azar, K. Wang, G. N. Wong, F. Gutierrez, and T. S. Rappaport, "28 GHz millimeter wave cellular communication measurements for reflection and penetration loss in and around buildings in new york city," in *2013 IEEE International Conference on Communications (ICC)*, June 2013, pp. 5163–5167.

[45] A. Ghosh, "The 5G mmwave radio revolution." *Microwave Journal*, vol. 59, no. 9, 2016.

[46] A. V. Alejos, M. G. Sanchez, and I. Cuinas, "Measurement and analysis of propagation mechanisms at 40 GHz: Viability of site shielding forced by obstacles," *IEEE Transactions on Vehicular Technology*, vol. 57, no. 6, pp. 3369–3380, Nov 2008.

[47] J. Ryan, G. R. MacCartney, and T. S. Rappaport, "Indoor office wideband penetration loss measurements at 73 GHz," in *2017 IEEE International Conference on Communications Workshops (ICC Workshops)*, May 2017, pp. 228–233.

[48] D. Wisely, N. Wang, and R. Tafazolli, "Capacity and costs for 5G networks in dense urban areas," *IET Communications*, vol. 12, no. 19, pp. 2502–2510, 2018.

[49] Y. A. Sambo, G. C. Valastro, G. M. Patane, M. Ozturk, S. Hussain, M. A. Imran, and D. Panno, "Motion sensor-based small cell sleep scheduling for 5G networks," in *IEEE International Workshop on Computer Aided Modeling and Design of Communication Links and Networks, Limassol, Cyprus, 11-13 Sep 2019*, 2019.

[50] D.-Y. Liao and X. Wang, *5G Wireless Micro Operators for Integrated Casinos and Entertainment in Smart Cities*. Cham: Springer International Publishing, 2018, pp. 115–149.

[51] D. Sahinel, C. Akpolat, M. A. Khan, F. Sivrikaya, and S. Albayrak, "Beyond 5G vision for IOLITE community," *IEEE Communications Magazine*, vol. 55, no. 1, pp. 41–47, January 2017.

[52] F. Wiegel, V. Hagenmeyer, and G. Oberschmidt, "Cross-media mesh networks for smart home and smart grid applications," in *2018 IEEE International Conference on Smart Energy Grid Engineering (SEGE)*, Aug 2018, pp. 205–211.

[53] Z. Genc, B. L. Dang, J. Wang, and I. Niemegeers, "Home networking at 60 GHz: challenges and research issues," *annals of telecommunications - annales des télécommunications*, vol. 63, no. 9, pp. 501–509, Oct 2008.

[54] J. Guillory, E. Tanguy, A. Pizzinat, B. Charbonnier, S. Meyer, H. W. Li, and C. Algani, "Radio over fiber tunnel for 60 GHz wireless home network," in *2011 Optical Fiber Communication Conference and Exposition and the National Fiber Optic Engineers Conference*, March 2011, pp. 1–3.

[55] B. L. Dang, M. G. Larrode, R. V. Prasad, I. Niemegeers, and A. Koonen, "Radio-over-fiber based architecture for seamless wireless indoor communication in the 60 GHz band," *Computer communications*, vol. 30, no. 18, pp. 3598–3613, 2007.

[56] N. E. Farid, S. M. M. Hassan, R. Sanusi, and A. I. A. Rahim, "A 2-stage 40 GHz CMOS power amplifier driver for mm-wave radio-over-fiber applications," in *2015 IEEE International Circuits and Systems Symposium (ICSyS)*, Sep. 2015, pp. 55–59.

[57] S. Shin, C. Liu, S. Fan, Y. Hsueh, S. Hsiao, and G. Chang, "A versatile 60 GHz CMOS phased-array transmitter chipset for broadband radio-over-fiber systems," in *Asia-Pacific Microwave Conference 2011*, Dec 2011, pp. 1718–1721.

[58] Z. Genc, G. M. Olcer, E. Onur, and I. Niemegeers, "Improving 60 GHz indoor connectivity with relaying," in *2010 IEEE International Conference on Communications*, May 2010, pp. 1–6.

[59] M. Zhao, D. Liu, and F. Yu, "Improving the robustness of 60 GHz indoor connectivity by deployment of mirrors," in *2018 IEEE 29th Annual International Symposium on Personal, Indoor and Mobile Radio Communications (PIMRC)*, Sep. 2018, pp. 188–193.

[60] Z. Genc, U. H. Rizvi, E. Onur, and I. Niemegeers, "Robust 60 GHz indoor connectivity: Is it possible with reflections?" in *2010 IEEE 71st Vehicular Technology Conference*, May 2010, pp. 1–5.

[61] W. Khawaja, O. Ozdemir, Y. Yapici, I. Guvenc, and Y. Kakishima, "Coverage enhancement for mm wave communications using passive reflectors," in *2018 11th Global Symposium on Millimeter Waves (GSMM)*. IEEE, 2018, pp. 1–6.

[62] L. A. Linares and J. G. Sánchez, "Empirical modeling of femtocell pathloss in a femto-to-macroindoor-to-outdoor interference scenario," Master's thesis, Aalborg University, Denmark, 2011.

[63] R. Baldemair, T. Irnich, K. Balachandran, E. Dahlman, G. Mildh, Y. Selén, S. Parkvall, M. Meyer, and A. Osseiran, "Ultra-dense networks in millimeter-wave frequencies," *IEEE Communications Magazine*, vol. 53, no. 1, pp. 202–208, January 2015.

[64] Y. Niu, C. Gao, Y. Li, L. Su, D. Jin, and A. V. Vasilakos, "Exploiting device-to-device communications in joint scheduling of access and backhaul for mmwave small cells," *IEEE Journal on Selected Areas in Communications*, vol. 33, no. 10, pp. 2052–2069, Oct 2015.

[65] M. Kamel, W. Hamouda, and A. Youssef, "Ultra-dense networks: A survey," *IEEE Communications Surveys Tutorials*, vol. 18, no. 4, pp. 2522–2545, Fourthquarter 2016.

[66] P. Popovski, V. Braun, H. Mayer, P. Fertl, Z. Ren, D. Gonzales-Serrano, E. Ström, T. Svensson, H. Taoka, P. Agyapong *et al.*, "Scenarios requirements and KPIs for 5G mobile and wireless system," *ICT-317669-METIS/D1. 1, ICT-317669 METIS project*, 2013.

[67] D. López-Pérez, M. Ding, H. Claussen, and A. H. Jafari, "Towards 1 Gbps/UE in cellular systems: Understanding ultra-dense small cell deployments," *IEEE Communications Surveys Tutorials*, vol. 17, no. 4, pp. 2078–2101, Fourthquarter 2015.

[68] S. Stefanatos and A. Alexiou, "Access point density and bandwidth partitioning in ultra dense wireless networks," *IEEE Transactions on Communications*, vol. 62, no. 9, pp. 3376–3384, Sep. 2014.

[69] M. Ding, D. Lopez-Perez, G. Mao, P. Wang, and Z. Lin, "Will the area spectral efficiency monotonically grow as small cells go dense?" in *2015 IEEE Global Communications Conference (GLOBECOM)*, Dec 2015, pp. 1–7.

[70] B. V. Quang, R. V. Prasad, and I. Niemegeers, "A survey on handoffs lessons for 60 GHz based wireless systems," *IEEE Communications Surveys & Tutorials*, vol. 14, no. 1, pp. 64–86, 2012.

[71] B. L. Dang, M. G. Larrode, R. V. Prasad, I. Niemegeers, and A. Koonen, "Radio-over-fiber based architecture for seamless wireless indoor communication in the 60GHz band," *Computer Communications*, vol. 30, no. 18, pp. 3598–3613, dec 2007.

[72] S. Lien, S. Shieh, Y. Huang, B. Su, Y. Hsu, and H. Wei, "5G new radio: Waveform, frame structure, multiple access, and initial access," *IEEE Communications Magazine*, vol. 55, no. 6, pp. 64–71, 2017.

[73] E. Dahlman, S. Parkvall, and J. Sköld, "Radio-interface architecture," in *5G NR: the Next Generation Wireless Access Technology.* Elsevier, 2018, pp. 73–102.

[74] M. Tayyab, X. Gelabert, and R. Jantti, "A survey on handover management: From LTE to NR," *IEEE Access*, vol. 7, pp. 118 907–118 930, 2019.

[75] M. Jaber, M. Imran, R. Tafazolli, and A. Tukmanov, "An adaptive backhaul-aware cell range extension approach," in *2015 IEEE International Conference on Communication Workshop (ICCW)*, 2015, pp. 74–79.

[76] E. et al., "Text proposal for evaluation methodology," R1-083807: 3GPP TSG RAN WG1 Meeting, Tech. Rep., Sept. 20O8.

[77] Q. Europe, "R1-083813:Range expansion for efficient support of heterogeneous networks," 3GPP TSG RAN WG1 Meeting, Tech. Rep., Sept. 20O8.

[78] T. Kudo and T. Ohtsuki, "Cell range expansion using distributed Q-learning in heterogeneous networks," in *2013 IEEE 78th Vehicular Technology Conference (VTC Fall)*, 2013, pp. 1–5.

[79] D. Lopez-Perez and X. Chu, "Inter-cell interference coordination for expanded region picocells in heterogeneous networks," in *2011 Proceedings of 20th International Conference on Computer Communications and Networks (ICCCN)*, 2011, pp. 1–6.

[80] T. S. Rappaport, *Wireless Communications: Principles and Practice*. 2nded. Upper Saddle River, NJ, USA: Prentice-Hall, 2013.

[81] A. Karandikar, N. Akhtar, and M. Mehta, *Mobility management in LTE heterogeneous networks*. Springer, 2017.

[82] S. Sesia, I. Toufik, and M. Baker, *LTE the UMTS long term evolution: from theory to practice*. John Wiley Sons, 2011.

[83] S. M. Razavi, D. Yuan, F. Gunnarsson, and J. Moe, "Dynamic tracking area list configuration and performance evaluation in lte," in *2010 IEEE Globecom Workshops*, 2010, pp. 49–53.

[84] M. Tayyab, X. Gelabert, and R. Jäntti, "A survey on handover management: From lte to nr," *IEEE Access*, vol. 7, pp. 118 907–118 930, 2019.

[85] A. Taufique, A. Mohamed, H. Farooq, A. Imran, and R. Tafazolli, "Analytical modeling for mobility signalling in ultradense hetnets," *IEEE Transactions on Vehicular Technology*, vol. 68, no. 3, pp. 2709–2723, 2019.

[86] 5G New Radio - NR and NG-RAN Overall Description-Stage 2, 3GPP TS 38.300 Release 15, Version 15.5.0, March Mar. 2019.

[87] 5G; System Architecture for the 5G System, "3GPP TS 23.501 Release 15," Version 15.2.0, Jun. 2019.

[88] O. G. Aliu, A. Imran, M. A. Imran, and B. Evans, "A survey of self organisation in future cellular networks," *IEEE Communications Surveys Tutorials*, vol. 15, no. 1, pp. 336–361, First 2013.

[89] P. V. Klaine, M. A. Imran, O. Onireti, and R. D. Souza, "A survey of machine learning techniques applied to self-organizing cellular networks," *IEEE Communications Surveys Tutorials*, vol. 19, no. 4, pp. 2392–2431, Fourthquarter 2017.

[90] 3GPP, "5G; Study on scenarios and requirements for next generation access technologies," 3rd Generation Partnership Project (3GPP), TS 38.913, Sept. 2018.

[91] ——, "5G; NR; Base Station (BS) radio transmission and reception," 3rd Generation Partnership Project (3GPP), TS 38.104, July 2018.

[92] S. Rangan, T. S. Rappaport, and E. Erkip, "Millimeter-wave cellular wireless networks: Potentials and challenges," *Proceedings of the IEEE*, vol. 102, no. 3, pp. 366–385, March 2014.

[93] S. J. Russell and P. Norvig, *Artificial intelligence: a modern approach*. Malaysia; Pearson Education Limited,, 2016.

[94] D. S. Wickramasuriya, C. A. Perumalla, K. Davaslioglu, and R. D. Gitlin, "Base station prediction and proactive mobility management in virtual cells using recurrent neural networks," in *2017 IEEE 18th Wireless and Microwave Technology Conference (WAMICON)*, April 2017, pp. 1–6.

[95] Z. Hamza and T. Abdallah, "Mapping fault tree into bayesian network in safety analysis of process system," in *2015 4th International Conference on Electrical Engineering (ICEE)*, Dec 2015, pp. 1–5.

[96] S. Akoush and A. Sameh, "Bayesian learning of neural networks for mobile user position prediction," in *2007 16th International Conference on Computer Communications and Networks*, Aug 2007, pp. 1234–1239.

[97] V. Raghavan, A. Partyka, L. Akhoondzadeh-Asl, M. A. Tassoudji, O. H. Koymen, and J. Sanelli, "Millimeter wave channel measurements and implications for PHY layer design," *IEEE Transactions on Antennas and Propagation*, vol. 65, no. 12, pp. 6521–6533, Dec 2017.

[98] M. Döhler and A. Aghvami, "An outdoor-indoor interface model for radio wave propagation for 2.4, 5.2 and 60 GHz," *MSc Project, King's College London*, 1999.

[99] C. Larsson, F. Harrysson, B. Olsson, and J. Berg, "An outdoor-to-indoor propagation scenario at 28 GHz," in *The 8th European Conference on Antennas and Propagation (EuCAP 2014)*, April 2014, pp. 3301–3304.

[100] J. Du, D. Chizhik, R. Feick, G. Castro, M. Rodríguez, and R. A. Valenzuela, "Suburban residential building penetration loss at 28 GHz for fixed wireless access," *IEEE Wireless Communications Letters*, vol. 7, no. 6, pp. 890–893, Dec 2018.

[101] C. U. Bas, R. Wang, T. Choi, S. Hur, K. Whang, J. Park, J. Zhang, and A. F. Molisch, "Outdoor to indoor penetration loss at 28 GHz for fixed wireless access," in *2018 IEEE International Conference on Communications (ICC)*, May 2018, pp. 1–6.

[102] I. Rodriguez, H. C. Nguyen, I. Z. Kovács, T. B. Sørensen, and P. Mogensen, "An empirical outdoor-to-indoor path loss model from below 6 GHz to cm-

wave frequency bands," *IEEE Antennas and Wireless Propagation Letters*, vol. 16, pp. 1329–1332, 2017.

[103] C. Umit Bas, R. Wang, S. Sangodoyin, T. Choi, S. Hur, K. Whang, J. Park, C. J. Zhang, and A. F. Molisch, "Outdoor to indoor propagation channel measurements at 28 GHz," *IEEE Transactions on Wireless Communications*, vol. 18, no. 3, pp. 1477–1489, March 2019.

[104] E. Semaan, F. Harrysson, A. Furuskär, and H. Asplund, "Outdoor-to-indoor coverage in high frequency bands," in *2014 IEEE Globecom Workshops (GC Wkshps)*, Dec 2014, pp. 393–398.

[105] N. Tran, T. Imai, and Y. Okumura, "Outdoor-to-indoor channel characteristics at 20 GHz," in *2016 International Symposium on Antennas and Propagation (ISAP)*, Oct 2016, pp. 612–613.

[106] T. Imai, K. Kitao, N. Tran, N. Omaki, Y. Okumura, and K. Nishimori, "Outdoor-to-indoor path loss modeling for 0.8 to 37 GHz band," in *2016 10th European Conference on Antennas and Propagation (EuCAP)*, April 2016, pp. 1–4.

[107] C. A. L. Diakhate, J. Conrat, J. Cousin, and A. Sibille, "Millimeter-wave outdoor-to-indoor channel measurements at 3, 10, 17 and 60 GHz," in *2017 11th European Conference on Antennas and Propagation (EUCAP)*, March 2017, pp. 1798–1802.

[108] I. Rodriguez, H. C. Nguyen, N. T. K. Jørgensen, T. B. Sørensen, J. Elling, M. B. Gentsch, and P. Mogensen, "Path loss validation for urban micro cell scenarios at 3.5 GHz compared to 1.9 GHz," in *2013 IEEE Global Communications Conference (GLOBECOM)*, Dec 2013, pp. 3942–3947.

[109] I. Rodriguez, H. C. Nguyen, T. B. Sorensen, J. Elling, J. A. Holm, P. Mogensen, and B. Vejlgaard, "Analysis of 38 GHz mmwave propagation char-

acteristics of urban scenarios," in *Proceedings of European Wireless 2015; 21th European Wireless Conference*, May 2015, pp. 1–8.

[110] J. Medbo, D. Sundman, H. Asplund, N. Jaldén, and S. Dwivedi, "Wireless urban propagation measurements at 2.44, 5.8, 14.8 58.68 GHz," in *2017 XXXIInd General Assembly and Scientific Symposium of the International Union of Radio Science (URSI GASS)*, Aug 2017, pp. 1–4.

[111] K. Saito, Q. Fan, N. Keerativoranan, and J. Takada, "4.9 GHz band outdoor to indoor propagation loss analysis in high building environment using unmanned aerial vehicle," in *2019 13th European Conference on Antennas and Propagation (EuCAP)*, March 2019, pp. 1–4.

[112] K. Haneda, J. Zhang, L. Tan, G. Liu, Y. Zheng, H. Asplund, J. Li, Y. Wang, D. Steer, C. Li, T. Balercia, S. Lee, Y. Kim, A. Ghosh, T. Thomas, T. Nakamura, Y. Kakishima, T. Imai, H. Papadopoulos, T. S. Rappaport, G. R. MacCartney, M. K. Samimi, S. Sun, O. Koymen, S. Hur, J. Park, C. Zhang, E. Mellios, A. F. Molisch, S. S. Ghassamzadeh, and A. Ghosh, "5G 3GPP-Like channel models for outdoor urban microcellular and macrocellular environments," in *2016 IEEE 83rd Vehicular Technology Conference (VTC Spring)*, May 2016, pp. 1–7.

[113] T. S. Rappaport, Y. Xing, G. R. MacCartney, A. F. Molisch, E. Mellios, and J. Zhang, "Overview of millimeter wave communications for fifth-generation 5G wireless networks—with a focus on propagation models," *IEEE Transactions on Antennas and Propagation*, vol. 65, no. 12, pp. 6213–6230, Dec 2017.

[114] F. S. Chaves and K. Bechta, "5G network deployment: Interplay of key elements in the challenging outdoor-to-indoor scenario," in *2016 European Conference on Networks and Communications (EuCNC)*, June 2016, pp. 293–297.

[115] K. Saito and M. Omiya, "A computational study of indoor-to-outdoor propagation in office environment at 2.4 GHz and 5.2 GHz bands," in *2018 IEEE International Workshop on Electromagnetics:Applications and Student Innovation Competition (iWEM)*, Aug 2018, pp. 1–2.

[116] H. Fukudome, K. Akimoto, S. Kameda, N. Suematsu, T. Takagi, and K. Tsubouchi, "Measurement of 3.5 GHz band small cell indoor-outdoor propagation in multiple environments," in *European Wireless 2016; 22th European Wireless Conference*, May 2016, pp. 1–6.

[117] ——, "Modeling indoor-outdoor propagation in wooden residential area at 2.5 GHz and 3.5 GHz bands," in *2017 International Conference on Computing, Networking and Communications (ICNC)*, Jan 2017, pp. 277–281.

[118] S. Hamid, A. Al-Dweik, M. Mirahmadi, K. Mubarak, and A. Shami, "Indoor-to-outdoor channel characterization for modeling and prediction of interference in next generation wireless networks," in *2015 9th European Conference on Antennas and Propagation (EuCAP)*, April 2015, pp. 1–5.

[119] A. Valcarce and J. Zhang, "Empirical indoor-to-outdoor propagation model for residential areas at 0.9–3.5 GHz," *IEEE Antennas and Wireless Propagation Letters*, vol. 9, pp. 682–685, 2010.

[120] I. Rodriguez, H. C. Nguyen, N. T. K. Jorgensen, T. B. Sorensen, and P. Mogensen, "Radio propagation into modern buildings: Attenuation measurements in the range from 800 MHz to 18 GHz," in *2014 IEEE 80th Vehicular Technology Conference (VTC2014-Fall)*, Sep. 2014, pp. 1–5.

[121] S. Sadowski and P. Spachos, "Rssi-based indoor localization with the internet of things," *IEEE Access*, vol. 6, pp. 30 149–30 161, 2018.

[122] Q. Zeng, J. Wang, Q. Meng, X. Zhang, and S. Zeng, "Seamless pedestrian navigation methodology optimized for indoor/outdoor detection," *IEEE Sensors Journal*, vol. 18, no. 1, pp. 363–374, Jan 2018.

[123] D. Dardari, P. Closas, and P. M. Djurić, "Indoor tracking: Theory, methods, and technologies," *IEEE Transactions on Vehicular Technology*, vol. 64, no. 4, pp. 1263–1278, April 2015.

[124] B. Allen, S. Mahato, Y. Gao, and S. Salous, "Indoor-to-outdoor empirical path loss modelling for femtocell networks at 0.9, 2, 2.5 and 3.5 GHz using singular value decomposition," *IET Microwaves, Antennas Propagation*, vol. 11, no. 9, pp. 1203–1211, 2017.

[125] Y. Corre, J. Stephan, and Y. Lostanlen, "Indoor-to-outdoor path-loss models for femtocell predictions," in *2011 IEEE 22nd International Symposium on Personal, Indoor and Mobile Radio Communications*, Sep. 2011, pp. 824–828.

[126] M. Kacou, V. Guillet, G. El Zein, and G. Zaharia, "Coverage and throughput analysis at 60 GHz for indoor wlan with indirect paths," in *2018 IEEE 29th Annual International Symposium on Personal, Indoor and Mobile Radio Communications (PIMRC)*, Sep. 2018, pp. 1–5.

[127] M. Mirahmadi, A. Shami, and A. Al-Dweik, "A building architecture model for predicting femtocell interference in next-generation networks," in *2012 IEEE International Conference on Communications (ICC)*, June 2012, pp. 5059–5063.

[128] M. A. Imran, A. Turkmen, M. Ozturk, J. Nadas, and Q. H. Abbasi, "Seamless indoor/outdoor coverage in 5G," pp. 1–23, may 2020.

[129] N. Sinclair, D. Harle, I. A. Glover, and R. C. Atkinson, "A kernel methods approach to reducing handover occurrences within lte," in *European*

Wireless 2012; 18th European Wireless Conference 2012, April 2012, pp. 1–8.

[130] L. Bai, C.-X. Wang, J. Huang, Q. Xu, Y. Yang, G. Goussetis, J. Sun, and W. Zhang, "Predicting wireless mmwave massive mimo channel characteristics using machine learning algorithms," *Wireless Communications and Mobile Computing*, vol. 2018, 2018.

[131] N. Sinclair, D. Harle, I. A. Glover, J. Irvine, and R. C. Atkinson, "An advanced som algorithm applied to handover management within lte," *IEEE Transactions on Vehicular Technology*, vol. 62, no. 5, pp. 1883–1894, Jun 2013.

[132] M. Milijić, Z. Stanković, and I. Milovanović, "Hybrid-empirical neural model for indoor/outdoor path loss calculation," in *2011 10th International Conference on Telecommunication in Modern Satellite Cable and Broadcasting Services (TELSIKS)*, vol. 2, Oct 2011, pp. 548–551.

[133] M. Sattarian, J. Rezazadeh, R. Farahbakhsh, and A. Bagheri, "Indoor navigation systems based on data mining techniques in internet of things: a survey," *Wireless Networks*, vol. 25, no. 3, pp. 1385–1402, Apr 2019. [Online]. Available: https://doi.org/10.1007/s11276-018-1766-4

[134] M. M. Molu, P. Xiao, M. Khalily, K. Cumanan, L. Zhang, and R. Tafazolli, "Low-complexity and robust hybrid beamforming design for multi-antenna communication systems," *IEEE Transactions on Wireless Communications*, vol. 17, no. 3, pp. 1445–1459, March 2018.

[135] 3GPP, "3G;Home NodeB Study Item Technical Report," 3rd Generation Partnership Project (3GPP), TS 38.913 , Sept. 2008.

[136] A. Alexiou, C. Bouras, V. Kokkinos, K. Kontodimas, and A. Papazois, "Interference behavior of integrated femto and macrocell environments," in *2011 IFIP Wireless Days (WD)*, Oct 2011, pp. 1–5.

[137] A. F. Molisch, A. Karttunen, R. Wang, C. U. Bas, S. Hur, J. Park, and J. Zhang, "Millimeter-wave channels in urban environments," in *2016 10th European Conference on Antennas and Propagation (EuCAP)*, 2016, pp. 1–5.

[138] M.-D. Kim, J. Liang, Y. K. Yoon, and J. H. Kim, "28ghz path loss measurements in urban environments using wideband channel sounder," in *2015 IEEE International Symposium on Antennas and Propagation USNC/URSI National Radio Science Meeting*, 2015, pp. 1798–1799.

[139] S. Hur, Y.-J. Cho, J. Lee, N.-G. Kang, J. Park, and H. Benn, "Synchronous channel sounder using horn antenna and indoor measurements on 28 ghz," in *2014 IEEE International Black Sea Conference on Communications and Networking (BlackSeaCom)*, 2014, pp. 83–87.

[140] C. U. Bas, R. Wang, S. Sangodoyin, S. Hur, K. Whang, J. Park, J. Zhang, and A. F. Molisch, "Dynamic double directional propagation channel measurements at 28 ghz - invited paper," in *2018 IEEE 87th Vehicular Technology Conference (VTC Spring)*, 2018, pp. 1–6.

[141] J. Ko, K. Lee, Y.-J. Cho, S. Oh, S. Hur, N.-G. Kang, J. Park, D.-J. Park, and D.-H. Cho, "Feasibility study and spatial temporal characteristics analysis for 28 ghz outdoor wireless channel modelling," *IET Communications*, vol. 10, no. 17, pp. 2352 – 2362, 2016.

[142] C. Larsson, F. Harrysson, B.-E. Olsson, and J.-E. Berg, "An outdoor-to-indoor propagation scenario at 28 ghz," in *The 8th European Conference on Antennas and Propagation (EuCAP 2014)*. IEEE, 2014, pp. 3301–3304.

[143] H. Zhao, R. Mayzus, S. Sun, M. Samimi, J. K. Schulz, Y. Azar, K. Wang, G. N. Wong, F. Gutierrez, and T. S. Rappaport, "28 ghz millimeter wave cellular communication measurements for reflection and penetration loss in and around buildings in new york city," in *2013 IEEE international conference· on communications (ICC)*. IEEE, 2013, pp. 5163 – 5167.

[144] R. Rudd, K. Craig, M. Ganley, and R. Hartless, "Building Materials and Propagation Final Report," Ofcom, Tech. Rep., Sept. 2014.

[145] A. Regmi, "Reflection measurement of building materials at microwaves," *Diss . Master's thesis*, 2016.

[146] H. C. Rhim and O. Buyukozturk, "Electromagnetic properties of concrete at microwave frequency· range," *Materials Journal*, vol. 95, no. 3, pp. 262 – 271, 1998.

[147] T. S. Rappaport, S. Sun, R. Mayzus, H. Zhao, Y. Azar, K. Wang, G. N. Wong, J. K. Schulz, M. Samimi, and F. Gutierrez, "Millimeter wave mobile communications for 5G cellular: It will work!" *IEEE Access*, vol. 1, pp. 335–349, 2013.

[148] M. E. Leinonen, G. Destino, O. Kursu, M. Sonkki, and A. Pärssinen, "28 GHz wireless backhaul transceiver characterization and radio link budget," *ETRI Journal*, vol. 40, no. 1, pp. 89–100, 2018.

[149] D. Pena, R. Feick, H. D. Hristov, and W. Grote, "Measurement and modeling of propagation losses in brick and concrete walls for the 900-MHz band," *IEEE Transactions on Antennas and Propagation*, vol. 51, no. 1, pp. 31–39, Jan 2003.

[150] M. U. Sheikh, K. Hiltunen, and J. Lempiainen, "Enhanced Outdoor to Indoor Propagation Models and Impact of Different Ray Tracing Approaches

at Higher Frequencies," *Advances in Science, Technology and Engineering Systems Journal*, vol. 3, no. 2, pp. 58–68, 2018.

[151] I. Shayea, M. Ergen, M. Hadri Azmi, S. Aldirmaz Çolak, R. Nordin, and Y. I. Daradkeh, "Key challenges, drivers and solutions for mobility management in 5G networks: A survey," *IEEE Access*, vol. 8, pp. 172 534–172 552, 2020.

[152] M. R. Akdeniz, Y. Liu, M. K. Samimi, S. Sun, S. Rangan, T. S. Rappaport, and E. Erkip, "Millimeter wave channel modeling and cellular capacity evaluation," *IEEE journal on selected areas in communications*, vol. 32, no. 6, pp. 1164–1179, 2014.

[153] A. M. Al-Samman, T. Al-Hadhrami, A. Daho, M. Hindia, M. H. Azmi, K. Dimyati, M. Alazab *et al.*, "Comparative study of indoor propagation model below and above 6 GHz for 5G wireless networks," *Electronics*, vol. 8, no. 1, p. 44, 2019.

[154] Y. Wang, G. Feng, Y. Sun, S. Qin, and Y.-C. Liang, "Decentralized learning based indoor interference mitigation for 5g-and-beyond systems," *IEEE Transactions on Vehicular Technology*, vol. 69, no. 10, pp. 12 124–12 135, 2020.

[155] N. Amirrudin, S. H. Syed Ariffin, N. N. Nik Abd Malik, and G. N.Effiyana, "Mobility prediction via markov model in lte femtocell," *International Journal of Computer Applications*, vol. 18, 01 2013.

[156] N. A. Amirrudin, S. H. S. Ariffin, N. N. N. A. Malik, and N. E. Ghazali, "User's mobility history-based mobility prediction in LTE femtocells network," in *2013 IEEE International RF and Microwave Conference (RFM)*, 2013, pp. 105–110.

[157] M. Ozturk, P. V. Klaine, and M. A. Imran, "3D transition matrix solution for a path dependency problem of markov chains-based prediction in cellular networks," in *2017 IEEE 86th Vehicular Technology Conference (VTC-Fall)*, 2017, pp. 1–5.

[158] A. Mohamed, O. Onireti, S. A. Hoseinitabatabaei, M. Imran, A. Imran, and R. Tafazolli, "Mobility prediction for handover management in cellular networks with control/data separation," in *2015 IEEE International Conference on Communications (ICC)*, 2015, pp. 3939–3944.

[159] The Guardian, "Vodafone reports 50% rise in internet use as more people work from home," https://www.theguardian.com/business/2020/mar/18/vodafone-rise-data-usage-more-people-work-from-home-coronavirus, 2020.

[160] N. Sinclair, D. Harle, I. A. Glover, and R. C. Atkinson, "A kernel methods approach to reducing handover occurrences within LTE," in *European Wireless 2012; 18th European Wireless Conference 2012*, 2012, pp. 1–8.

[161] T.-H. Kim and J.-W. Kim, "Handover optimization with user mobility prediction for femtocell-based wireless networks," *International Journal of Engineering and Technology (IJET)*, vol. 5, no. 2, pp. 1829–1837, 2013.

[162] T. Inoue, Y. Watanabe, T. Nobukiyo, and Y. Matsunaga, "Dual handover triggers to improve QoE for indoor and outdoor mobility," in *2014 IEEE 25th Annual International Symposium on Personal, Indoor, and Mobile Radio Communication (PIMRC)*, 2014, pp. 1727–1731.

[163] P. S. Prasad and P. Agrawal, "Mobility prediction for wireless network resource management," in *2009 41st Southeastern Symposium on System Theory*, 2009, pp. 98–102.

[164] D. M. Rose, T. Jansen, S. Hahn, and T. Kürner, "Impact of realistic indoor mobility modelling in the context of propagation modelling on the user and

network experience," in *2013 7th European Conference on Antennas and Propagation (EuCAP)*, 2013, pp. 3979–3983.

[165] J. Kolodziej, S. U. Khan, L. Wang, N. Min-Allah, S. A. Madani, N. Ghani, and H. Li, "An application of markov jump process model for activity-based indoor mobility prediction in wireless networks," in *2011 Frontiers of Information Technology*, 2011, pp. 51–56.

[166] B. Tang, C. Jiang, H. He, and Y. Guo, "Probabilistic human mobility model in indoor environment," in *2016 International Joint Conference on Neural Networks (IJCNN)*, 2016, pp. 1601–1608.

[167] A. Turkmen, S. Ansari, P. V. Klaine, L. Zhang, and M. A. Imran, "Indoor mobility prediction for mmWave communications using Markov Chain," in *2021 IEEE Wireless Communications and Networking Conference (WCNC)*, 2021, pp. 1–5.

[168] F. Zafari, A. Gkelias, and K. K. Leung, "A survey of indoor localization systems and technologies," *IEEE Communications Surveys & Tutorials*, vol. 21, no. 3, pp. 2568–2599, 2019.

[169] R. S. Sutton and A. G. Barto, *Reinforcement learning: An introduction*. MIT press, 2018.

[170] A. Goldsmith, *Wireless Communications*. Cambridge university press, 2005.

[171] A. Turkmen, M. S. Mollel, M. Ozturk, Y. Sun, L. Zhang, R. Ghannam, and M. A. Imran, "Coverage analysis for indoor-outdoor coexistence for millimetre-wave communication," in *4th International Conference on UK - China Emerging Technologies (UCET 2019), Glasgow, UK, 21-22 Aug 2019*, 2019.

[172] S. Zhao, Y. Feng, and G. Yu, "D2d communication channel allocation and resource optimization in 5g network based on game theory," *Computer Communications*, vol. 169, pp. 26–32, 2021.

[173] D. Wisely, N. Wang, and R. Tafazolli, "Capacity and costs for 5g networks in dense urban areas," *IET Communications*, vol. 12, no. 19, pp. 2502–2510, 2018.

[174] C. B. Barneto, L. Anttila, M. Fleischer, and M. Valkama, "Ofdm radar with lte waveform: Processing and performance," in *2019 IEEE Radio and Wireless Symposium (RWS)*. IEEE, 2019, pp. 1–4.

[175] Y. Sun, G. Feng, S. Qin, Y.-C. Liang, and T.-S. P. Yum, "The smart handoff policy for millimeter wave heterogeneous cellular networks," *IEEE Transactions on Mobile Computing*, vol. 17, no. 6, pp. 1456–1468, 2017.

[176] Z. Li, C. Wang, and C.-J. Jiang, "User association for load balancing in vehicular networks: An online reinforcement learning approach," *IEEE Transactions on Intelligent Transportation Systems*, vol. 18, no. 8, pp. 2217–2228, 2017.

[177] S. Hussain, "Efficient ray-tracing algorithms for radio wave propagation in urban environments," Ph.D. dissertation, Dublin City University, 2017.

[178] J. Ho and I. Akyildiz, "Local anchor scheme for reducing signaling costs in personal communications networks," *IEEE/ACM Transactions on Networking*, vol. 4, no. 5, pp. 709–725, 1996.

[179] L. Wang, Y. Zhang, and Z. Wei, "Mobility management schemes at radio network layer for LTE femtocells," in *VTC Spring 2009 - IEEE 69th Vehicular Technology Conference*, 2009, pp. 1–5.

[180] K.-S. Kim, S.-L. Ju, and H.-R. Choi, "Performance evaluation for 5g nr based uplink millimeter-wave mimo systems under urban micro cell," in

2019 2nd International Conference on Communication Engineering and Technology (ICCET), 2019, pp. 48–51.

[181] E. Basar, M. Di Renzo, J. De Rosny, M. Debbah, M.-S. Alouini, and R. Zhang, "Wireless communications through reconfigurable intelligent surfaces," *IEEE Access*, vol. 7, pp. 116 753–116 773, 2019.

[182] F. C. Okogbaa, Q. Z. Ahmed, F. A. Khan, W. B. Abbas, F. Che, S. A. R. Zaidi, and T. Alade, "Design and application of intelligent reflecting surface (irs) for beyond 5 g wireless networks: A review," *Sensors*, vol. 22, no. 7, p. 2436, 2022.

[183] E. Bjornson, L. Van der Perre, S. Buzzi, and E. G. Larsson, "Massive mimo in sub- 6 ghz and mmwave: Physical , practical· , and use-case differences," *IEEE Wireless Communications*, vol. 26, no. 2, pp. 100 – 108, 2019.

[184] O. Alluhaibi, Q. Z. Ahmed, C. Pan, and H. Zhu, "Capacity maximisation for hybrid digital-to-analog beamforming mm-wave systems," in *2016 IEEE Global Communications Conference (GLOBECOM)*, 2016, pp. 1–6.

[185] M. Nair, Q. Z. Ahmed, and H. Zhu, "Hybrid digital-to-analog beamforming for millimeter-wave systems with high user density," in *2016 IEEE Global Communications Conference (GLOBECOM)*, 2016, pp. 1–6.

[186] O. E. Ayach, S. Rajagopal, S. Abu-Surra, Z. Pi, and R. W. Heath, "Spatially sparse precoding in millimeter wave mimo systems," *IEEE Transactions on Wireless Communications*, vol. 13, no. 3, pp. 1499–1513, 2014.

[187] W. Hong, Z. H. Jiang, C. Yu, D. Hou, H. Wang, C. Guo, Y. Hu, L. Kuai, Y. Yu, Z. Jiang, Z. Chen, J. Chen, Z. Yu, J. Zhai, N. Zhang, L. Tian, F. Wu, G. Yang, Z.-C. Hao, and J. Y. Zhou, "The role of millimeter-wave technologies in 5g/6g wireless communications," *IEEE Journal of Microwaves*, vol. 1, no. 1, pp. 101–122, 2021.

[188] C. Huang, R. Mo, and C. Yuen, "Reconfigurable intelligent surface assisted multiuser miso systems exploiting deep reinforcement learning," *IEEE Journal on Selected Areas in Communications*, vol. 38, no. 8, pp. 1839–1850, 2020.

[189] J. Dang, Z. Zhang, and L. Wu, "Joint beamforming for intelligent reflecting surface aided wireless communication using statistical csi," *China Communications*, vol. 17, no. 8, pp. 147–157, 2020.

[190] R. Arshad, H. Elsawy, S. Sorour, T. Y. Al-Naffouri, and M.-S. Alouini, "Handover management in 5g and beyond: A topology aware skipping approach," *IEEE Access*, vol. 4, pp. 9073–9081, 2016.

[191] Ericsson Blog, "5G positioning: What you need to know," https://www.ericsson.com/en/blog/2020/12/5g-positioning--what-you-need-to-know, 2019, Accessed: 2022-05-16.

[192] W. Chen, X. Ma, Z. Li, and N. Kuang, "Sum-rate maximization for intelligent reflecting surface based terahertz communication systems," in *2019 IEEE/CIC International Conference on Communications Workshops in China (ICCC Workshops)*, 2019, pp. 153–157.

[193] Özdogan, E. Björnson, and E. G. Larsson, "Intelligent reflecting surfaces: Physics, propagation, and pathloss modeling," *IEEE Wireless Communications Letters*, vol. 9, no. 5, pp. 581–585, 2020.

[194] E. Björnson and L. Sanguinetti, "Power scaling laws and near-field behaviors of massive mimo and intelligent reflecting surfaces," *IEEE Open Journal of the Communications Society*, vol. 1, pp. 1306–1324, 2020.

[195] Q. Wu, S. Zhang, B. Zheng, C. You, and R. Zhang, "Intelligent reflecting surface-aided wireless communications: A tutorial," *IEEE Transactions on Communications*, vol. 69, no. 5, pp. 3313–3351, 2021.

[196] S. Yang, H. Han, Y. Liu, W. Guo, and L. Zhang, "Intelligent reflecting surface-induced randomness for mmwave key generation," *arXiv preprint arXiv: 2111.00428*, 2021.

[197] Y. Liu, L. Zhang, P. V. Klaine, and M. A. Imran, "Optimal multi-user transmission based on a single intelligent reflecting surface," in *2021 IEEE 4th International Conference on Electronic Information and Communication Technology (ICEICT)*, 2021, pp. 1–4.